TM-66-2

HADOPAD RADAR ACTUATOR DESIGN AND PERFORMANCE

by

John J. Roach

Malcolm L. Wiseman

February 1965

U.S. ARMY MATERIEL COMMAND

HARRY DIAMOND LABORATORIES

WASHINGTON, D.C. 20438

The findings in this report are not to be construed as an official Department of the Army position, unless so designated by other authorized documents.

Destroy this report when it is no longer needed. Do not return it to the originator.

AVAILABILITY/LIMITATION NOTICES

Qualified requesters may obtain copies of this report from DDC. DDC release to Clearinghouse for Federal Scientific and Technical Information is authorized.

BLANK PAGE

AD

DA 1W542703D346
AMCMS Code 5520.22.46803
HDL Proj 47100

TM-66-2

HADOPAD RADAR ACTUATOR DESIGN AND PERFORMANCE

by
John J. Roach
Malcolm L. Wiseman

February 1965

U.S. ARMY MATERIEL COMMAND
HARRY DIAMOND LABORATORIES
WASHINGTON, D.C. 20438

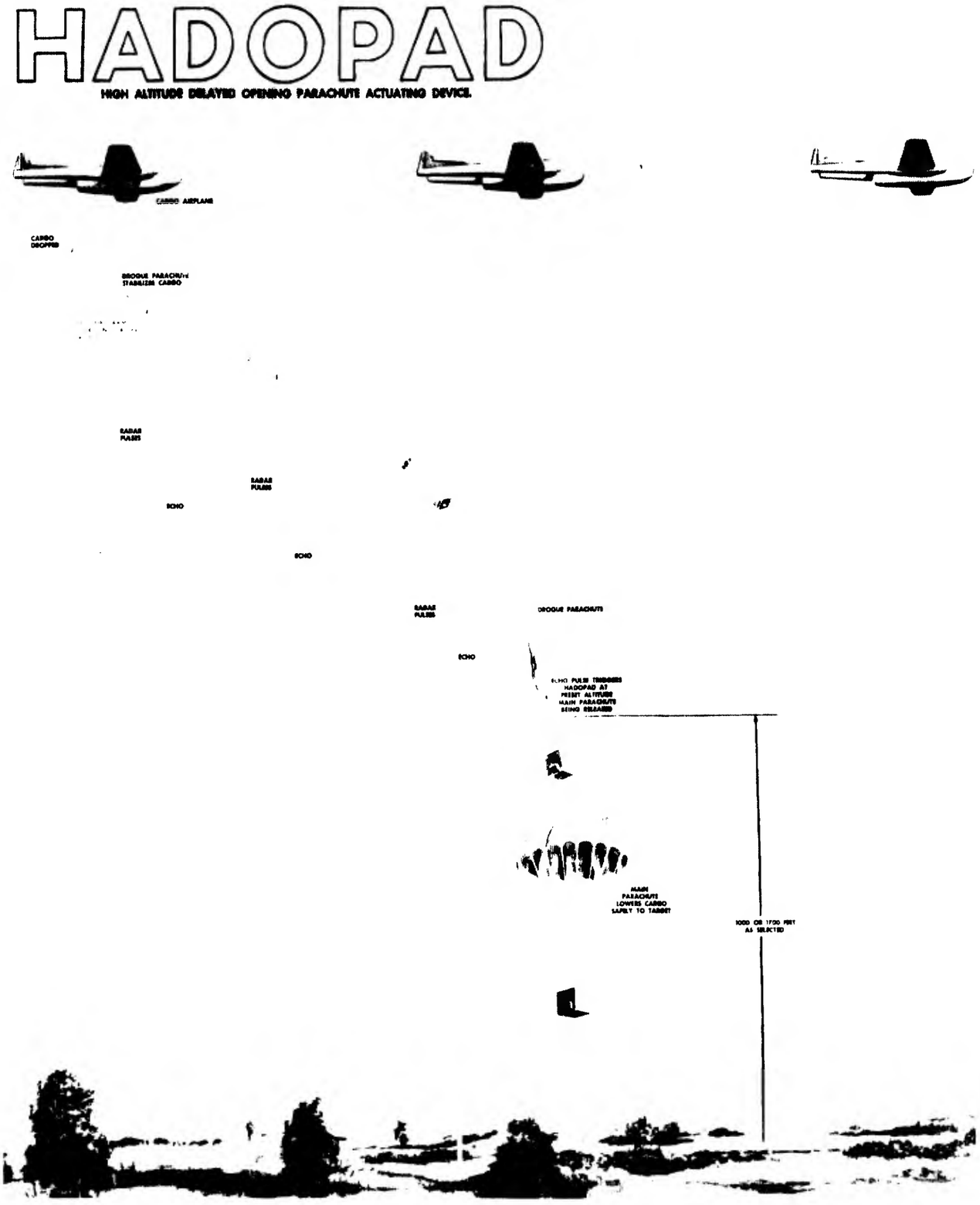

040-64

FRONTISPIECE: Pictorial Diagram of the HADOPAD.

CONTENTS

BLANK PAGE

ABSTRACT

A low-cost radar actuator for use as a component in a delayed-opening parachute aerial-delivery system has been developed at HDL at the request of the U.S. Army Natick Laboratories. This device is known as HADOPAD (High-Altitude Delayed-Opening Parachute Actuating Device).

The device, based on radar principles, will open a main recovery parachute at either of two preset heights (1000 or 1700 ft) above the ground. The complete system utilizes a drogue-parachute stabilizing stage for free fall from high altitude followed by a main- parachute recovery stage which is initiated at low altitude by the radar actuator.

Limited field testing of the radar actuator at Fort Devens, Mass. has shown the feasibility of the device as a parachute actuator, but some additional engineering and complete environmental tests are necessary before initiation of quantity production.

Forty actuators were constructed by HDL during the research and development phase.

1. INTRODUCTION

The Harry Diamond Laboratories have developed, during the past two years, a low-cost reusable radar actuator as part of an accurate air delivery system. This effort was sponsored by the U.S. Army Natick Laboratories who have the development mission for a High-Altitude Delayed-Opening Parachute Actuating Device (HADOPAD).

The radar is capable of sensing either of two altitudes (1000 or 1700 ft) as selected by a manual switch. By delaying the opening of the main parachute, it is possible to improve the delivery accuracy of material dropped from high altitude. A pictorial diagram of the HADOPAD system is shown in the frontispiece.

The air delivery system consists of the cargo package, two parachutes (drogue and main), and the radar actuator. When the cargo is dropped from the aircraft, the drogue parachute is released, and the radar is turned on. The radar has a built-in time delay to insure that the radar will not function on the aircraft. The radar is designed to determine when the cargo has reached a preset altitude and to generate a firing signal which actuates a mechanism releasing the main parachute at that time. The radar actuator may be reused by replacing the thermal power source and the bellows-type squib used in the release mechanism.

A limited production of 40 units during the developmental phase resulted in a cost per unit of about $1300. The estimated cost of production in large quantities would be about $700 per unit.

2. PRINCIPLE OF OPERATION

Radar operation is initiated by the generation of a pulse by the modulator, which is applied to the plate of the transmitter tube. The pulse causes the transmitter to oscillate at 420 Mc.

The transmitter is coupled to the radiating system or antenna through a hybrid coupler (a three-terminal device), which allows a single antenna to serve for both transmission and reception. The coupler attenuates the transmitted pulse across the receiver input during the transmission period, while offering relatively small attenuation along the transmitter-to-antenna path. During the period of reception the received signal is divided equally between transmitter and receiver.

The transmitted energy is thus delivered to the radiating antenna system, which propagates the energy in a pattern determined by the design of the antenna. In the case of the HADOPAD actuator, the energy is dispersed over a wide angle. When this energy impinges on a reflecting surface, some of it returns to the antenna greatly attenuated and delayed in time, in accordance with the distance travelled to the reflector and back to the antenna. The time delay is in direct proportion to the distance to the reflecting object. The velocity of propagation is 984 ft/μs. This information is utilized by the actuator to determine altitude over the terrain (the reflector).

The reflected energy is delivered to the receiver input, again through the coupler, by the antenna. The receiver, which is of the superheterodyne type, mixes and amplifies the signal at 50 Mc. The signal is then detected and delivered to the video amplifier, where it is again amplified and applied to one input terminal of a coincidence circuit.

Simultaneously with the application of the modulator pulse to the transmitter plate, a sample of this pulse is routed through a delay system, which drives a blocking oscillator. The blocking oscillator emits one tailored pulse at its output for each driving pulse placed across its input. The duration of the output pulse is dependent on the constants of the delay circuitry and is relatively independent of the pulse applied to its input.

The pulse applied to the blocking oscillator is delayed relative to the transmitted pulse by the time interval necessary for the radiated pulse to traverse the round trip path from the antenna to reflector and back to antenna. Thus an internal time gate pulse has been generated that can be made proportional to the desired height of function. This gate pulse is applied to the other input terminal of the coincidence circuit. The coincidence circuit is designed to deliver an output pulse only when signals are present at both of its inputs simultaneously. This sequence of events occurs for each pulse from the modulator at a rate of about 825 times per second.

During the drop period of the HADOPAD actuator, the actuator approaches the reflector (terrain) from a higher altitude than the desired function altitude. Consequently the delay time between the transmitted pulse and the received echo pulse is constantly decreasing. At a given time during the drop period the echo pulse coincides with the gate pulse. This causes the coincidence circuit to emit an output pulse.

The time of coincidence may be lengthened any reasonable amount by controlling the width of the gating pulse. For example, if the width of the gate pulse is 0.25 μs, the echo pulse remains coincident with the gate pulse during this interval, which corresponds to about 125 ft of fall after initial coincidence. This is commonly done to insure operation since it is impossible to be sure of operation with a very short gate interval, such as 0.05 μs. After the actuator falls through the altitude interval represented by the gate width, the reflected echo pulse no longer operates the coincidence circuit and the actuator can no longer initiate the firing circuitry.

The pulses emitted from the coincidence circuit output are further amplified. The width of the individual pulses is increased during the process of amplification resulting in an increase of energy per pulse due to both amplification and stretching. The pulse stretcher amplifiers are designed to deliver relatively high energy pulses into an integrating circuit, which is basically a capacitor charged through a resistance element. Each succeeding pulse delivered to the integrating capacitor raises the voltage across it in direct proportion to the energy content of the driving pulse. The integrating circuit is designed to accept a number of these pulses before attaining a given voltage level.

When the voltage across the integrating capacitor reaches a preset level, a silicon controlled rectifier (SCR) is triggered.

The SCR then acts to discharge a storage capacitor through the bellows squib, actuating the main parachute.

3. STATEMENT OF REQUIREMENTS

(1) The actuator should be capable of normal operation within 2 sec after application of power.

(2) Accuracy of actuation should be within 10 percent of the assigned function altitudes of 1000 and 1700 ft above average terrain level.

(3) The device should have a reliability factor of 0.95, and the design should be as economical as possible consistent with this factor.

(4) The actuator should be capable of operation over the temperature range -65° to +165°F. The device must withstand all world environment and climatic extremes, in addition to the airborne and parachute recovery environments.

(5) The device should be reusable for training purposes, and the service requirements before reuse should be minimal.

(6) Any function checkout just prior to use should be minimal and efficient.

4. DESCRIPTION OF RADAR ACTUATOR

The altitude-sensing device for use in the HADOPAD system is a pulse-modulated radar set operating at about 420 Mc. Figure 1 is a block diagram of the system which comprises a modulator, transmitter, hybrid coupler, antenna, receiver (including mixer, local oscillator, i-f amplifier, detector, and emitter follower), video amplifier, decision circuitry, pulse stretcher, integrator, and firing circuit.

Semiconductor devices are utilized throughout except for the transmitter, mixer, and local oscillator, where subminiature vacuum tubes are used. The system is modularized for ease of test and assembly. The various circuits are housed within shielded containers, as follows:

RECEIVER HOUSING

High-frequency mixer
Local oscillator
I-F amplifier
Second detector
Emitter follower

TRANSMITTER/MODULATOR HOUSING

Transmitter
Modulator

DECISION/FIRING CIRCUIT HOUSING

Video amplifier
Coincidence circuit
Gate generator
Pulse stretcher
Integrator
Firing circuit

POWER SUPPLY HOUSING

Thermal battery
DC-DC converter

The hybrid coupler and thermal time-delay relay are contained in individual housings.

A 2-amp fuse has been shunted across the thermal power supply terminals to monitor battery condition. When the power supply is actuated the fuse opens. This fuse is provided to supply an indication that the power supply has been actuated accidentally or otherwise. However, the actuator may be dropped with or without the fuse in place with no effect on operation assuming the power supply is operational. The fuse is mounted in an externally accessible receptacle.

Power distribution is accomplished through the use of a single cable harness terminated in miniature plugs at entry points to the various housings. All signal circuits utilize RG58U coaxial cables. Other accessory devices are mounted on the main actuator housing.

The complete actuator is packaged inside a rectangular aluminum box approximately 18 by 4 by 10 in. The cavity antenna (1 1/2 x 10 x 17 in.) is fastened to the outside of this box and is fed from inside by coaxial cable. The individual electronic subassemblies are supported on shelves. The power supply is inclosed in a removable aluminum tube. Figures 2, 3, and 4 are photographs of the complete actuator along with the parachute release mechanism.

Considerable effort has been expended in an attempt to design a low-cost, high-reliability system. Military approved components and standard parts have been utilized where possible; no special components or critical materials have been specified. The following subsections describe the system in detail.

4.1 Modulator/Transmitter

The modulator and transmitter are packaged in a commercial drawn aluminum can with cover. The can is compartmented to shield the modulator from the transmitter.

The modulator supplies the plate power for the transmitting tube in the form of pulses at a repetition rate of about 825 per second. A typical modulator pulse is shown in figure 5. The shape of the modulator pulse is determined by the discharge of a rudimentary delay line, which is energized by a resonant charging circuit. A silicon controlled rectifier (SCR), driven by a unijunction transistor, is utilized as a switch to generate the modulator output pulse. The pulse repetition rate of the circuit is determined by constants in the unijunction circuit. An auxiliary pulse, derived from the modulator output pulse is used to trigger the gate generator contained in the video subassembly. More complete detail on the operation and design of the modulator is contained in reference 1.

The transmitter utilizes a type SN1551B subminiature filamentary triode as the oscillator. The peak power (averaged over the pulse interval) is about 350 w. The average pulse interval is 0.14 μs. The duty factor is about 9000, with a form factor of 1.55, yielding a total average power multiplier of 14,000. The mean center frequency is 423 Mc. Starting delay is about 0.12 μs. Complete details of operation and design may be found in reference 2. The power envelope of a typical detected transmitted pulse is shown in figure 6, and a typical power envelope of the transmitted spectrum in figure 7. The width of the spectrum is about 5.3 Mc. A schematic of the transmitter and modulator subassembly is given in figure 8.

4.2 Hybrid Coupler

The hybrid coupler is a device permitting the use of a single antenna for both transmit and receive functions as described in section 2. The basic hybrid coupler or ring is shown in figure 9. Isolation between transmitter and receiver is obtained as the result of phase cancellation because of the difference in path length between two alternate channels. The phase differences at the various terminals are shown in figure 10 during both transmit and receive intervals.

Figure 10 shows that, during the transmit period, cancellation is obtained at the receiver while reinforcement

occurs at the antenna and termination terminals. During the receive period cancellation occurs at the termination terminal while reinforcement is obtained at both receiver and transmitter terminals. The total theoretical power loss resulting from the insertion of this device is 6 db (3 db on each function). This loss is tolerable in the interest of obtaining receiver recovery or sensitivity at the low-function altitude of 1000 ft and lower.

This type of coupler is usually constructed of coaxial line or waveguide of lengths that result in the required phasing, each half wavelength section shifting phase by 180 deg resulting in a cancellation condition referred to the input. These line lengths can be simulated electrically by the use of lumped constants (inductance and capacity). The practical coupler as used in the HADOPAD actuator is such a device and is similar to the coupler or ring described in reference 3.

Figure 11 shows the two basic lumped constant networks necessary to assemble an equivalent ring. These networks were calculated on the basis of formulae given in reference 4. Figure 11 also shows the evolution of the final delay circuitry resulting from combining the four lumped delay networks. In this figure, L41 and C32 are parallel resonant as are L42 and C11. The resonant impedance of these combinations is high compared with 50 ohms and can be neglected. Thus these elements do not appear in the final network assembly. C12 and C21 can be combined by addition into one capacitance, as can C22 and C31. Since the HADOPAD system utilizes only three of the four terminals, terminal 1 in figure 10 is terminated in Ro (50 ohms). The final circuit is shown in figure 12, on which selected 5-percent tolerance components are used. Photographs of the HADOPAD coupler are shown in figure 13. At final assembly the cover is soldered into place. No potting is used. The coupler could be foam potted.

Of 40 couplers fabricated at HDL, 10 were tested over a frequency band with unused ports properly terminated with results as summarized below. The averages of the data are plotted in figure 14.

The detailed data showed that the most important parameter—isolation or insertion loss between ports 2 and 4, peaks at a frequency slightly higher than the operational frequency band of the HADOPAD transmitter. A 10-Mc downward movement would be about optimum. Summation of the forward insertion losses (ports 3-4 plus ports 2-3) resulted in a range of 6.3 to 6.8 db. Thus the average two-way coupler loss

is about 6.5 db. The voltage standing wave ratio measured on four couplers did not exceed 2:1 over the frequency band of interest.

INSERTION LOSS DB

	360 Mc	380 Mc	400 Mc	420 Mc	440 Mc	460 Mc	480 Mc
Ports 2-3							
Ave	4.3	3.9	3.8	3.5	3.2	3.2	3.0
Max	4.5	4.1	4.0	3.7	3.6	3.6	3.2
Min	4.0	3.6	3.5	3.1	2.8	2.9	2.7
Ports 2-4							
Ave	20.6	23.2	27.8	31.1	32.0	28.9	24.9
Max	24.1	28.2	36.0	38.5	39.0	30.8	34.0
Min	19.0	20.0	22.0	24.5	26.5	24.0	20.0
Ports 3-4							
Ave	2.5	2.4	2.7	2.8	2.9	3.3	3.5
Max	3.2	2.9	3.2	3.0	3.2	3.6	4.0
Min	2.1	2.1	2.3	2.5	2.7	3.0	3.2

Further data were obtained on all 40 couplers in the final test of the complete actuator where the coupler was terminated by the actuator receiver and transmitter. Power output from the transmitter was measured first at the output of the transmitter; the meter was then moved to the antenna terminal of the coupler and the power was again measured. The receiver remained connected to the coupler during this test. The ratio of the two power measurements was recorded as db loss during transmission.

A similar test was performed through the receiver channel. A signal was injected into the receiver input and increased until a 100-mv level was obtained at the detector. The receiver was then connected to the coupler and the signal injected into the antenna terminal of the coupler and again increased to obtain the 100-mv level at the detector. The ratio of the two input signal amplitudes was recorded as db loss during reception. The transmitter remained connected to the coupler during this test.

The overall results were as follows:

DB Loss	Transmission (db)	Reception (db)	Total (db)
Ave	2.5	3.8	6.3
Max	5.0	8.7	11.0
Min	0.7	1.8	3.6

It should be emphasized that the coupler during the final tests, described above, was not terminated in passive 50-ohm loads. The receiver impedance is about 10 ohms during reception while the transmitter in the turned-off state is about 150 ohms. During transmission the impedance of the transmitter is about 50 ohms and that of the receiver remains in the vicinity of 10 ohms.

These data, therefore, must be assessed accordingly and not be accepted as absolute; but they do provide a fair indication of the coupler operation when incorporated into the actuator. Obviously certain of these couplers should have been rejected on the basis of the numbers obtained, and would have been, except for the limited quantity available. The actual criterion for acceptance or rejection was overall actuator performance. No simple correlation exists between coupler losses and frequency or system attenuation. Time limitations precluded a more complete investigation of coupler operation in the system.

4.3 Cavity Antenna

The antenna is a waveguide fed slot. It consists of a length of waveguide short-circuited at one end with the open end terminated in a vestigial ground plane (ref 5). Figures 15 and 16 are photographs of the complete antenna. The inside of the waveguide is 1 3/8 in. by 9 7/8 in. by 16 3/4 in. The cutoff frequency is about 350 Mc. The open end of the antenna is covered by an epoxy glass board.

The waveguide section is fed off center by a coaxial cable terminated in a post electrically connected to the far side of the cavity. An additional post is positioned near the shorted end of the cavity as a tuning adjustment. Final tuning adjustment is accomplished by two screws located symmetrically about the center of the opening. One screw (fixed) functions as a bandsetting device while the other (adjustable) operates as a vernier. Figure 17 is an outline drawing of the antenna showing the positioning of the feed point and tuning adjustments. Dimensioning is in inches and in wavelengths. The antenna is fastened to the actuator housing by four ears or lugs and is fed coaxially through a hole in the housing. The dimensions of the antenna were the major determinant in the final size of the actuator.

The ideal antenna for the HADOPAD application would radiate minimum energy in the back direction (toward the aircraft) and maximum in the direction of the terrain. The half power beam width in the forward (terrain) direction should be less than about 13 deg to avoid pulse width limiting (fig. 38) in the region of the

of the expected function altitudes. The antenna should be relatively insensitive to the type of cargo and should have a bandwidth of about 20 Mc (VSWR $\leq$ 2.0). The antenna should require no maintenance or service consistent with training requirements.

Since the antenna is attached directly to the fuze housing, damage from drop conditions is minimized and no service or maintenance is required beyond visual inspection. This type of antenna is usually operated in conjunction with a ground plane surrounding the mouth, but due to space limitations the only ground plane consists of the actuator housing. To be effective, the ground plane should be at least λ square.

The basic antenna is a slot excited by a cavity. The radiation pattern produced by a slot in a ground plane is closely related to that which would be produced by a thin flat dipole which would just fill the slot. The difference in pattern is one of polarization only. The electric field distribution obtained with a slot radiator is identical with the magnetic field distribution in the radiation field of an equivalent dipole. In order to confine the pattern to one hemisphere, the slot is usually backed with a cavity. Figure 18 shows the effect of the cavity on the directivity. The radiation pattern of a cavity with no ground plane attached is similar to that obtained from a half-wave dipole and resembles the pattern shown in figure 18 for the basic slot.

The radiation pattern for the half-wave dipole in free space is given by

$$E = A\left[\frac{\cos\frac{\pi}{2}\sin\theta}{\cos\theta}\right]$$

The pattern of an equivalent slot is

$$E = A\left[\frac{\cos\frac{\pi}{2}\cos\theta}{\sin\theta}\right]$$

The radiation pattern of the HADOPAD antenna which resembles that obtained from the second equation is shown in figures 19 and 20. The plot shown in these figures is the power pattern plotted in db, where the reference is the maximum point on the forward lobe.

The forward lobe gain of the HADOPAD antenna is about 2 db. The gain of the back lobe is about -3 db. The large back lobe gain restricts the lowest altitude at which a drop may be made, since about 1600 ft separation from the aircraft is required before final arming of the actuator can occur (ref 6). The

impedance of the antenna is about 43 ohms at 422 Mc. Laboratory measurements of the VSWR show it averages less than 2:1 over a 7.6 Mc band. The average tuning range was found to be 11.9 Mc. The epoxy glass cover shifts the center frequency downward by about 3 Mc. Detailed data were taken on 36 antennas and the results are summarized below.

VSWR $\leq$ 2.0:	Ave	Max	Min
Lowest frequency (Mc)	419.2	426.0	415.0
Highest frequency (Mc)	426.9	432.0	422.0
Bandwidth (Mc)	7.7	10.0	5.5
Tuning Range:			
Lowest frequency (Mc)	418.4	421.0	414.5
Highest frequency (Mc)	430.4	434.0	426.0
Range (Mc)	12.0	19.5	8.5

The data tabulated above were obtained in the laboratory where location of the antenna in relation to other objects was a major factor. The antenna was set as far in the clear as possible with only necessary equipment in the vicinity. Data indicate that the bandwidth is somewhat narrow for this application, being just slightly wider than the transmitted spectrum. This necessitated individual tuning to match the particular transmitter. It was found that the bandwidth was highly dependent on the inductance of the feed post. Increasing the diameter of the post resulted in a wider bandwidth. The original design utilized a length of No. 18 wire as a feed post. By substitution of a No. 10 screw, about 3 Mc increase in bandwidth was noted. Further increase in diameter might result in better performance but this was not checked because of the tight time schedule. The effect of changing the diameter of the tuning post was not checked due to inaccessibility.

Initially, some of these antennas were potted with lightweight foam but these could not be satisfactorily tuned to the high frequency end of the band. The purpose of potting was to add to the rigidity of the antenna. Improper foaming resulted in higher density than anticipated. The high density material across the mouth added enough capacity to lower the tuning range by an unacceptable amount. Experimentation with the foam potting was concluded because of time. HDL is confident that these cavities can be successfully potted if environmental conditions require it.

The present HADOPAD antenna is not fully satisfactory in two respects, back lobe gain and broad-banding. It is felt that the necessary broad-banding can be accomplished with little sacrifice

in gain through optimization. The high back lobe gain is inherent in the device because of the absence of a satisfactory ground plane. The effect of various types of cargo on the lobe structure is not known, and it would require considerable effort to obtain this information.

4.4 Receiver

The HADOPAD receiver is a 420-Mc superheterodyne containing a mixer, local oscillator, i-f strip, detector, and emitter follower. The local oscillator operates at 370 Mc, and the intermediate frequency is 50 Mc. The receiver has an overall average noise figure of 19 db and a nominal power gain of 60 db. The receiver is assembled on a brass plate and is shielded on both sides by standard-size drawn aluminum cans.

The signal frequency (420 Mc) circuits utilize subminiature filamentary tubes. The local oscillator is a 1551B, and the mixer is a 1551C. An electron tube was selected for the mixer for two reasons: economy and the known ability to withstand indefinitely the overload conditions during transmission. A tube was chosen as local oscillator because of the cost factor. The nominal input impedance of the receiver is about 10 ohms.

The mixer stage is untuned, while the local oscillator tuning adjustment is by means of a powdered iron slug threaded into the coil form. The local oscillator can be tuned over a 16-Mc range.

The intermediate amplifier consists of five transistorized (2N1742) stages which are stagger tuned to achieve the desired bandwidth. The nominal bandwidth of the amplifier is 7.5 Mc at low level signals. Tuning adjustment is by means of powdered iron slugs threaded into each coil form. No neutralizing means are included, feedback being controlled by swamping the input circuits with a fixed capacitor which is the low level element of a capacitive divider. The capacitive divider provides the necessary interstage impedance match. The amplifier is temperature compensated with a sensitor and thermistor. Video frequency bypassing as well as i-f bypassing is used to achieve fast recovery.

The detector is a series-connected crystal diode working into a short time-constant load. The short time constant minimizes distortion of the amplified echo pulse.

The receiver output stage is an emitter follower which provides about 13 db of power gain along with an impedance transformation down to about 150 ohms. The voltage gain is about 0.9. The emitter follower utilizes a 2N1742 transistor also.

A typical bandpass characteristic of the receiver at low signal levels is shown in figure 21. Figure 22 shows the characteristic at high signal level. The recovery characteristic of the receiver is displayed in figure 23. A schematic diagram of the receiver is given in figure 24 while photographs of the assembly appear in figures 25, 26, and 27.

A detailed report on the HADOPAD receiver is given in reference 7.

4.5 Decision and Firing Circuits

The decision and firing circuit assembly consists of a video amplifier, coincidence circuit, gate generator, d-c amplifier, pulse stretcher, integrator, and firing circuit. These circuits utilize semiconductors throughout and are mounted on an etched circuit board. A drawn aluminum can with mating cover forms an electrical shield for the assembly. A schematic drawing of the decision-firing assembly is shown in figure 28.

The video amplifier (Q301) is used to amplify the receiver output voltage to a level capable of driving the coincidence circuit. This amplifier has a voltage gain of about 13 and a bandpass of about 10 Mc. The amplifier places about 1.3 v peak across the coincidence circuit at firing level.

A blocking oscillator (Q304) serves as a gate generator. This oscillator delivers one pulse each time it is triggered. The trigger pulse originates at the modulator and is derived from the same pulse that triggers the transmitter. The trigger pulse from the modulator is delayed by a lumped-constant delay line (DL301) before application to the blocking oscillator.

An additional delay section (DL302 and DL303) is shunted across the base-to-emitter circuit of the blocking oscillator transistor. This delay section receives the original blocking oscillator turn-on trigger pulse from the modulator (which has a positive polarity), delays it in time, and reflects it back to the transistor with negative polarity causing the transistor to cease conduction. The section is terminated in a short circuit in order to maximize amplitude of the reflected pulse. The blocking oscillator transformer has a natural period of 3 μsec. Consequently if the reflected negative turn-off pulse appears at any time less than 3 μsec after the oscillator is initiated by the original trigger pulse, the reflected pulse will turn off the blocking oscillator. Utilizing this type of circuit allows the output or gate pulse length to be controlled only by the delay line constants and minimizes the effect of changes in the transistor and transformer parameters.

Since the trailing edge of the gate pulse determines the function height of the actuator, changing the length of the gate generator output pulse will result in a change in function height. A switch is incorporated in the actuator to perform this function by switching the delay lines (DL302 and DL303) which supply the turn-off pulses. For the low function altitude (1000 ft), a delay section of 0.4 μsec is used, resulting in a gate length of 0.8 μsec. For the high altitude function (1700 ft), two lines are used (0.4 and 0.6 μsec) resulting in a gate length of 2.0 μsec.

The leading edge of the gate pulses are fixed in time by the 1.6-μsec delay line in series with the modulator trigger pulse, which results in the trailing edges appearing at either 2.4 or 3.6 μsec after the initiation of the modulator pulse. Position of the trailing edges of the gate measured at room temperature on forty units show that for the low function height (1000 ft) the position varies between 2.15 and 2.50 μsec (1057 and 1230 ft) averaging 2.34 μsec (1152 ft). For the upper function (1700 ft), the average position is 3.47 μsec (1708 ft) with a range of 3.32 to 3.72 μsec (1640 to 1830 ft). The spread in equivalent heights is the result of the ±5 percent tolerance in the delay lines. The values are off design center because these lines are procurable only in step values, and also because of an intentional bias toward the upper altitudes to partially compensate for pulse overlap over low reflectivity terrain.

The coincidence circuit consists of two semiconductor diodes (CR303 and CR304) which normally are in a conducting state, connecting two parallel equal voltage sources of positive bias to the base of a transistor (Q302). The polarity of the bias is such as to hold the transistor in a nonconducting state until both of the bias sources are removed. Either bias source alone will maintain the transistor in the nonconductive state. The gate generator output is applied across one diode (CR304) while the video amplifier output is applied across the other (CR303). Both of these outputs are negative and, when present, act to cut the respective diodes off, thus removing the sources of cutoff bias on the transistor. If these sources are removed simultaneously, the transistor will conduct.

A potentiometer (R310) located in the emitter circuit of the transistor controls the sensitivity of the coincidence circuitry. A thermistor (RT301) is also incorporated in the emitter circuit of the coincidence transistor to obtain temperature compensation.

The coincidence circuit is somewhat amplitude sensitive, requiring a varying time overlap that is a function of signal amplitude. Figure 29 is a plot of video amplifier input signal versus time overlap between the echo pulse and the gate pulse. Figure 29 shows a possible 100-ft error in function height between the lowest signal condition and the highest.

The function of the d-c amplifier (Q303) is to raise the power level of the coincidence circuit output by amplification and a small amount of stretching. The d-c amplifier voltage gain is about 18. The load of the preceding stage is a small inductance (L302) which is shunted across the emitter-base circuit of the d-c amplifier. An inductance is used as a load in order to provide leakage current stability (I_{CBO} versus I_C) for the d-c amplifier transistor (Q303). Because of this, the input signal to the d-c amplifier consists of a poorly damped "ring" at a frequency of about 1.0 Mc. The d-c amplifier output is heavily clamped by a semiconductor diode (CR306) in the emitter circuit of the following stage, resulting in a single pulse at this point.

The purpose of the pulse stretcher is to deliver constant-amplitude, constant-energy pulses to the integrator, which is basically a form of counter circuit. In order to count consistently, the energy per pulse must not vary from pulse to pulse. Pulse stretching is accomplished by the use of a four-layer diode (CR305).

The four-layer diode is a switching device consisting of three junctions. The construction of the device is shown in figure 30. Figure 30 also graphically shows the voltage-current characteristic of a four-layer diode. The voltage-current characteristic shows three essential operating regions: I, "off" or high-resistance state; II, transition or negative resistance state; and III, "on" or low-resistance state. The curve is shown on an expanded scale for illustration purposes.

As may be noted when the applied voltage rises and reaches the switching voltage, the device begins to switch "on." The current at this point is typically several microamperes. The device switches because of an internal feedback mechanism allowing the diode to pass a steadily increasing current as the voltage decreases (Region II). When fully "on" (Region III), the four-layer diode passes a current which is limited principally by the external circuit.

In the "on" state, the device has a dynamic resistance of less than a few ohms and a voltage drop of about one volt. As long as sufficient current is passed by the circuit, the device will

remain in the "on" condition. At the point on the curve marked I_h, the circuit is passing just enough current to keep the device in the "on" condition. If the current drops below I_h, the diode switches back to the high resistance or "off" condition.

The four-layer diode (CR305) used in the pulse stretcher circuit is normally in the nonconducting state. This particular four-layer diode has a rated switching voltage of 28 v. In the quiescent state, a positive bias of 18 v is applied to the anode, which is not sufficient to switch the device. However, when a negative polarity pulse is applied across CR306 (the crystal diode in the four-layer diode cathode circuit) by the d-c amplifier, the sum of the quiescent bias voltage (18) and the applied pulse voltage (15) exceeds the switching voltage of the four-layer diode and the device conducts heavily. This connects C306 to ground through approximately 50 ohms, allowing C306 to charge through the crystal diode, CR308. Prior to the switching operation, C306 could not charge because both of its terminals were essentially at the same potential due to the presence of R314. Because of the low charging time constant, C306 charges to nearly 18 v peak.

During the charging process, the voltage developed across CR308 is not sufficient to fully turn on CR307; hence C308 receives only a negligible charge. The pulse-stretching four-layer diode, CR305, remains in conduction for about 50 μsec after application of the turn-on pulse, at which time it returns to the "off" or quiescent state, since the turn-on pulse is no longer present. It is then ready to receive the next turn-on pulse which will occur about 1.2 msec later.

When the four-layer diode (CR305) turns off, C306 no longer charges, and its voltage (about 18) is applied across CR307 and C308. CR307 turns on, and C308 receives charge from C306 through R314 and CR307. Each time C306 discharges into C308, the voltage across C308 increases in proportion to the amount of charge delivered (initially at the rate of about 0.25 v per discharge) resulting in an exponential "staircase." During this time, the voltage across C308 is in series with the voltage across C307 (about 18 v). At the end of about 70 such charge cycles, the sum of the voltages (about 28 v) across C308 and C307 is sufficient to drive the four-layer diode CR309 into a state of conduction. When CR309 conducts, it discharges the series combination of C307 and C308 into the bellows squib, initiating main chute action. The number of pulses integrated is adjusted by the value of R315 which establishes the leakage rate of C308.

The requirement imposed by the coincidence circuit of time coincidence and the requirement of periodicity imposed by

the integrator afford good protection against both internal and external disturbances. The system requires about 290-mv peak-to-peak wideband noise to cause a function on the high altitude (1700 ft) gate and about 100 mv for the low altitude (1000 ft) gate.

The firing circuit will deliver a minimum of 20,000 ergs into a 5-ohm load. An inductance (L303) is inserted in series with the firing output terminal to prevent damage to the four-layer diode (CR309) in the event a short circuit is placed across the output terminal.

The decision-firing subassembly requires 23 v at 10 ma for operation. The d-c amplifier, pulse stretcher, integrator, and firing-circuit supply voltages are regulated by an 18-v Zener diode (VR301) and filtered by C307. A 0.1-mfd capacitor (C309) was found necessary to remove the effects of gate generator reaction on the supply line. Without C309, this reaction appears in the receiver output as a spurious pulse coinciding with the gate generator turn-on.

A more complete explanation of the operation of the decision and firing circuit along with pertinent detailed data appears in reference 8. As noted in reference 8, the operation of the firing circuit is somewhat marginal because of the temperature coefficient of the Zener diode (VR301). The temperature coefficient, when coupled with its tolerance, lowers the reference 18 v by a matter of about 1.5 v at low temperature resulting in a marginal firing condition. This temperature sensitivity is partially compensated by CR315. An alternate circuit which has not been fully tested is shown in reference 8. This circuit, which is simpler than the present circuit, does not depend on a Zener diode reference, and consequently its temperature sensitivity should be improved.

The decision and firing assemblies used in the present actuator are not potted. In the event of future production, foam potting can be utilized.

Figure 31 is a photograph of the decision and firing assembly. Figure 32 shows the waveforms at various points in the circuit.

4.6 DC-DC Converter

Power for the HADOPAD radar actuator is supplied by a transistorized dc-dc converter which supplies outputs of +190, +23, and +125 v. The heater circuit (-1.30 v) is supplied through

a dropping resistor connected across the output of a transistorized regulating circuit packaged as part of the converter assembly. The primary circuit of the converter is also supplied by the regulator output. The power source for the converter assembly is a 6- to 8-v thermal supply which is activated by a striker mechanism released when the cargo is ejected from the aircraft.

The converter is packaged within a cylindrical steel can 3 in. in diameter x 3 3/4 in. in length. Components are mounted on four circular etched boards. The present converter was not potted, but a future design can be potted.

A schematic diagram of the dc-dc converter is given in figure 33. A photograph of the converter is shown as figure 34. Reference 9 details the basic design of a preliminary model of the converter.

The converter assembly consists of two sections, a regulator circuit and the conversion circuit.

The regulator circuit consists of transistors Q403, Q404, and Q405. Q403 is the series-controlled transistor which is driven by an emitter follower Q404. The regulating transistor Q405 utilizes the Zener diode CR418 for a voltage reference. Power for the regulator is obtained from the secondary (terminals 13 and 14) circuit of transformer T401. This source of power is regulated by the semiconductor diode CR417. The regulator delivers a nominal 5.5 v.

Heater power for the tubes is obtained through the parallel dropping resistors R408 and R410 which are connected to the regulator output. Additional shunt-padding terminals are mounted on the lid of the can for final adjustment of the heater voltage to 1.30 v with the actuator as a load. Resistor R411 is selected and inserted at that time.

The switching function in the converter section is performed by Q401 and Q402, which switch the regulated voltage at nominal rate of 1250 times per second. Transformer T404 steps up the resulting voltage to obtain the higher voltage outputs. Each circuit utilizes a semiconductor bridge for rectification. Filtering is supplied by shunt capacitance across the output terminals.

The nominal output terminal voltage and currents that may be obtained from the converter are as follows:

Voltage (v)	Current (Ma)
-1.30	900
+23	40
+125	30
+190	4.5

The input current at 7.5 v averages 2.27 amp (17 w).

It was found necessary to adjust the individual regulator circuits to maintain the tolerance on the 23-v circuit. Two external terminals were provided on the lid of the housing for the addition of the shunt-padding resistor R412. This resistor is in parallel with internal R407. Selection of R412 was made using the radar actuator as a load during final test. The value of R412 was chosen to obtain 23 ± 0.25 v at the output terminals.

Forty of these converter assemblies were fabricated by a local manufacturer. Data obtained on 35 of these units working into dummy loads at HDL are summarized below.

Parameter	Ave	Max	Min
Output Terminal Volt at 7.5-v Input			
190-v circuit	194	211	189
125-v circuit	129	140	124
23-v circuit	23.3	23.5	23.0
Output Ripple Voltage (pk-pk)			
190-v circuit	1.10	2.9	0.5
125-v circuit	0.90	2.0	0.5
23-v circuit	0.25	0.70	0.15
Regulator Output Term Volt at:			
6.5-v Input	5.33	5.80	5.00
8.0-v Input	5.40	6.10	5.05
1.30-v Circuit Output Term Volt at:			
6.5-v Input	1.36	1.47	1.29
8.0-v Input	1.37	1.55	1.30
Input Current (amp) at 7.5 v	2.27	2.50	2.10
Heater Shunt Padding Resistor (ohms)	16.2	36.0	0
Regulator Shunt Padding Resistor (ohms)	1037	3600	0

The values of the padding resistors were determined by substitution of a variable resistance. The final resistor inserted was fixed-composition resistor to the nearest 5 percent value. The heater voltages tabulated in the above summary were without the final padding resistor (R411) in place.

As the result of data taken with both actuator and dummy loads, it appears that more work is necessary on the dc-dc converter before completely satisfactory operation can be obtained. Better filtering on all circuits is desirable and speed-up capacitors should be added to the switching circuitry since the switching speed of the 2N1546 transistors is marginal. The use of a Zener diode CR418 as a voltage reference necessitates individual padding of the regulating circuit and matching the converter to the radar actuator.

4.7 Thermal Time Delay

A thermal time delay is utilized to prevent the radar from functioning prematurely on the dropping aircraft. With the present antenna, it appears that the separation between cargo and aircraft must be a minimum of 1600 ft before closure of the output circuit to the bellows squib, or that alternatively, the reflected signal from the aircraft must be outside the gate interval of the actuator (ref 6). A time delay of 12.0 sec appears to satisfy both alternatives.

The delay is a commercial device which is placed in series with the output firing circuit. It is energized upon cargo ejection by the thermal power supply and maintains an open output circuit for 12 sec. The delay is adjustable over a range of 8 to 12 sec. The original factory setting for these thermal time delay devices was 8 sec at 7.5 v. Subsequent field testing showed that this time delay was inadequate under certain conditions. Consequently all delays have been reset to 12 sec.

Data taken on 40 of these thermal delays as received from the factory are summarized below. Test number 1 checks the factory accuracy of setting at rated voltage, tests 2 and 3 at high and low voltage. Tests 4 and 5 check temperature sensitivity, while 6 and 7 give an indication of consistency. A manually operated clock was used in the tests.

It was necessary to discard two delays, one for erratic operation at low temperature and the other because of a consistently low time delay. Three timers were outside the ±10 percent factory setting limits (7.2 to 8.8 sec) as received on test No. 1. The times obtained on the three were 6.86, 7.10,

and 9.07 sec. It can be seen that the major factor in the accuracy of operation of these delays is voltage variation. Very little temperature effect was noted.

SUMMARY OF TEST RESULTS

Test No.	Applied Voltage (v)	Temperature	Heater Current (ma)	Time (sec) Ave	Max	Min
1	7.5	Room	490	7.95	9.07	7.10
2	8.0	Room	520	6.94	7.55	6.56
3	6.5	Room	420	10.98	11.59	10.38
4	6.5	-65°F	425	11.07	13.28	10.10
5	8.0	+165°F	520	6.96	7.56	6.48
6	7.5	Room (Test 5+16 hr)	490	7.84	8.25	7.39
7	7.5	Room (Test 5+17 hr)	490	7.91	8.46	7.50

Total spread in all tests: 6.48 to 13.28 sec = 8.0 sec $^{-19.0\%}_{+66.0\%}$

4.8 Housing

The radar actuator is packaged inside a rectangular aluminum box approximately 18 x 4 x 10 in. The cavity antenna is fastened to the outside of this box and is fed from inside by an RF cable. The individual subassemblies are supported on shelves or in a tube and can be removed from the main box for repair or adjustment. Figure 35 shows a view of the main housing with the various fasteners and end covers.

4.9 Battery Striker Mechanism

The thermal supply is initiated by a striker mechanism (fig. 36) which is actuated by deployment of the drogue parachute. The drogue parachute drag pulls the striker mechanism locking pin, until the hammer shaft is disengaged, which results in the delivery of a sharp blow to the thermal power supply primer initiating the battery. The flexible pull wire and the locking pin are designed so that release can be achieved regardless of angle of pull; i.e., the flexible pull wire is omnidirectional. The striker mechanism is resettable.

4.10 Parachute Release Mechanism

The parachute release mechanism (fig. 37) is used to hold the drogue parachute harness securely until a firing pulse is received from the radar actuator. The firing pulse actuates the release mechanism releasing the drogue parachute harness,

which in turn pulls the canopy cover from the main parachute resulting in the deployment of the main parachute. The firing pulse from the radar actuator initiates a bellows-type squib which exerts a 70-lb load against the release shaft lever. As the lever is pushed by the bellows squib, the cut-away section moves into position and the drogue parachute harness is released. The mechanism is designed to use two bellows squibs for improved reliability, but one squib has more than enough energy to actuate the release mechanism.

5. SYSTEM EVALUATION

5.1 Basic Sensitivity Calculations

The design sensitivity of the radar actuator is a function of electrical characteristics of the terrain and of the dropping aircraft. The radar must be sensitive enough to operate over low reflectivity terrain but must be insensitive to reflected signal from the aircraft. Directional sensitivity is controlled by the antenna pattern which should direct maximum illumination toward the ground and the minimum toward the aircraft.

In the design of the radar actuator, it was assumed that the power reflectivity of the worst terrain is .01 and that the terrain constitutes a diffuse-type reflector. It was also assumed that the radar is pulse width limited, i.e., no usable return power will be obtained from the terrain outside an area restricted by the width of the pulse.

A diffuse-type terrain was assumed since this is the worst type of characteristic in this application where the actuator approaches the terrain near vertical incidence. A vertical approach allows the utilization of the maximum antenna gain in the calculations. Vertical incidence also maximizes the specular component. The specular component is a function of D^{-2} (D = distance) while diffuse return is a function of D^{-3}. It is known that at this frequency, a fair percentage of the return is specular on the average, but no definite percentage can be assigned. In all probability, the distance function lies between D^{-2} and D^{-3}.

The pulse width limiting concept can be derived from the geometry presented in figure 38, where D is distance from the actuator to the terrain. The C is a constant representing the velocity of electromagnetic radiation (984 ft/μsec), and T is the width of the transmitted pulse in microseconds. Multiplication of the factors CT results in a product with the dimensions of distance.

In figure 38, the factor CT/2 represents the maximum distance that can be traversed during the pulse duration. Obviously the ground can be illuminated only during the duration of the transmitted pulse. The intercept point of the scalar D at the terrain represents the coincidence of the leading edge of the transmitted pulse with the terrain, and D+ CT/2, the intercept of the trailing edge. The area of intercept for the case of vertical incidence is circular, and is elliptical at angles off the vertical.

In the case of HADOPAD, it may be assumed that the intercept area is close to circular, because the region of operation is near vertical incidence. From considerations shown in figure 38, the intercepted area can be computed as approximately 660,000 sq ft for an altitude of 1700 ft and 442,000 sq ft at 1000 ft. The equivalent radii are 458 ft and 378 ft, respectively.

The equation used in computing the required sensitivity of the HADOPAD radar is given below. This is the standard radar equation modified to account for a diffuse reflecting surface and pulse width limiting.

$$\frac{Pr}{Pt} = \frac{G^2(4CTD + C^2T^2)\ K\ \lambda^2}{128\ \pi^2\ D^4}$$

where

Pr = Power received (w)
Pt = Power transmitted (w)
G = Antenna Gain (same antenna used for transmission and reception = 0 db)
C = 984 x 10^6 ft/sec (velocity of electromagnetic radiation)
T = 0.14 x 10^{-6} sec (transmitted pulse width)
K = .01 (power reflection coefficient of terrain)
λ = 2.34 ft (wavelength of transmission, frequency = 420 Mc)
D = Altitude above terrain
π = 3.14

The factor C^2T^2 becomes of decreasing significance with increasing altitude. Neglecting this factor results in less than a 5-percent error at 500 ft and less than 2.5-percent at 1000 ft. This allows simplification of the above formula to

$$\frac{Pr}{Pt} = \frac{G^2\ K C T\ \lambda^2}{32\ \pi^2\ D^3} \text{ or } \frac{Pr}{Pt}\ (db) = 10 \log \frac{G^2\ K\ CT\ \lambda^2}{32\ \pi^2\ D^3}$$

This relationship is plotted as db path attenuation for altitudes from 600 through 1800 ft in figure 39. Also plotted in figure 39 is the path attenuation for a specular reflector

$$\frac{Pt}{Pr}\ (db) = (20 \log \frac{2D}{\lambda}) + 22 + 10 \log K - 20 \log G$$

(This formula was derived from the FRIIS Transmission formula first published in the May 1946 issue of the Proceedings of the Institute of Radio Engineers, p 254.) All parameters are in db, and the same constants are used as in the preceding formula for the diffuse pulse-limited case. In order to work with the bare path attenuation, these plots assume an antenna gain of 1.0 (0 db). Actual antenna gain was considered as part of the actuator circuitry.

Reference to figure 39 shows that the required path attenuation in the worst case for 1700-ft operation is 113 db, and 106 db for the 1000-ft function.

5.2 Laboratory Tests

Laboratory tests on the overall actuator were conducted in two phases, preliminary and final. The preliminary tests were conducted with all subassemblies interconnected. Heater and regulator pads were installed on the converter as described in section 4.6, and the coupler characteristics were measured as described in section 4.2. The time delay relay was checked for operation, and a preliminary measurement of path attenuation was made after final tuning adjustments. The purpose of this preliminary testing was to verify proper operation before final assembly into the housing. Final tuning adjustments consisted of tuning the local oscillator to frequency, adjusting the receiver input tuning, and setting the output coupling condition on the transmitter.

The local oscillator tuning slug was adjusted to maximize the echo pulse at the receiver output. The transmitter output coupling and the receiver input tuning adjustments were set to maximize the received echo while simultaneously minimizing spurious responses on the receiver output base line adjacent to the main bang. Because of some interaction between these last two adjustments, the process was repeated at least two or three times. Both adjustments are noncritical and were terminated at the midpoint of desired response range. Tuning and the preliminary path attenuation measurements were made using a delay cable equal to 780 electrical feet.

A block diagram showing the necessary test equipment and interconnections for final and preliminary testing of the

actuator is shown in figure 40. Two reels of RG8A/U cable comprise the delay section and are operated with open ends for convenience. The cable propagation constant as measured at HDL at 420 Mc is 0.64. The physical cable lengths are 500 and 200 ft. The round trip delay times measured at 420 Mc are 1.59 and 0.65 μsec, respectively, resulting in a total usable delay of 2.24 μsec. Two-way attenuation was measured as 45 and 20 db, respectively.

The longer line (780 electrical feet) was used during the tune-up process and in checking the low altitude gating function. Both lines coupled together (1100 electrical feet) result in a reflected echo pulse which is outside the low altitude gate but well inside the high altitude gate. Hence, both lines are used to check the high altitude gate function.

The balance of the equipment depicted in figure 40 consists of commercial items which are easily specified and procured except for the firing indicator which was constructed at HDL. A schematic of this device is given in figure 41.

The final test of the actuator was conducted with the actuator completely assembled in its housing with antenna in place, but not connected. The test was conducted as described below.

The actuator was set up on the test bench with the coupler antenna terminal connected to the 780-ft delay cable with its far end open. The function selector was set to "L" (low). The scope was connected to the receiver output test point, and the firing indicator to the actuator output connector. The converter in the actuator was energized with a 7.5-v, 3-amp power supply.

The receiver output was monitored, and the variable attenuator in series with the delay cables was adjusted so that the receiver output pulse was 100 mv. The decision-firing circuit gain control was then adjusted to set the firing threshold at this input level, as indicated by the firing indicator. The variable attenuator setting was recorded. The sum of the variable attenuator reading in db plus the fixed attenuator (10 db) plus the cable attenuation (22.5 db) multiplied by two was then recorded as the path attenuation at 780 ft.

The free end of the 780-ft length was then attached to a free end of the 320-ft cable, and the function selector set to "H" (high). The other end of the 320-ft cable was left

open. The variable attenuator setting was reduced until the firing level was again reached, and its setting was recorded. The summation of the cable attenuation (32.5 db) and the two attenuator values again multiplied by two was then recorded as the path attenuation at 1100 ft.

The 320-ft cable was then disconnected from the 780-ft length, and the actuator was deenergized. The variable attenuator was set for zero attenuation and the fuze reenergized while monitoring the firing indicator. This test was to insure that the actuator would fire on an overload signal. The variable attenuator was then set at maximum (25 db), and the peak-to-peak noise level in the region of 4.0 μsec (following initiation of the transmitted pulse) was recorded.

The following photographic data were also taken in the course of the final test:

(1) Receiver output
(2) Decision/firing circuit coincidence mixer test point ("AND" gate test point on schematic diagram)
(3) Integrator test point in decision/firing circuit
(4) Transmitted spectrum
(5) Modulator pulse at the modulator-pulse test point
(6) Detected transmitted pulse
(7) Fire pulse out of the actuator output connector

Figures 42, 43, and 44 show typical photographic data. The spectrum was photographed by connecting the spectrum analyzer to the far end of the 780-ft delay cable thus interposing the line attenuation between the spectrum analyzer and the transmitter, providing a well-shielded system against outside interference. Simultaneously, a marker generator was connected to the spectrum analyzer input. The marker was used to determine the transmitter center frequency and also to provide a calibration line on the photo. Another calibration line was provided by utilizing the internal marker from the spectrum analyzer.

The detected transmitted pulse was also taken through the 780-ft delay line with the detector placed at the free end. The detector output was connected to the scope vertical amplifier.

Since the local oscillator is not intentionally decoupled from the antenna, changes in the antenna loading reflect directly into the local oscillator. The initial local oscillator design showed a tendency to squegg under certain conditions of loading (ref 7); a test for squegging was included in the final tests. The test consisted of connecting a 50-cm adjustable stub to the

antenna terminal of the coupler. The stub was slowly pulled through its entire range while the receiver output was monitored by the oscilloscope. Indication of a squegg condition was the appearance of multiple echo pulses on the base line. Following alteration in the value of the local oscillator grid leak resistance, none of the local oscillators have been found to squegg.

After final testing of the actuator in the laboratory, it was taken to the roof of the building. The actuator was energized with a scope connected to the receiver output. The actuator was then positioned to illuminate the surrounding terrain through its own antenna. The receiver output was examined for close-in recovery, and the peak-to-peak noise at 4.0 μsec was recorded as well as the return amplitude at 3.0 μsec (1500 ft). Lack of close-in recovery as indicated by the absence of target signals below about 2.5 μsec indicates local oscillator squegging.

Data recorded during final testing of 35 actuators are summarized below.

	Ave	Max	Min
Transmitter center frequency (Mc)	442.9	428	419
Path attenuation, 780-ft cable (db)	109.9	117	105
Path attenuation, 1100-ft cable (db)	111.5	117	107
Peak-to-peak noise, 4-μsec in lab (mv)	20.4	40	10
Peak-to-peak noise, 4-μsec on roof (mv)	31.0	80	10
Echo amplitude, 3-μsec on roof (mv)	690	1000	600

Examination of the detailed data showed that on the 1100-ft cable length, one unit had a path attenuation of 107 db, and six units were at 109 db. On the shorter cable (780 ft), two units were 105 db, two were 107 db, and five were 108 db.

With an antenna gain of 2 db one way, one unit therefore, was 2 db lower than the required sensitivity for 1700-ft operation. The required path attenuation for this altitude was calculated at 113 db. This unit was the only unit deficient in sensitivity at either of the two function altitudes.

5.3 Field Tests

The first test of the prototype of the present actuator design on the two-stage parachute system was made at Maynard, Mass. on 27 June 1963. Previous testing was performed at the HDL Test Area.

The preliminary testing at Blossom Point utilized a single stage system with flash bulb function indication, since the recovery parachute was opened immediately upon ejection by a static line. The suspended actuator descended at a rate of 20 fps, firing the flash bulbs at the function altitude. The drop aircraft was an H21 helicopter. An electrical time delay of about 8 sec was incorporated in these actuators to obtain clearance between the drop aircraft and the actuators. The clearance between actuator and the aircraft was calculated at about 650 ft at the end of the delay interval.

Two prototype actuators utilizing cavity antennas were dropped at Blossom Point on 19 June 1963 from 2000 ft. One fuze did not operate while the other functioned at 930 ft (theodolite data). The fuze that failed to operate was recovered and found to have an open coupling capacitor at the receiver output.

At the request of the U.S. Army Natick Laboratories, three prototype actuators were dropped on two-stage systems at Maynard, Mass. on 27 June 1963. The systems were rigged to pallets carrying 200-lb dummy cargoes. The pallets were dropped from a C119 aircraft at 130 knots from 2000 ft. No instrumentation was available for height determination, but motion picture coverage was available. The prototypes were representative of the final design except the power was supplied from dry batteries instead of the dc-dc converter and thermal battery. A mechanical timer supplied a 3-sec time delay for clearance from the aircraft. Manual switching before ejection was utilized to energize the actuators.

Two of the three actuators dropped at Maynard appeared to operate properly while the third functioned early at about 4 sec after release.

The three actuators were returned to HDL. Except for attachment of flash bulb function indicators, the actuators were not altered or adjusted at HDL. The actuators were dropped on single stage systems at Blossom Point under instrumented conditions from a H21 helicopter at 2000 ft. The results were identical with those obtained at Maynard; the same actuator functioned early again. Function heights were obtained on the two proper functions: 1003 and 923 ft.

The cause of the early function was carefully investigated. The presence of a metal drill chip shorting the coincidence test point on the decision-firing assembly was ascertained as the cause of malfunction.

After delivery of thirty-five units to Natick Laboratories by HDL, field testing was resumed in March 1964 at Fort Devens, Mass (ref 6 and 10).

All drops made during the Fort Devens test utilized the two-stage parachute rigging. Two standard simulated cargoes (2200 and 500 lb) were mounted on plywood pallets. The 2200-lb cargo consisted of four 55-gal drums which were filled with water. The lighter cargo (500 lb) was a rectangular cardboard container ballasted with iron ingots. Figures 45 and 46 are photographs of the type of loads dropped. All drops were from a C119 aircraft at 130 knots.

When possible, the actuators were tested before and after drop using the 780-ft delay cables, similar to the test setup shown in figure 40. In the case of the field tests, however, only the scope was used in conjunction with the delay line system.

The first five actuators dropped at Fort Devens resulted in two proper functions, two early functions, and one dud. These actuators utilized an 8-sec time delay. Both early functions were on the 2200-lb loads. The balance were 500-lb loads.. The cause of the early functions was postulated to be reflections from the dropping aircraft. Ballistic data showed that the separation between aircraft and actuator was about 1100 ft for the lighter loads and about 1000 ft for the 2200-lb loads. Thus the echo signal would be outside the gate on the light loads, but inside the gate for the heavy loads at 8 sec.

Calculations based on measurement of actual signal return from a C119 aircraft showed that it was possible to trigger the fuze on aircraft reflections at separation distances up to about 1500 ft (ref 6). Calculations also showed that a minimum time delay of about 11 sec was necessary. It was therefore recommended that the minimum time delay for the heavy loads be set at 12 sec. Calculations also showed that the 8-sec delay was marginal for the light loads.

As the result of this analysis, all HADOPAD actuators dropped after June of 1964 utilized 12-sec arming delays on all loads.

A definite cause for the dud encountered in the first drop test could never be determined. The actuator, although damaged when recovered, still functioned properly in laboratory tests. The only component which could not be checked was the time delay relay which was damaged beyond repair. From the relative position

of the actuator to its socket and the nature of the damage to the socket, it was postulated that the socket had separated from the time delay during fall resulting in the dud condition. To prevent recurrence, all relay sockets were secured to the relay with No. 22 copper wire.

In two tests on 10 April and 23 April 1964, no failures were encountered in the radar actuator, but one mechanical parachute release opened prematurely (ref 6). As a result of the premature opening, the mechanical releases were modified to include a hood and a stronger release spring.

Two more drop tests were performed in May 1964 (ref 10). No radar malfunctions were encountered, but one thermal battery failed to initiate, resulting in a dud. Upon recovery, it was noted that the mechanical battery striker had indented the primer case, but the primer had failed to initiate. In the laboratory, it was possible to initiate the battery when the primer was struck sharply with a hammer. It was concluded that the primer was insensitive. Future battery procurement for this application must include more rigid inspection of the primers.

One test was performed in June 1964 at Fort Devens (ref 10). In this test, an early function was encountered on a 500-lb drop. In view of the use of an 8-sec time delay, and the results of calculations made previously which showed that the 8-sec time delay was marginal, this result was not unexpected. Laboratory tests of the recovered actuator showed no other reason for the early function.

The final drop test of this series made in 1964 was a test of a modified actuator at the HDL facility at Blossom Point, Md on 18 June 1964 (ref 11). This test was fully instrumented with theodolites.

The modification to the fuze consisted of changing the lower function option from 1000 to 800 ft. Mechanics of the change are described in reference 11. Laboratory measurements predicted a height of 830 ft; field measurements indicated a height of 809 ft.

The method used in modifying the low option resulted in an equivalent height reduction at the high option. Calculated height for the high option was 1390 ft.

A summary of the test drops at Fort Devens during the year of 1964 is given in table 1. More detailed information concerning all drop tests during 1964 is given in references 6, 10 and 11.

5.4 Environmental Tests

Because of expediency, no environmental testing of any significance was performed on these actuators as complete units. Temperature compensation of both the receiver and the decision and firing circuitry was installed during subassembly testing but there is no positive knowledge as to the overall performance as a complete unit.

5.5 Field Test Set

Equipment necessary for a quick go, no-go test of the actuator just prior to drop consists of five items: (1) reel of coaxial cable, (2) fixed attenuator, (3) variable attenuator, (4) power supply, and (5) firing indicator. This equipment may be identical to that used in laboratory tests described in section 5.2. This type of check-out was used with good results during the field testing program at Fort Devens.

The reel of cable consists of a continuous 500-ft piece of RG8A/U coaxial cable. The cable is terminated in type N connectors at both ends. The cable is used with one end open to obtain the reflection. The equivalent electrical length is 780 ft.

The fixed and variable attenuators are used to increase the cable attenuation to a usable level. These are chosen so that the combination permits a variation in total attenuation (cable + fixed attenuator + variable attenuator) between 100 and 120 db. For field testing, using the 500-ft cable length, a fixed attenuator of 20 db and a variable attenuator of 0 to 15 db may be used. This allows a variation in attenuation between 85 and 115 db, assuming a two-way cable loss of 45 db.

The power supply used for actuator testing should be capable of supplying about 3 amp at any voltage between 6.5 and 8.5 v dc, preferably about 7.5 v. This supply need not be well-regulated as long as the terminal voltage remains within the above limits. This supply could take the form of an ordinary low-voltage high-current power supply utilizing AC from the power line. Twelve-volt automobile or 28-v aircraft storage batteries could be used where AC power is not available by tapping across four of the cells.

The firing indicator is a semiconductor switching circuit which drives an indicator lamp. A schematic diagram of the circuit is shown as figure 41.

The cost of such a go, no-go test set should be less than $350 at current prices. This includes the low-voltage high-current power supply. Figure 47 shows a block diagram of a proposed go, no-go preflight test set.

6. CONCLUSIONS AND RECOMMENDATIONS

In the course of testing the HADOPAD actuator in both field and laboratory, certain undesirable features of the present design were noted. Also it was felt desirable to include other features not now in the design. The actuator in its present form is an engineering model which is capable of expansion into a production model with a minimum of effort. The modular type of construction permits a reasonable amount of circuit redesign or adjustment without interaction with other subassemblies. Recommended changes are listed below under subassembly headings.

6.1 Modulator/Transmitter

The chief deficiency of the modulator/transmitter subassembly lies in the limited life of the transmitting tube. The 2-sec warmup requirement dictated the use of filamentary tube. The extraction of high power pulses from a filament type cathode necessarily results in limited tube life. Indirectly heated cathode-type tubes usually require a minimum of 15 sec to warm up. Since the initiation of the HADOPAD project, fast-warmup indirectly heated cathode-type tubes have become available. These tubes are of the ceramic-type and have a warmup time of 3 sec. These tubes currently cost about $40 each, and are designed for pulse circuitry. Peak pulse power of some 250 w is obtainable from the smaller versions. These tubes will operate up to about 1800 Mc.

The use of a ceramic tube in the HADOPAD transmitter would greatly extend the useful life of the device for training purposes. The present radar has more than adequate life for its projected use, but appears to have a five- to seven-drop potential in training drops. However, in production where test time can be minimized, the device may have adequate life for ten drops.

A simple means of tuning the transmitter to frequency would also be desirable. The gate trigger pulse should be shortened and shaped to reduce trail-off. The modulator portion of the subassembly should be potted in place.

6.2 Hybrid Coupler

With the present circuitry, the losses encountered in the coupler when installed as part of the radar system under certain conditions are not tolerable. Two-way losses as high as 10 db were encountered. Institution of more rigid inspection should minimize the spread in operational quality. However, some of the high loss encountered must be ascribed to the lack of proper termination at the various ports. The receiver, for example, has a nominal input impedance of 10 ohms during reception. Although the power output of the transmitter is maximized into a 50-ohm load, the variation of its output impedance during the pulse may be such as to generate undesirable reflections.

6.3 Antenna

The present antenna is deficient in bandwidth, tends to radiate too much energy toward the dropping aircraft, and possesses a very wide downward beam. Increasing the diameter of the feed and tuning posts may overcome the bandwidth deficiency thus obviating the need for tuning each unit individually to the transmission frequency.

Since it is desirable to utilize an antenna which requires no maintenance, and this antenna appears to be the best compromise in this direction, little can be done to control the pattern, except by increasing frequency.

The antenna covers, which are presently cemented to the lips of the cavity, tend to loosen under stress. The covers should be screwed to appropriate blocks inside the cavity and the cement should be used as a sealant only. A final antenna design should include a potted cavity for increased rigidity. Lightweight foam can be used.

6.4 Receiver

The receiver can be improved in several respects. The principal deficiency is the front end. The local oscillator, which was altered because of the tendency to squegg under certain conditions of antenna loading, should be redesigned for lower plate-current drain. Lowering the value of the grid bias resistor in order to eliminate the squegg resulted in a plate current in excess of the tube rating. The plate voltage on the local oscillator should be reduced. The receiver input impedance should be raised from the present nominal 10 ohms to 50 ohms.

Some investigation should also be made into the variation of noise output from actuator to actuator. At present, the variation is about 2 to 1. Control of this parameter could result in a system sensitivity increase of about 3 db.

Installation of fast-switching back-to-back diodes across certain of the i-f resonant circuits should be considered to obtain a more consistent recovery characteristic. Such diodes are now available.

The emitter-follower output impedance should be readjusted for a closer match to the video load. Some work must be performed on the temperature-compensating circuitry which is not completely satisfactory.

Portions of the receiver that can be potted should be potted, particularly the lower half, which mounts the larger components. Lightweight foam would be satisfactory.

6.5 Decision and Firing Circuits

The major shortcoming of the decision and firing subassembly lies in the dependence on a Zener diode for a stable voltage reference. In some cases, this diode must be selected. Steps for correcting this deficiency are outlined in reference 8, wherein a simpler and probably more reliable circuit is presented.

Adjustment of the delay line tolerance in the gating circuit must await the result of field testing. At the present time, it is felt that the tolerance should be tighter, but this is based on very limited field test data.

The decision and firing subassembly should also be foam-potted.

6.6 DC-DC Converter

It is desirable to increase the output filtering of the converter to reduce ripple voltage. Speedup capacitors should be incorporated in the switching circuits to overcome the marginal switching characteristics of the 2N1546 transistors. Alternatively, faster switching transistors should be installed.

The use of a Zener diode as a voltage reference in the regulating circuit forces individual padding of each unit. It would be desirable to eliminate this condition.

Redesign of the present regulating circuit to increase the power capability would permit operation of the thermal time delay relay from a regulated voltage source and thus minimize the relatively wide variation in time that is now encountered.

The converter should be potted, preferably in epoxy, for better heat dissipation.

6.7 Thermal Time Delay

The utilization of a thermal type delay requires no field maintenance in training drops because it automatically resets.

The present thermal delay is sensitive to voltage, but not to temperature. A voltage regulated supply for the delay heater would be desirable, as discussed in section 6.6.

For more accurate timing, a mechanical timer would be superior to the present thermal delay with the unregulated power source. This would require resetting after each use.

A better mechanical mounting system for this component and its associated wiring should be considered in view of field performance (ref 6).

6.8 Housing

Some effort should be expended in improvement of the mounting of the various subassemblies within the housing. Some of the mounting screws are relatively inaccessible, causing great difficulty in final assembly. Sharp edges on the threaded mounting ears should be broken.

6.9 Battery Striker

In view of the results of the preliminary field testing at Fort Devens wherein one battery primer failed to initiate, the spring pressure and the striker travel should be increased. The present striker delivers the specified force to the primer, but some primers require more than the specification force to initiate. This was observed in the laboratory as well as in the field.

6.10 Parachute Release Mechanism

Because of the premature function encountered at Fort Devens on 10 April 1964, all moving parts of the release mechanism

should be hooded, and the spring tension should be increased. It was postulated that one or more of the suspension lines had tripped the main chute release rod during the drogue-chute initiation period.

6.11 System Sensitivity

The sensitivity of the system, as calculated, appears to be adequate to function over a diffuse type of reflector with a power reflection coefficient of .01 under pulse-limited condition. Verification of the calculations can be accomplished only by actual drops over low reflectivity terrain.

During the course of verification testing in the field, the sensitivity margin should be determined by insertion of fixed attenuators in the antenna line until a dud or very low-function condition is observed.

6.12 Field Testing

Field testing of these actuators has been very limited in scope. Tests at Fort Devens have yielded no height data and were largely qualitative as far as the actuator is concerned. The only instrumented data were those taken at Blossom Point, Md. These data are so sparse that no definite conclusions can be made.

Instrumented tests should be performed on these actuators as discussed in section 6.11 in order to provide data as to reliability and life as well as to supply delay line tolerance information.

6.13 Environmental Tests

No environmental testing of any consequence has been performed on the present complete actuator. Such testing must be initiated before any design changes can be made in order to locate the present weak points. These tests should include:

(1) Temperature Testing (Operation at the temperature extremes in conjunction with high- and low-voltage inputs.)
(2) Temperature Cycling (Nonoperational during cycling. Operation required before and after.)
(3) Vibration (Operation during vibration cycle.)
(4) Transportation Vibration (Actuator in shipping container. Nonoperational during vibration. Operation required before and after.)
(5) Drop Test (Actuator strapped on side of simulated cargo and subjected to twice the landing force expected

during actual drop. Operation required before and after drop.)

(6) Humidity Cycle (Operation required before and after cycle.)

Acknowledgments

The authors wish to acknowledge the efforts displayed by two HDL personnel in the design of the antenna and hybrid coupler. Mr. W. G. Heinard designed the antenna and Mr. H. Bruns the hybrid coupler.

7. REFERENCES

(1) "The HADOPAD Modulator," M. Miner and M. L. Wiseman, HDL Report No. R410-64-10, 8 June 1964.

(2) "HADOPAD Transmitter Development," J. J. Roach, HDL Report No. R410-64-11, 7 Nov 1964.

(3) "Characteristics of a Lumped Circuit Hybrid Ring in the VHF Region," Henry Bruns, Diamond Ordnance Fuze Laboratories Report No. TM-61-23, 5 May 1961.

(4) Radio Engineering Handbook by Keith Henny, Fourth Edition, 1959, chap 5, para 42.

(5) "Very High Frequency Techniques," RRL Staff, Vol I, chapter 7.

(6) "HADOPAD Field Tests at Fort Devens, Mass.," J. J. Roach, HDL Report R410-64-1, 20 May 1964.

(7) "A Radar Receiver for the HADOPAD System," A. J. Betag, M. L. Wiseman and J. J. Roach, HDL Report No. R410-64-12, 15 Nov 1964.

(8) "HADOPAD Decision and Firing Circuit," M. Miner, HDL Report No. R410-64-3, 1 Sept 1964.

(9) "Transistorized Regulator-Converter Power Supply for a High Altitude Delayed Action Parachute Actuator Device," Floyd Allen and H. J. Reed, HDL Report No. R940-63-13.

(10) "HADOPAD Field Tests at Fort Devens, Mass., May-June 1964," M. Miner, HDL Report R410-64-4.

(11) "HADOPAD Function Height Modifications," M. Miner, HDL Report No. R410-64-2, 17 Aug 1964.

BLANK PAGE

TABLE I. SUMMARY OF HADOPAD FIELD TESTS—1964—FORT DEVENS

Date 1964	Drop Order	Actuator S.N.	Load (lb)	Time Delay (sec)	Release Alt (ft)	Option (ft)	Results	Probable Cause Of Malfunction
13 Mar	1	52	300	8	3800	1000	OK	
	2	56	500	8	3800	1000	DUD -- Transmission heard	Time delay relay
	3	53	500	8	3800	1000	OK	
	4	55	2200	8	4800	1700	Early -- 8 sec after release	Aircraft reflections
	5	54	2200	8	4800	1700	Early -- 8 sec after release	Aircraft reflections
10 Apr	1	55	2200	12	4500	1000	Main chute opened at ejection from aircraft	Chute release mechanism
	2	54	2200	12	4500	1000	OK	
	3	53	2200	8	2950	1000	OK	
	4	52	500	8	3500	1000	OK	
23 Apr	1	55	2200	10	4500	1000	OK	
	2	54	2200	10	4500	1000	OK	
	3	53	2200	8	4500	1000	OK	
	4	52	500	8	2950	1000	OK	
7 May	1	72	2200	12	4400	1700	OK	
	2	73	2200	12	4400	1700	OK	
	3	77	2200	12	4400	1700	OK	
	4	65	500	8	3000	1000	DUD -- Battery striker lanyard not pulled	Rigging to lanyard
15 May	1	83	1500	12	4400	1700	DUD -- Battery not activated	Defective primer
	2	82	1500	12	4400	1700	OK	
	3	81	500	8	3300	1000	OK	
	4	80	500	8	3300	1000	OK	
11 June	1	77	500	8	3700	1000	OK	
	2	72	500	8	3700	1000	OK	
	3	85	500	8	3700	1000	Early -- 8 sec after release	Aircraft reflections

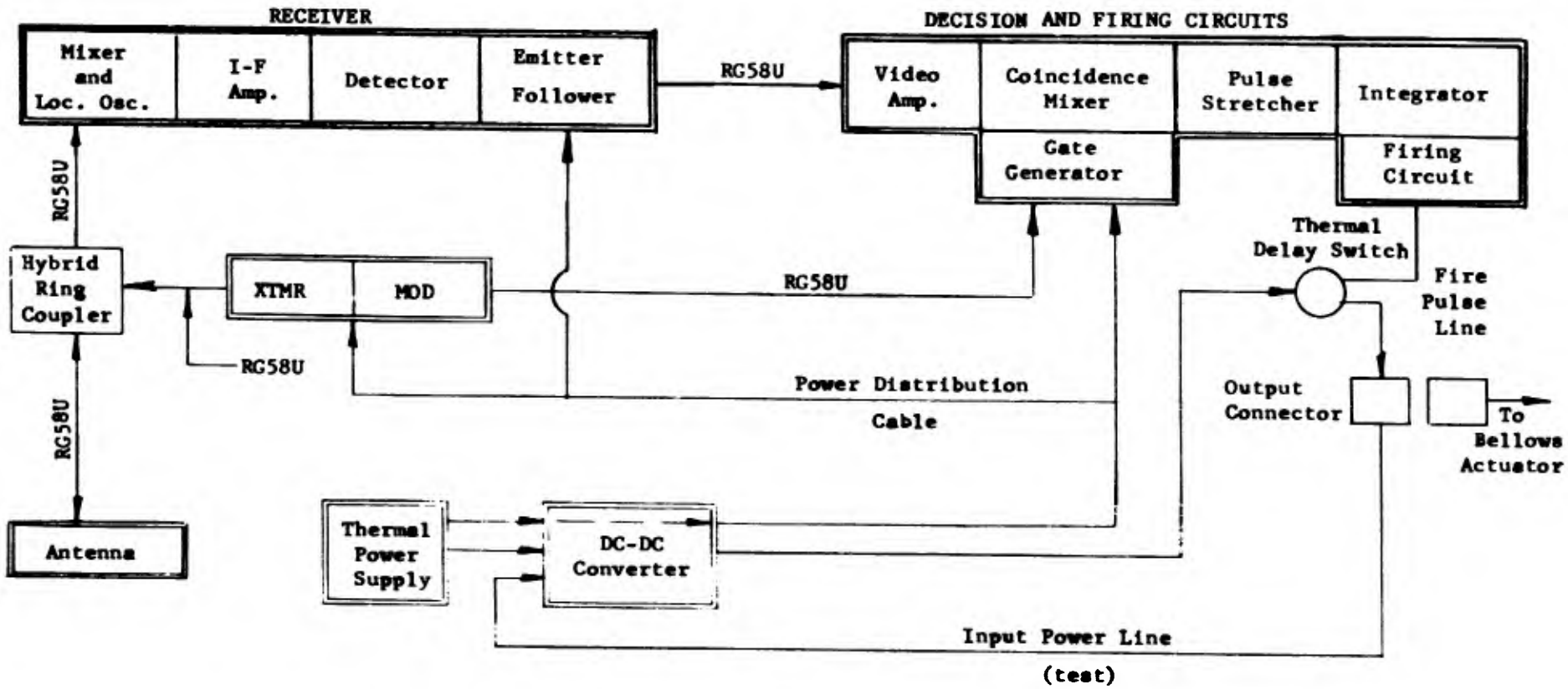

Figure 1. Block diagram, radar actuator.

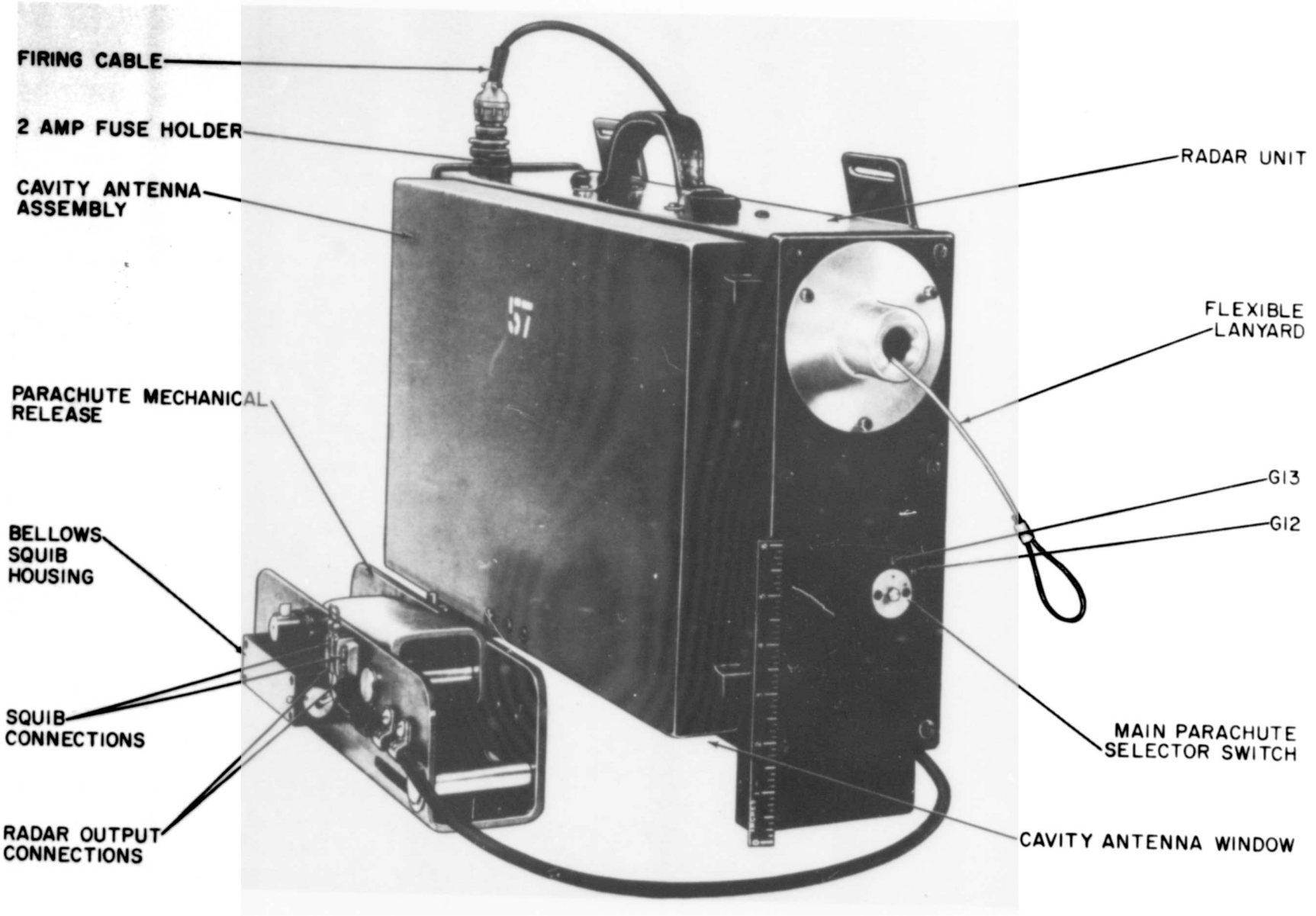

Fig. 2 Radar Actuator And Parachute Mechanical Release.

739-64

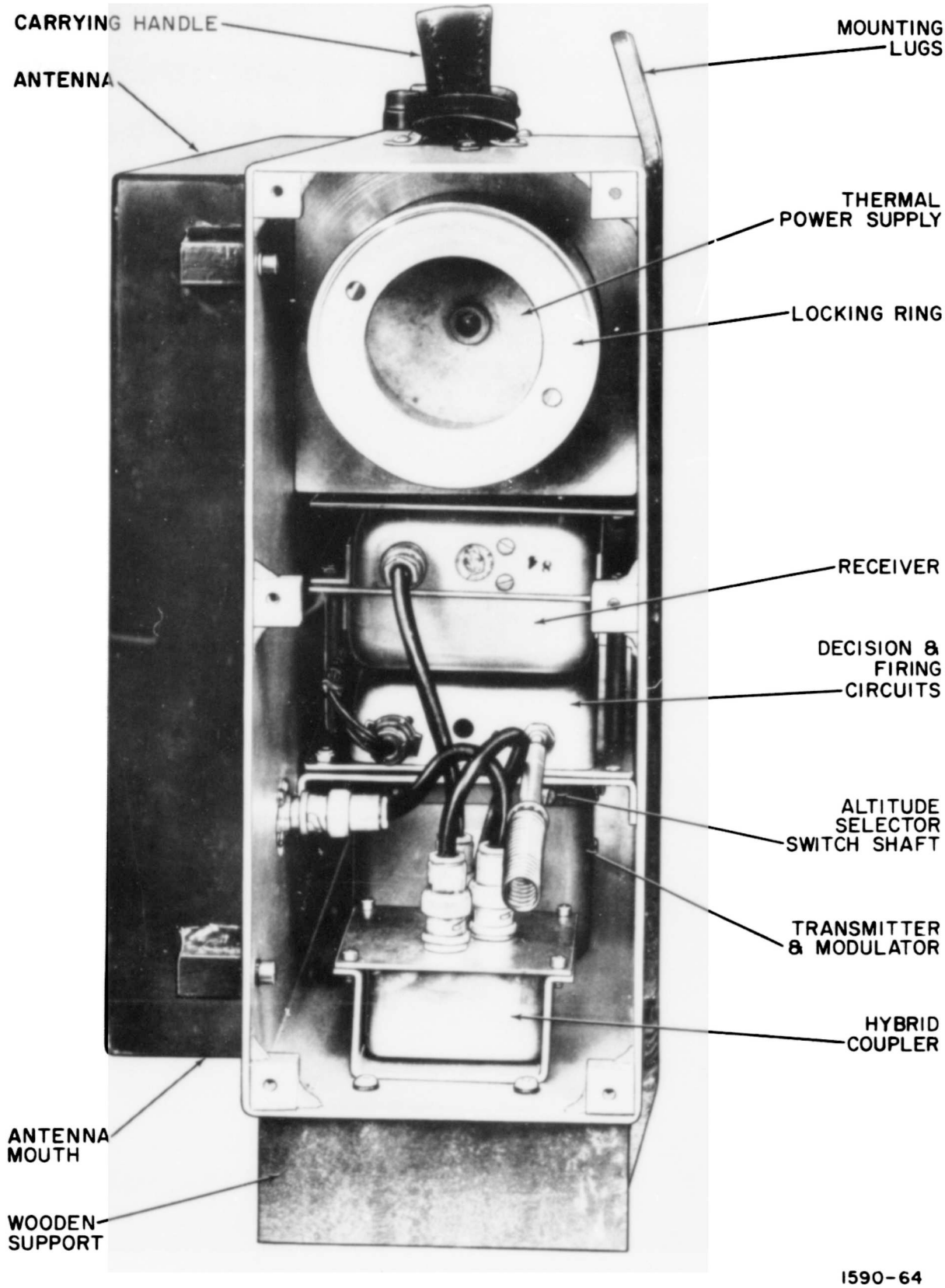

Fig. 3. HADOPAD Actuator, Battery End, End-Plate Removed.

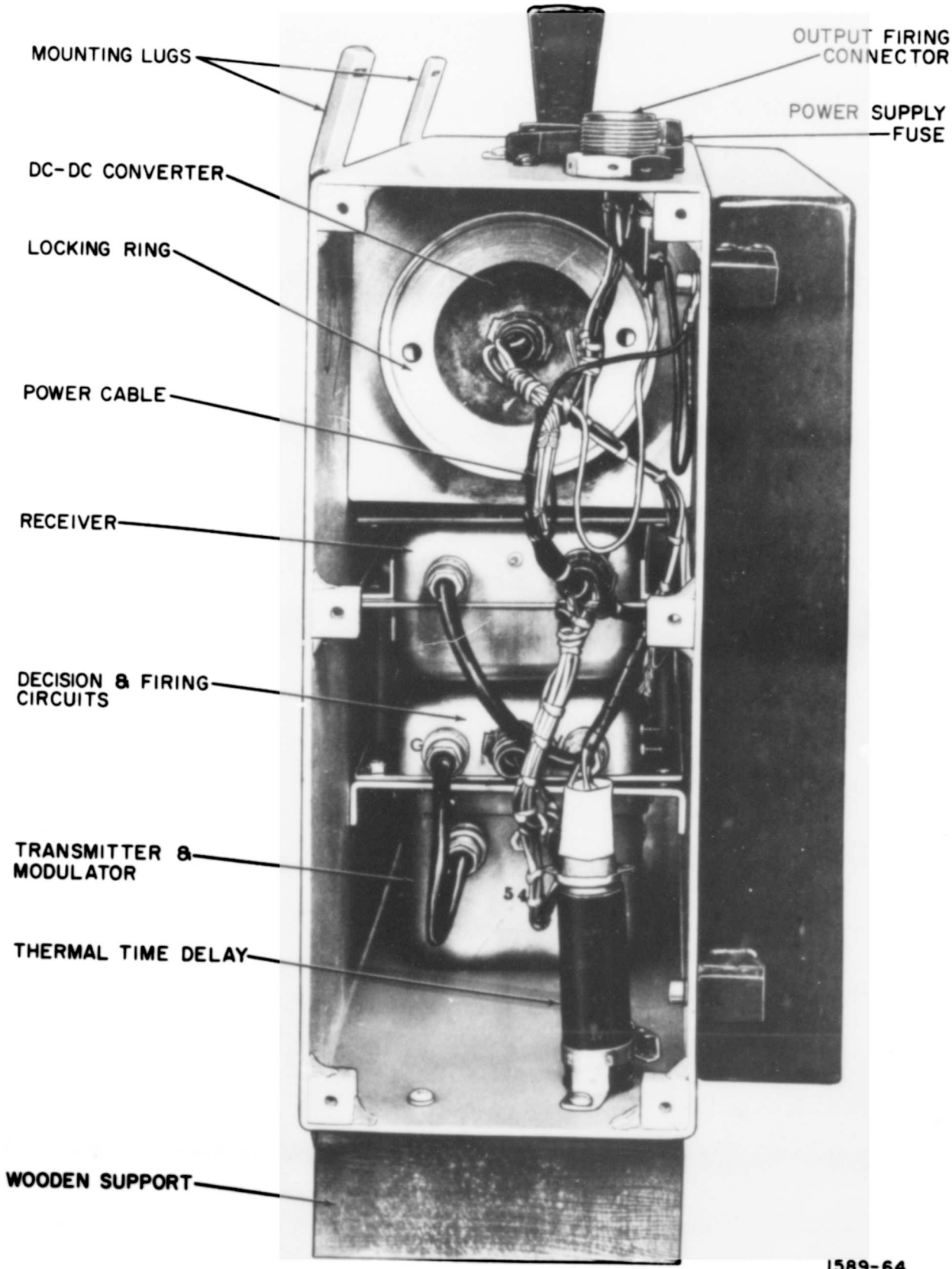

Fig. 4. HADOPAD Actuator, DC-DC Converter, End-Plate Removed.

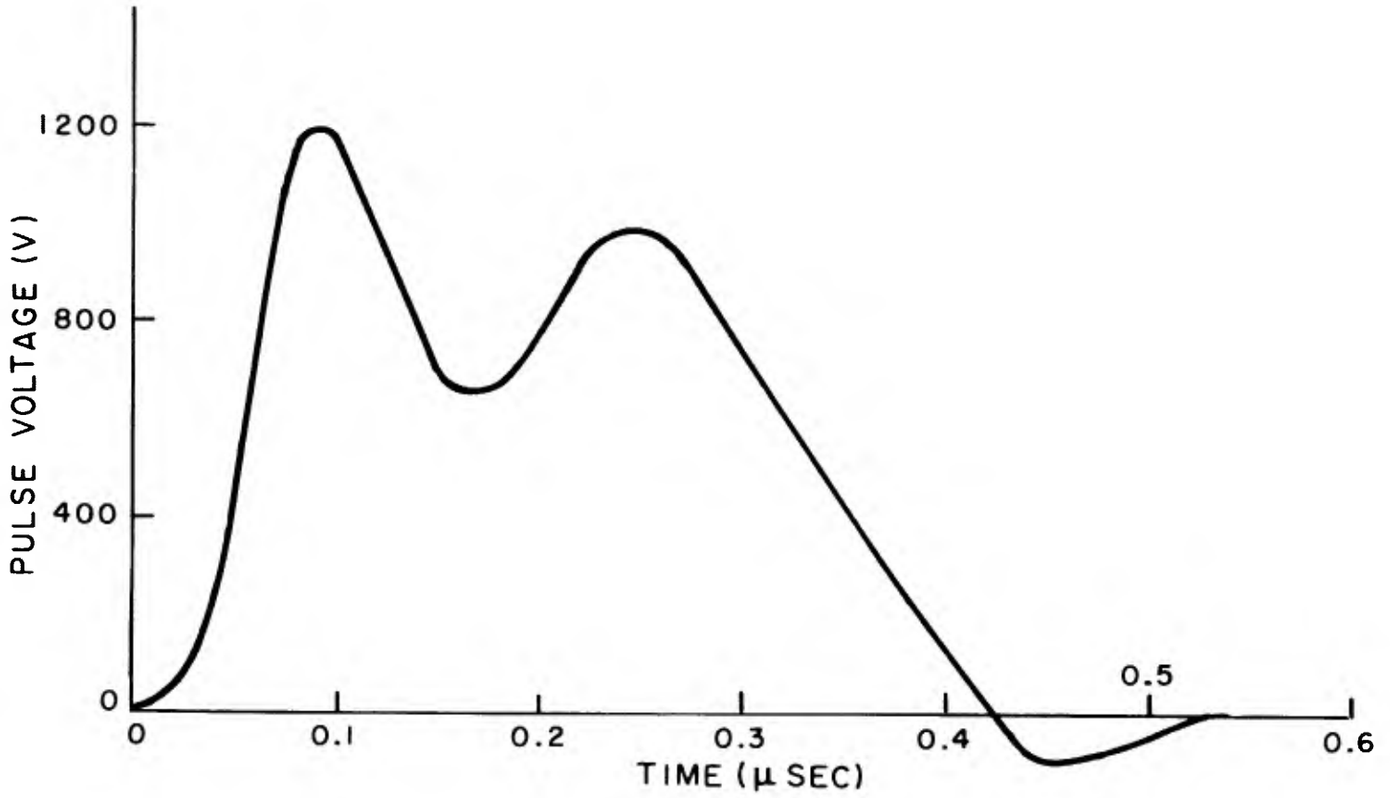

Figure 5. Typical modulator pulse—HADOPAD.

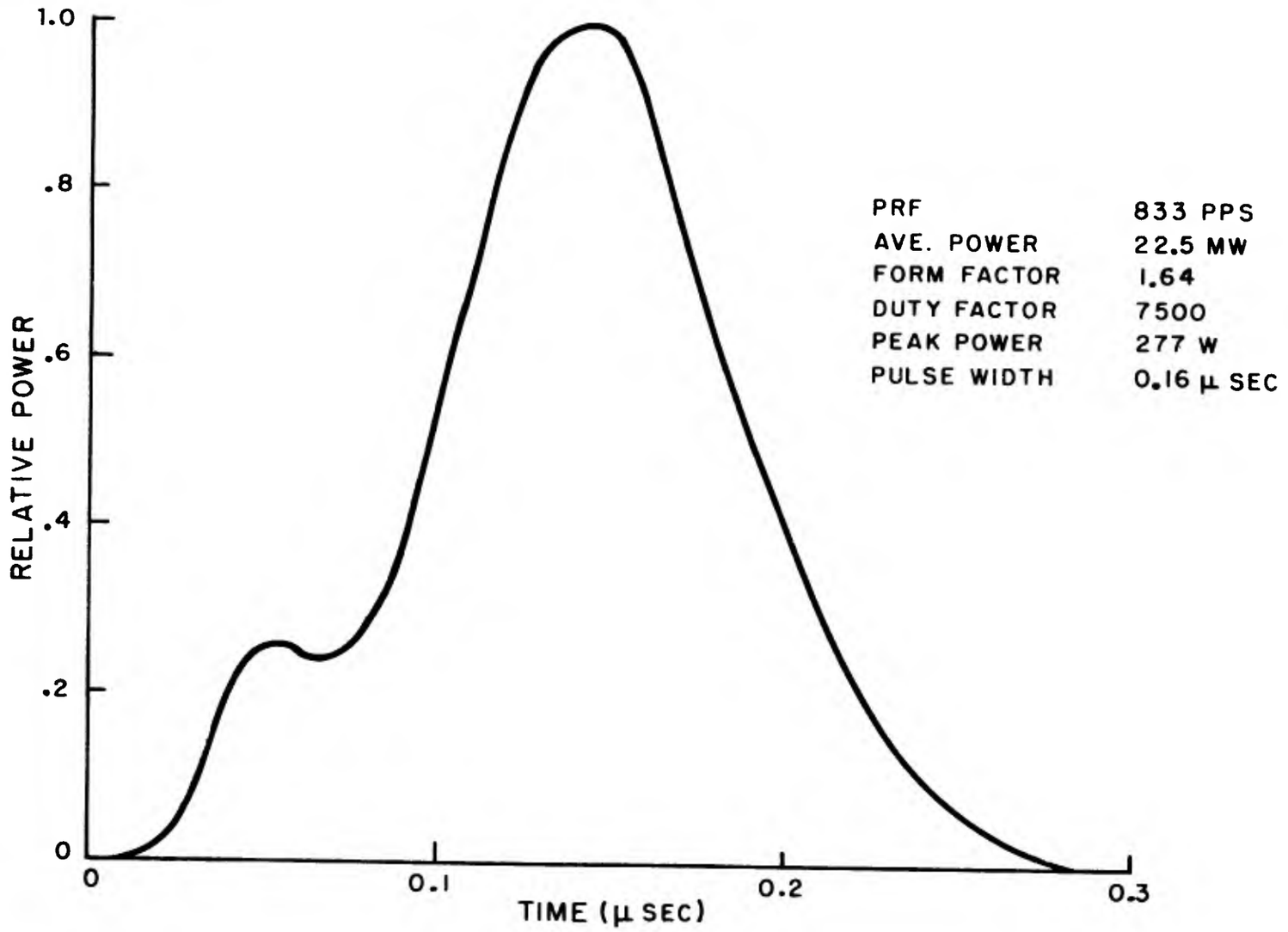

Figure 6. Transmitted-pulse power envelope.

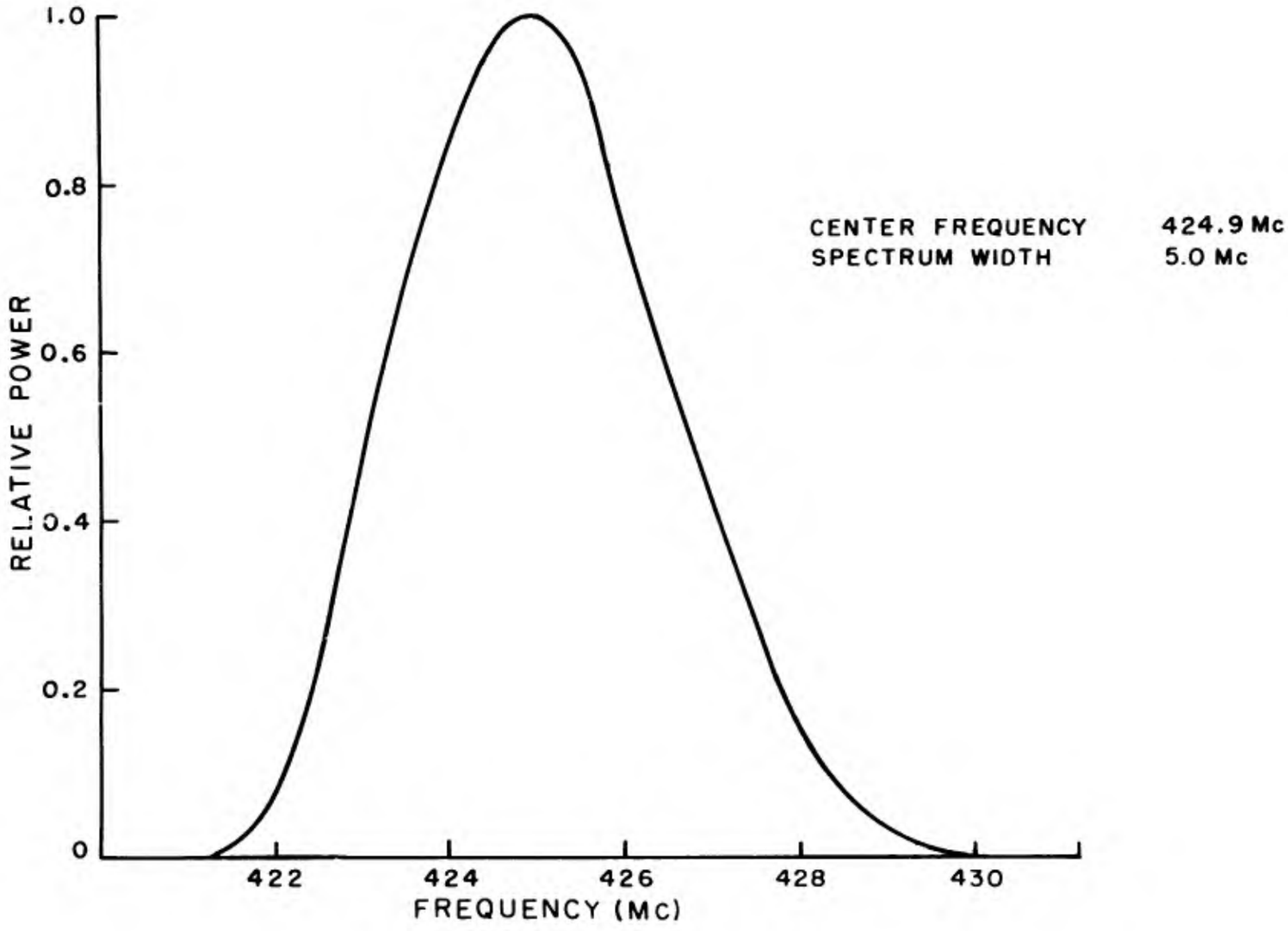

Figure 7. Typical power envelope of transmitted spectrum.

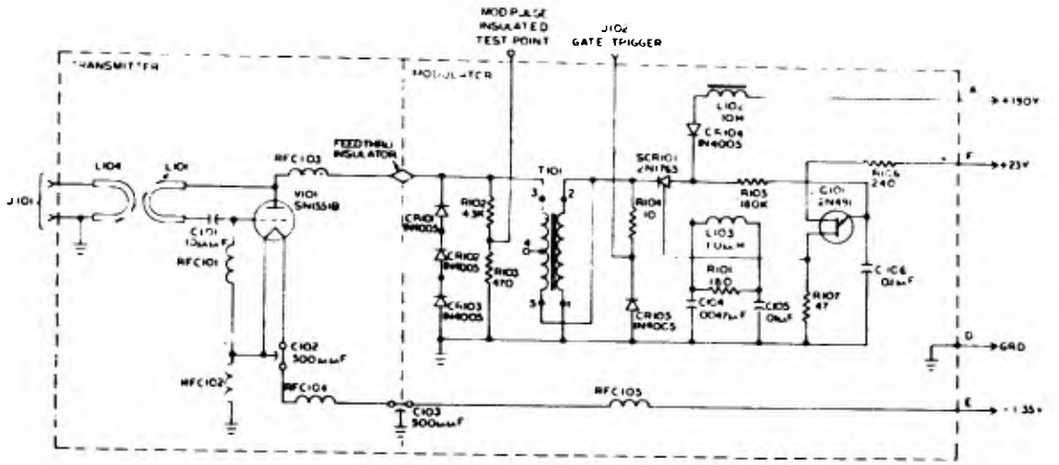

SYMBOL	PART NO
R101	RC07GF181J
R10_	RC07GF432J
R103	RC07GF471J
R1C4	RC07GF100J
R1C5	RCC7GF184J
R106	RC07GF241J
R107	RC07GF470J
C101	DWG B10991317
C102	DWG B10985665
C103	DWG B10985665
C104	DWG C10991339, ITEM 2
C105	DWG C10991339, ITEM 1
C106	DWG C10991338, ITEM 2
L101	ON XMTR PRINTED CIRCUIT BOARD, 10991307
L10_	DWG B10991303
L1C3	DWG B10991309
L104	WIRE, MIL-W-631, SEE B-991319
RFC101	DWG B10991246
RFC102	DWG B10991246
RFC103	DWG B10991246
RFC104	DWG B10991246
RFC105	DWG B10991246
V101	DWG C10984234
T101	DWG B10991293
G101	DWG B10991345
J101	MS 35179-1094A
J102	MS 35179-1094A
CR101	DWG B10991305, ITEM 1
CR102	DWG B10991305, ITEM 1
CR103	DWG B10991305, ITEM 1
CR104	DWG B10991305, ITEM 1
CR105	DWG B10991305, ITEM 1
SCR101	MIL-S-19500/249

NOTES
1. MIL-STD-12, MIL-STD-15 AND MIL-STD-16 APPLY
2. ALL RESISTOR VALUES ARE IN OHMS AND ARE 1/4 W, ±5%
3. ALL CAPACITORS OVER 1000 uuF ARE ±10% UNLESS OTHERWISE SPECIFIED THOSE BELOW 1000 uuF ARE GMV EXCEPT C101 WHICH IS ± 10%

Figure 8. Schematic diagram of transmitter/modulator.

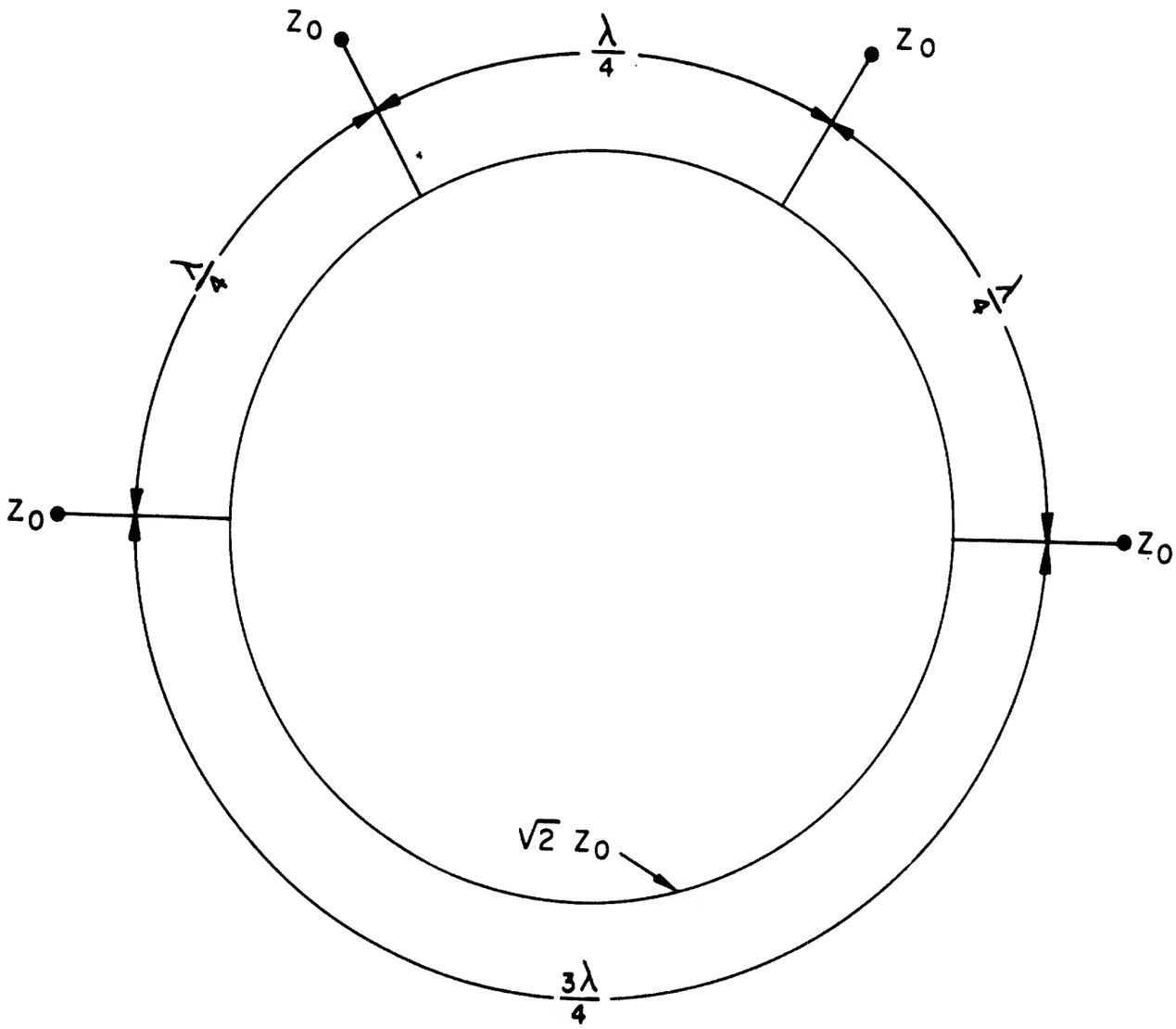

Z_0 = CHARACTERISTIC IMPEDANCE OF SYSTEM

Figure 9. Basic hybrid ring network.

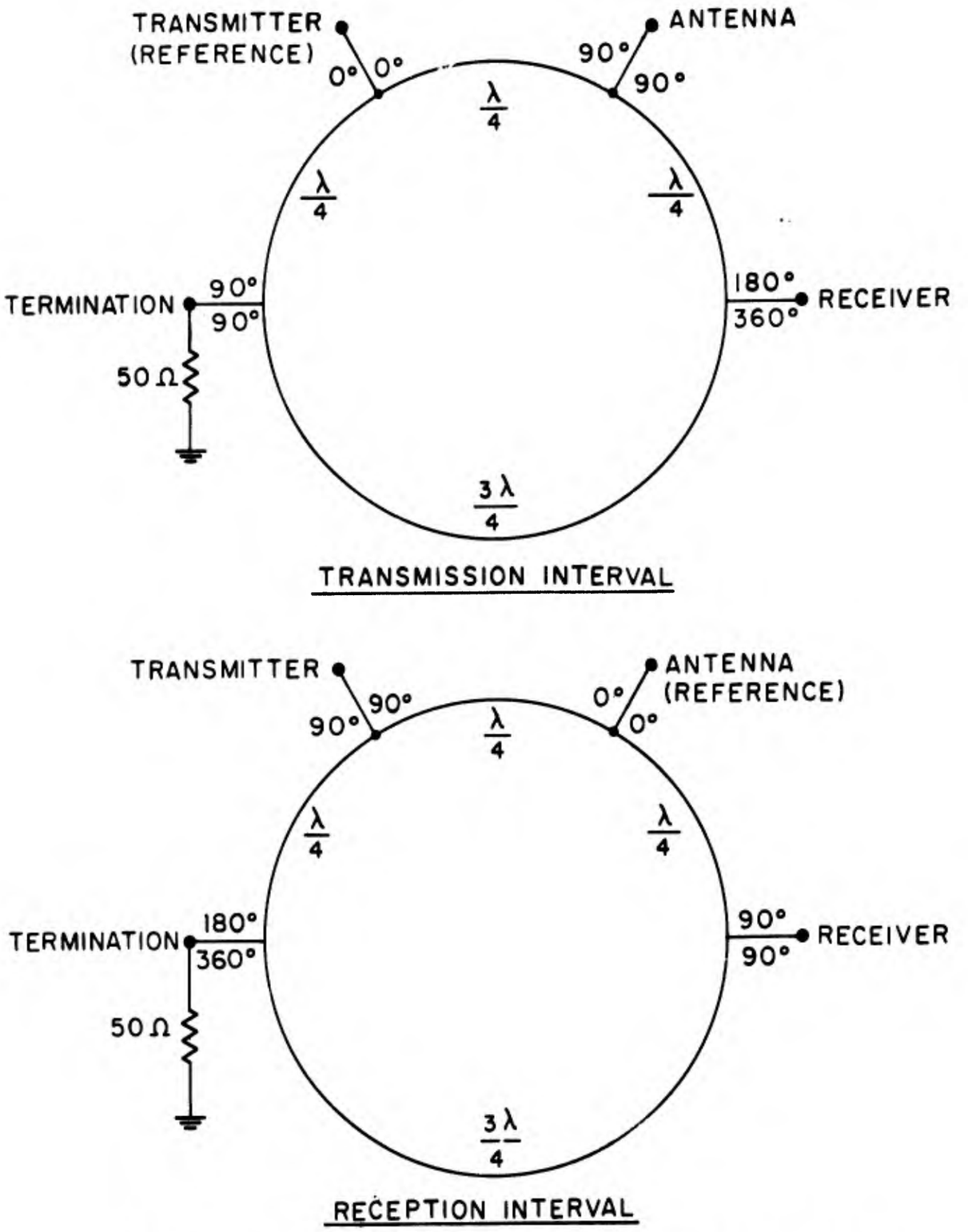

Figure 10. Phasing of basic hybrid ring used in HADOPAD.

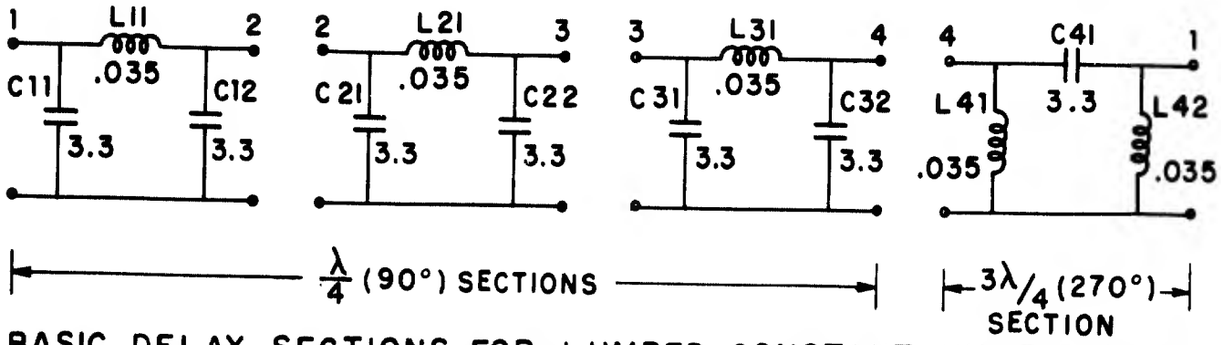

BASIC DELAY SECTIONS FOR LUMPED CONSTANT HYBRID RING

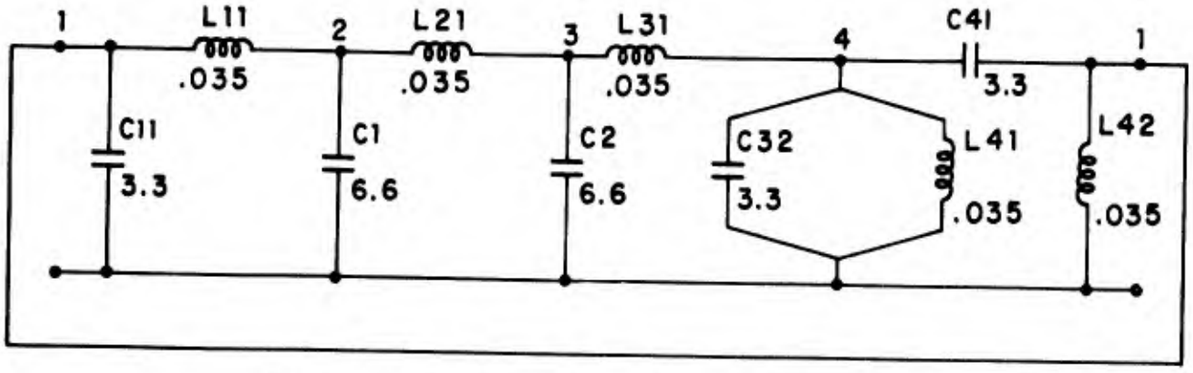

BASIC DELAY SECTIONS COMBINED

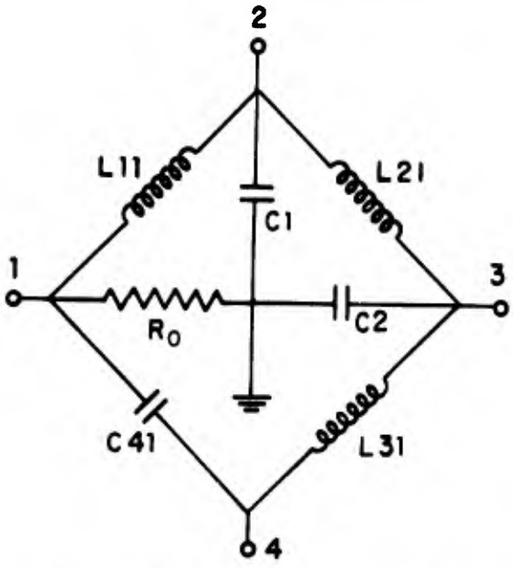

C1 = C12 + C21
C2 = C22 + C31
L42 & C11 ARE PARALLEL RESONANT
L41 & C32 ARE PARALLEL RESONANT
BOTH PARALLEL RESONANT CIRCUITS OMITTED BECAUSE OF HIGH Z.
$R_0 = 50\Omega$
COMPONENT VALUES ARE IN pf, μh, OR OHMS

FINAL LUMPED CONSTANT RING

Figure 11. Evolution of HADOPAD lumped-constant hybrid coupler.

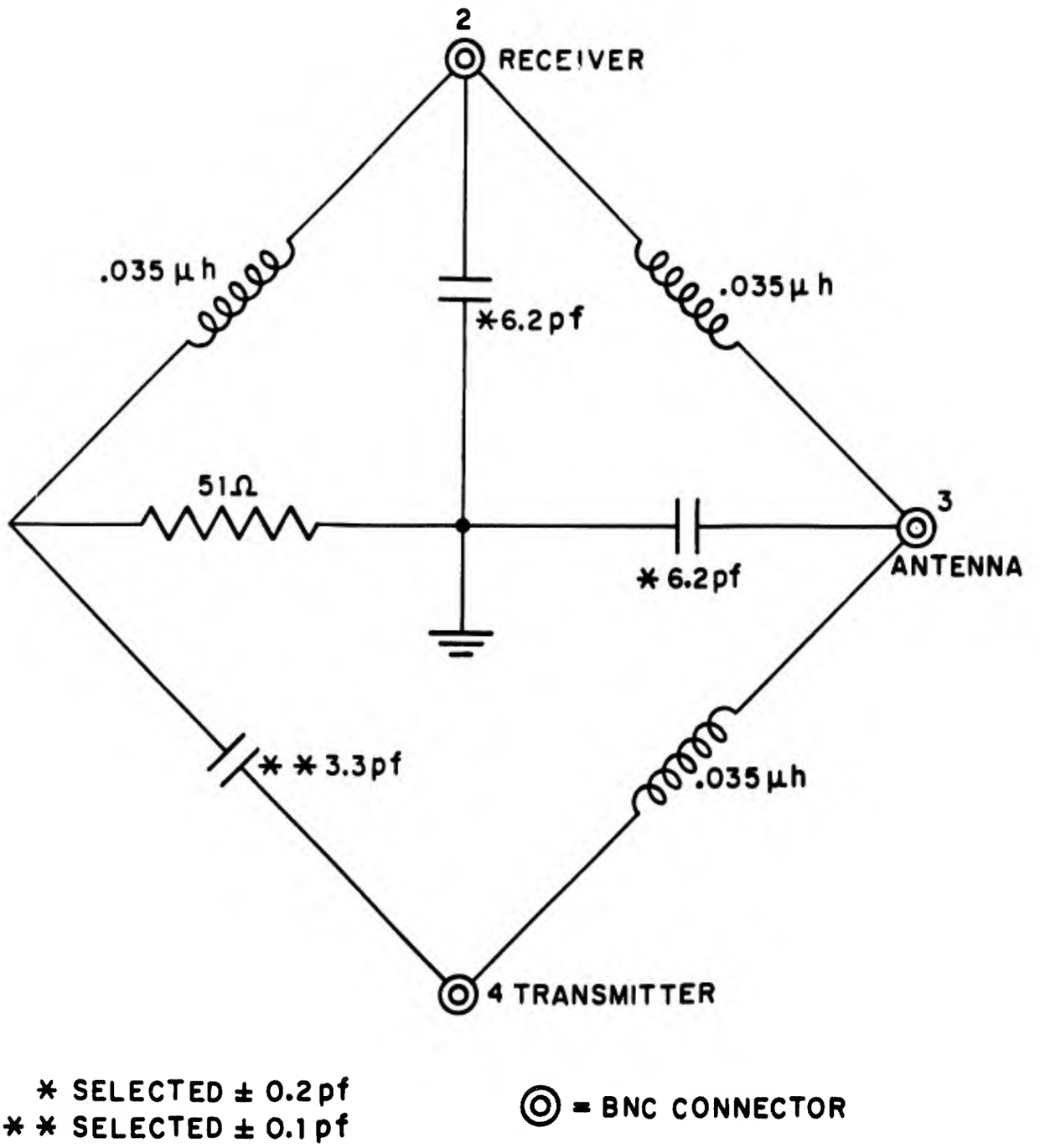

Figure 12. HADOPAD hybrid coupler.

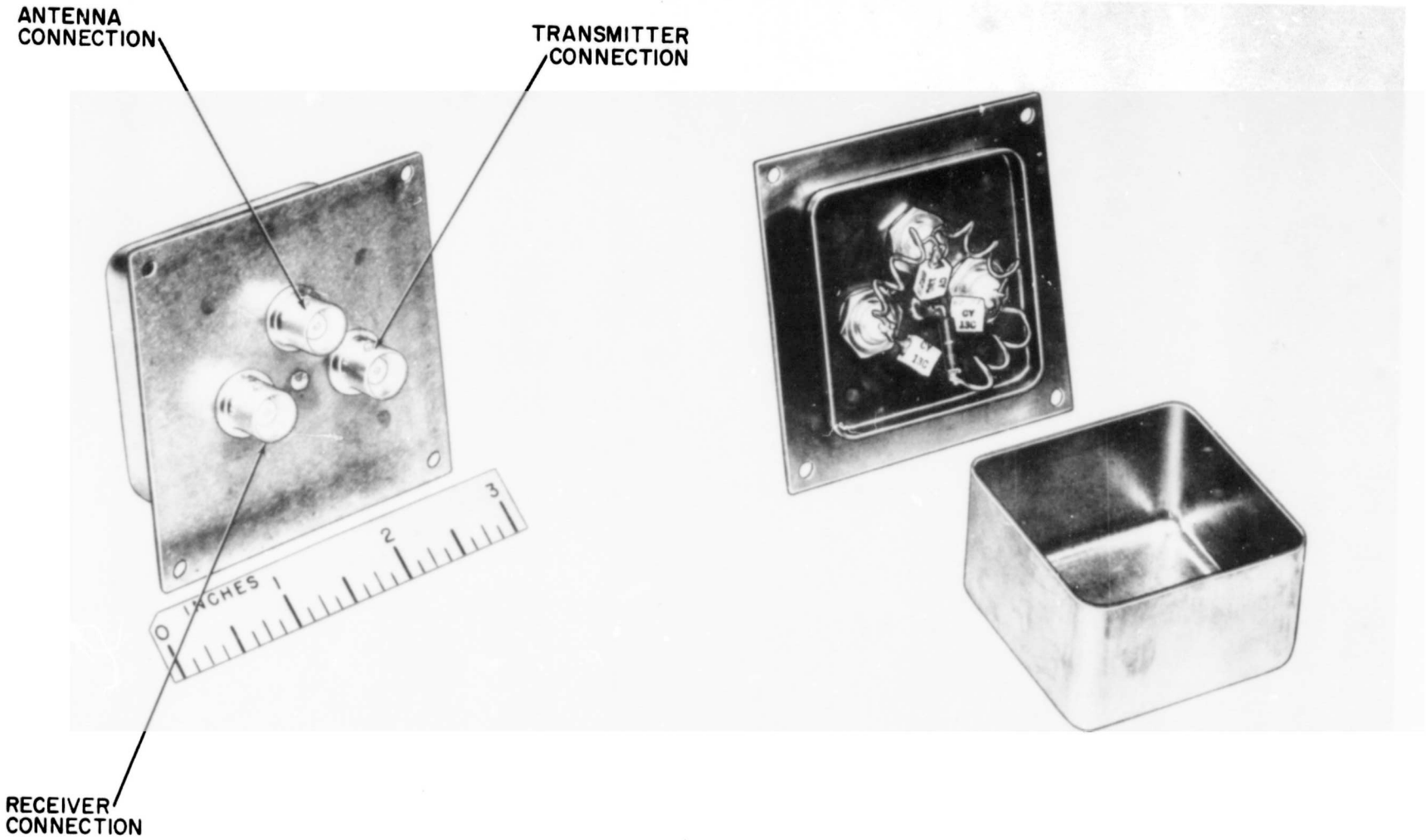

Fig. 13. Hybrid Ring Coupler For Radar Actuator.

096-64

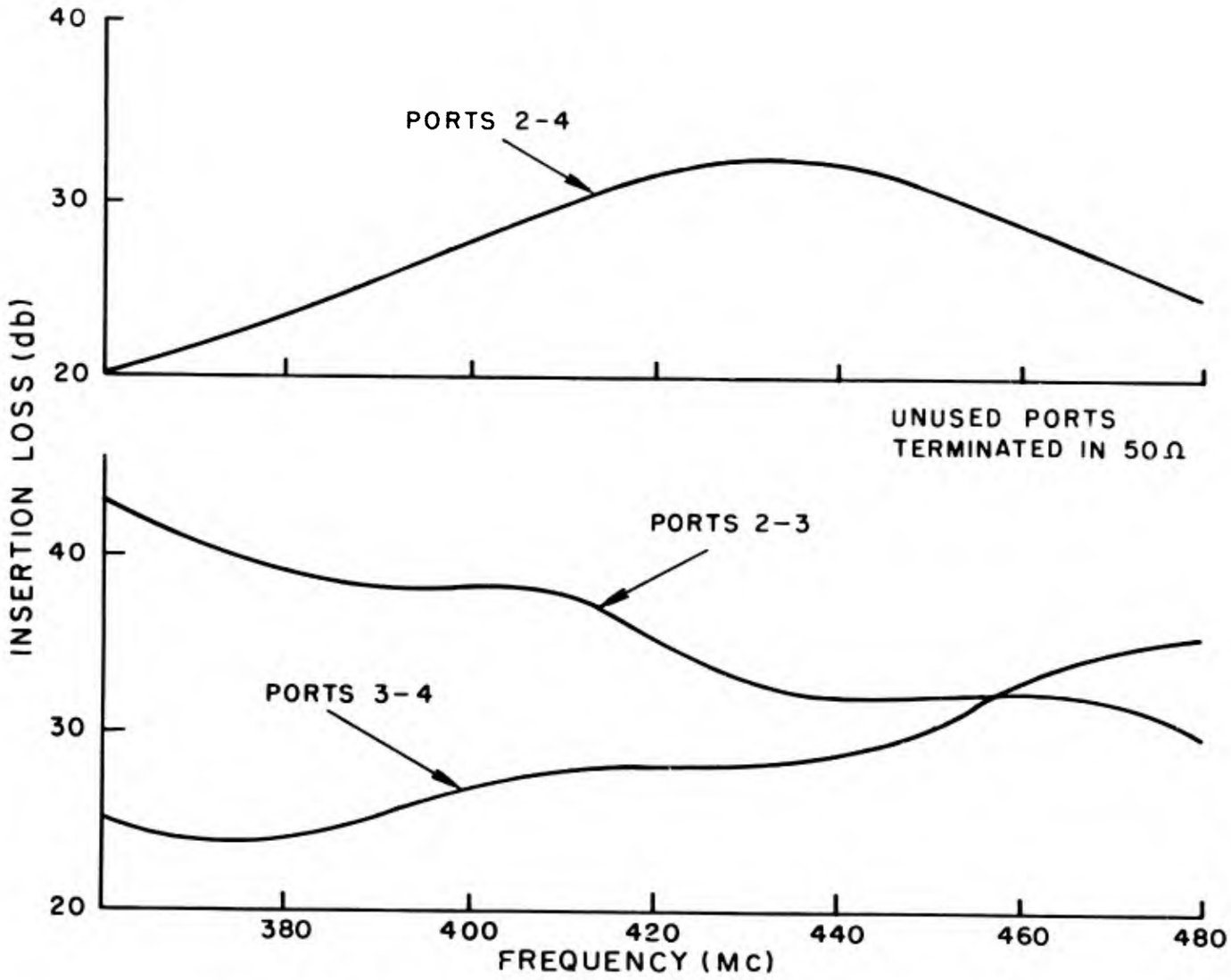

Figure 14. Average insertion loss of hybrid couplers.

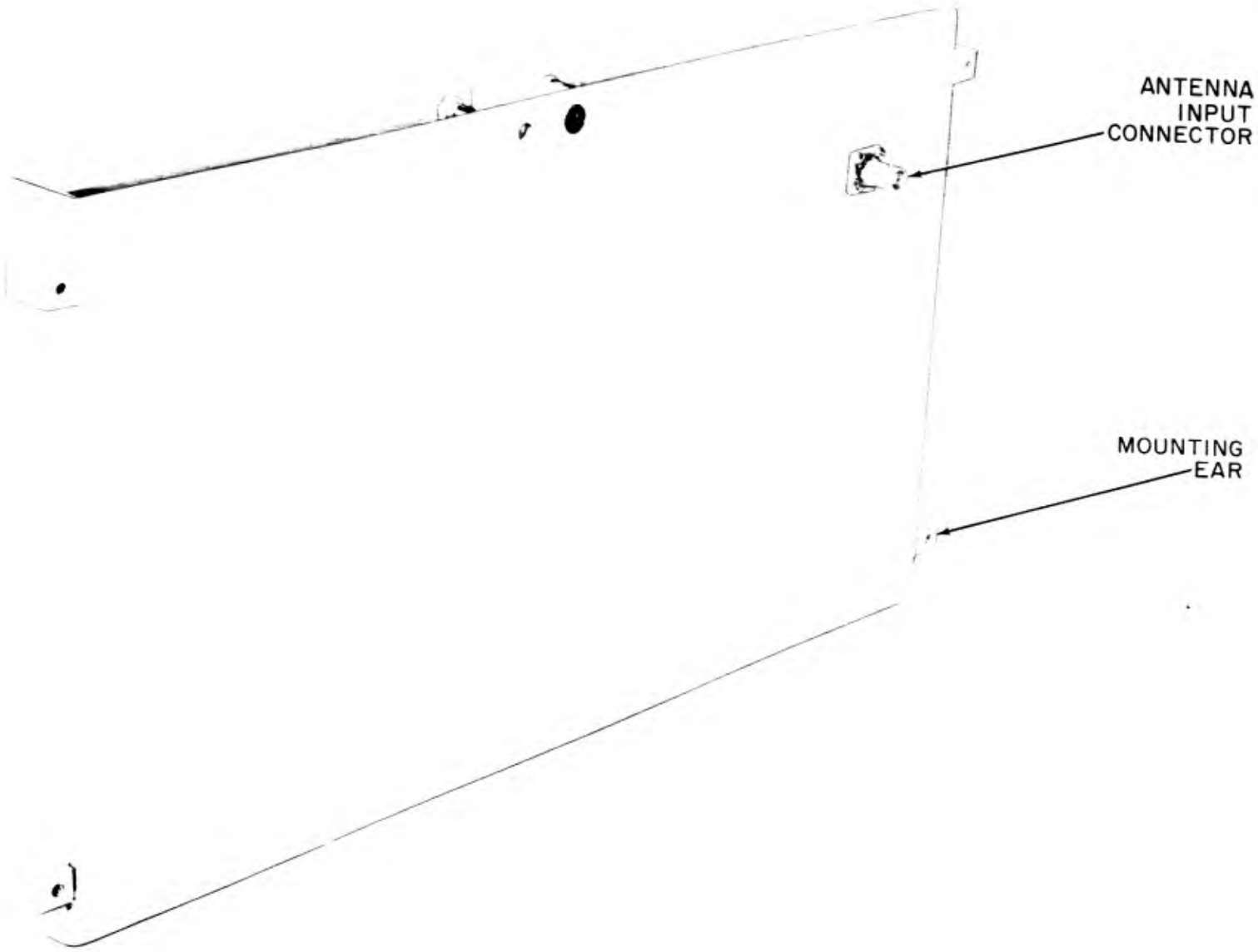

Fig. 15. HADOPAD Antenna, Side View, Cover Removed.

2694-64

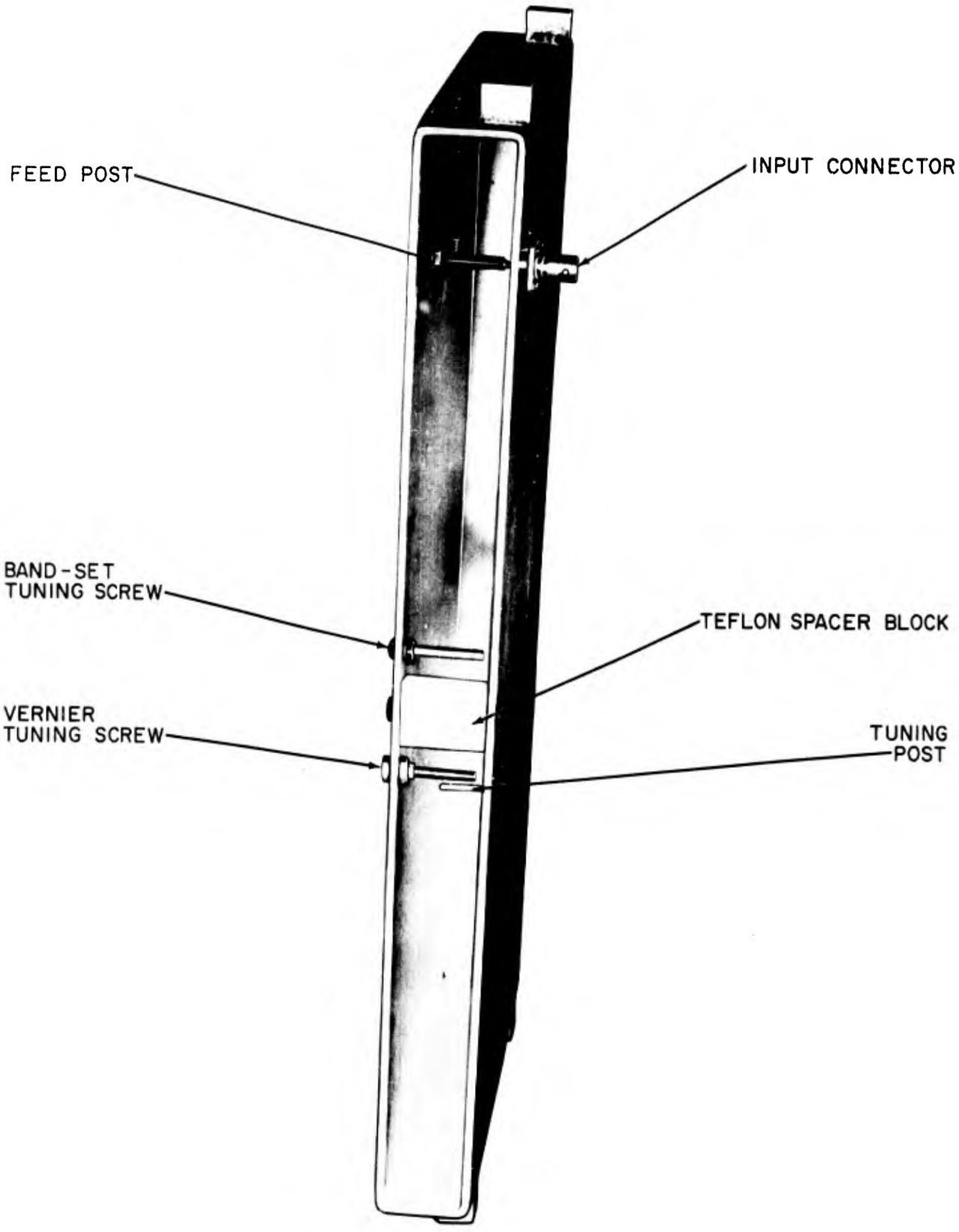

2695-64

Fig. 16. HADOPAD Antenna, View Into Mouth, Cover Removed.

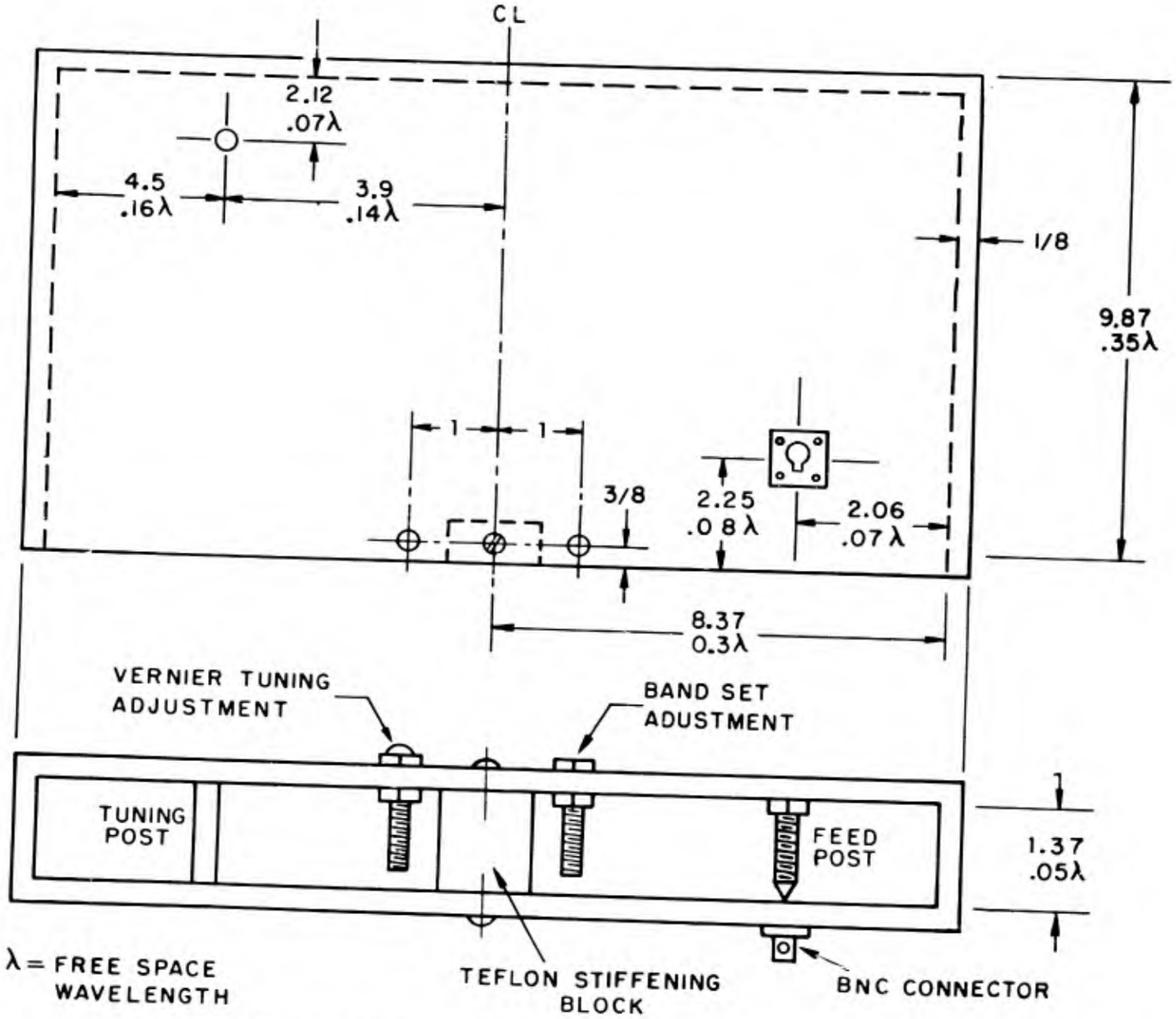

Figure 17. HADOPAD antenna dimensions—electrical.

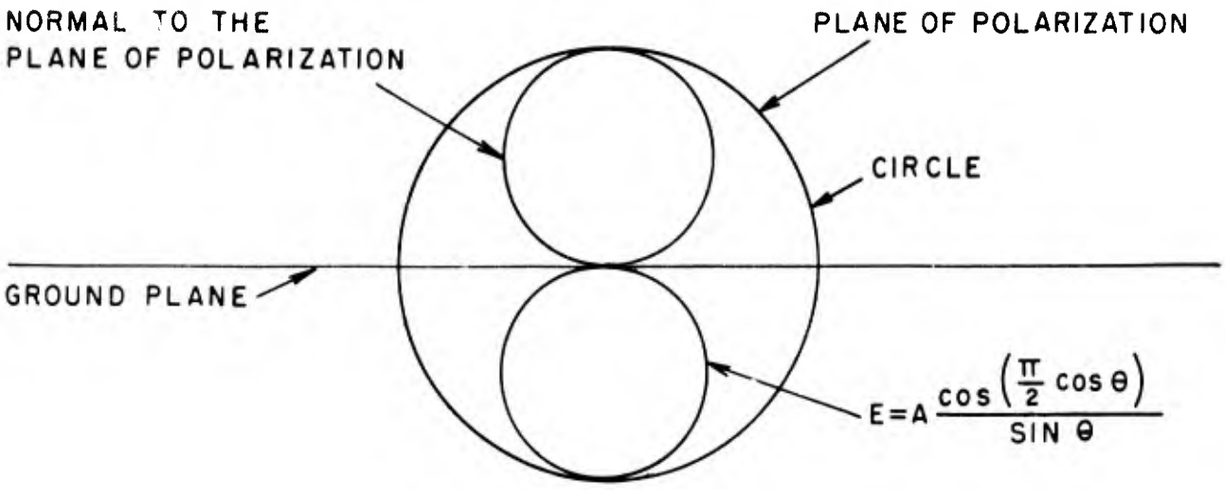

RADIATION PATTERN OF HALF-WAVE SLOT IN
INFINITE GROUND PLANE

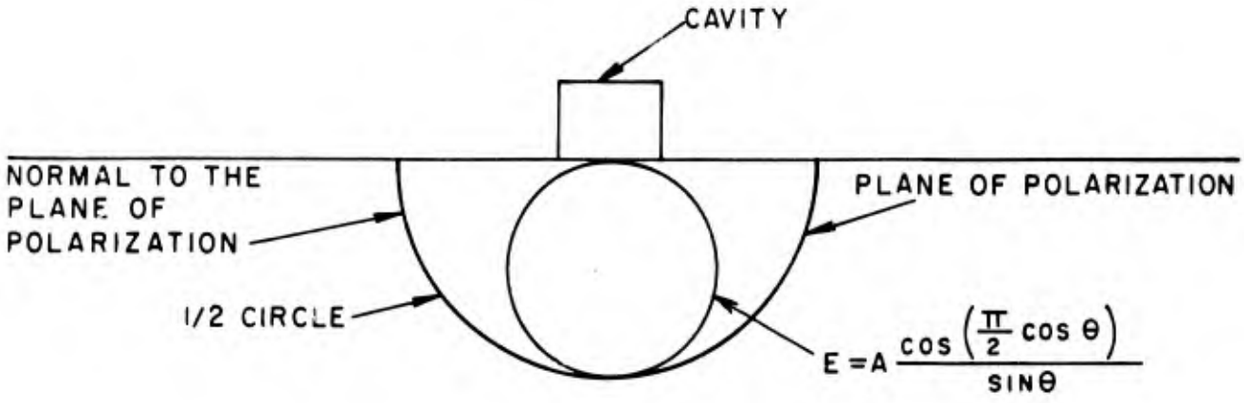

RADIATION PATTERN OF HALF-WAVE SLOT IN
INFINITE GROUND WITH CAVITY BEHIND SLOT

Figure 18. Effect of cavity on slot antenna.

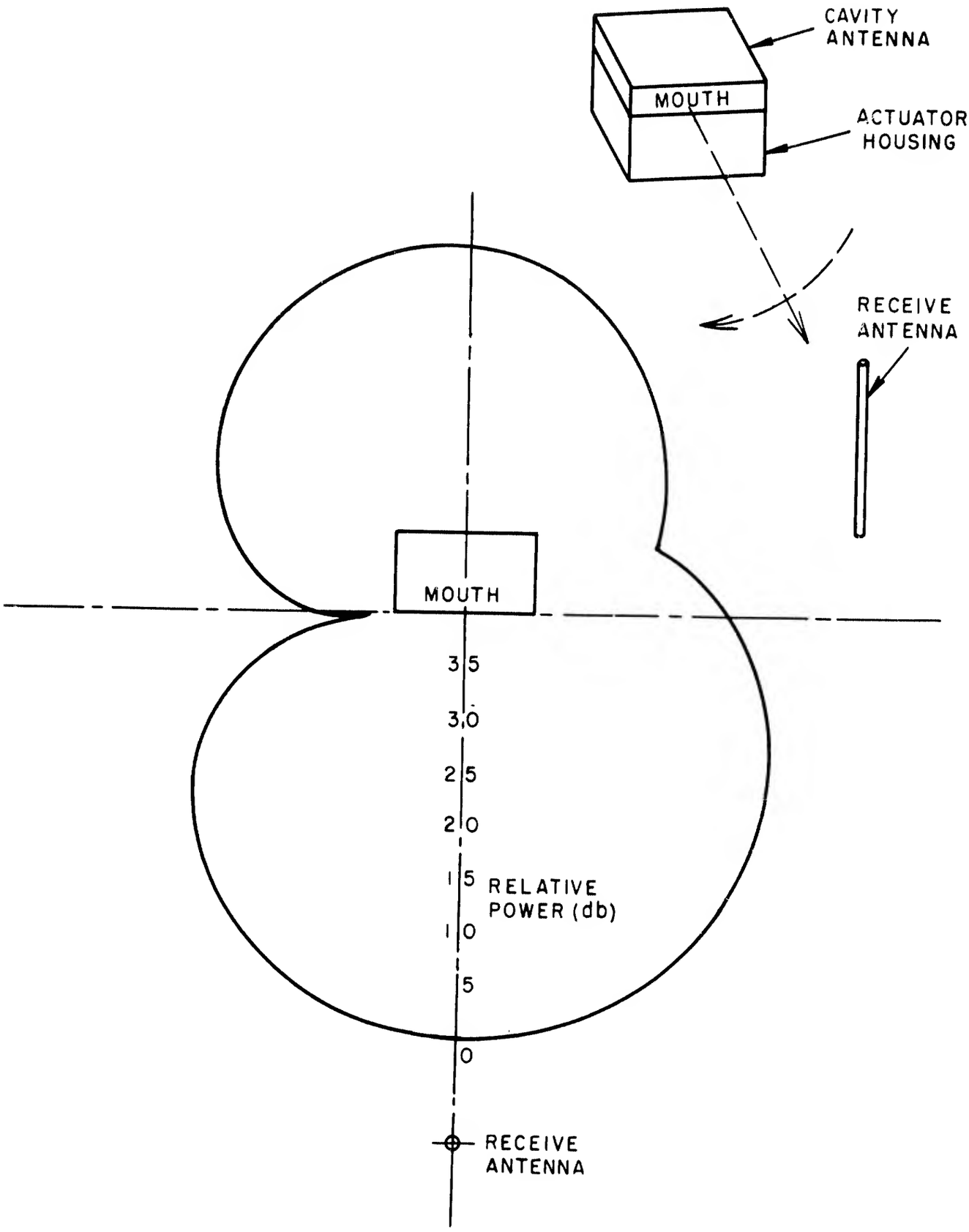

Figure 19. HADOPAD cavity antenna.

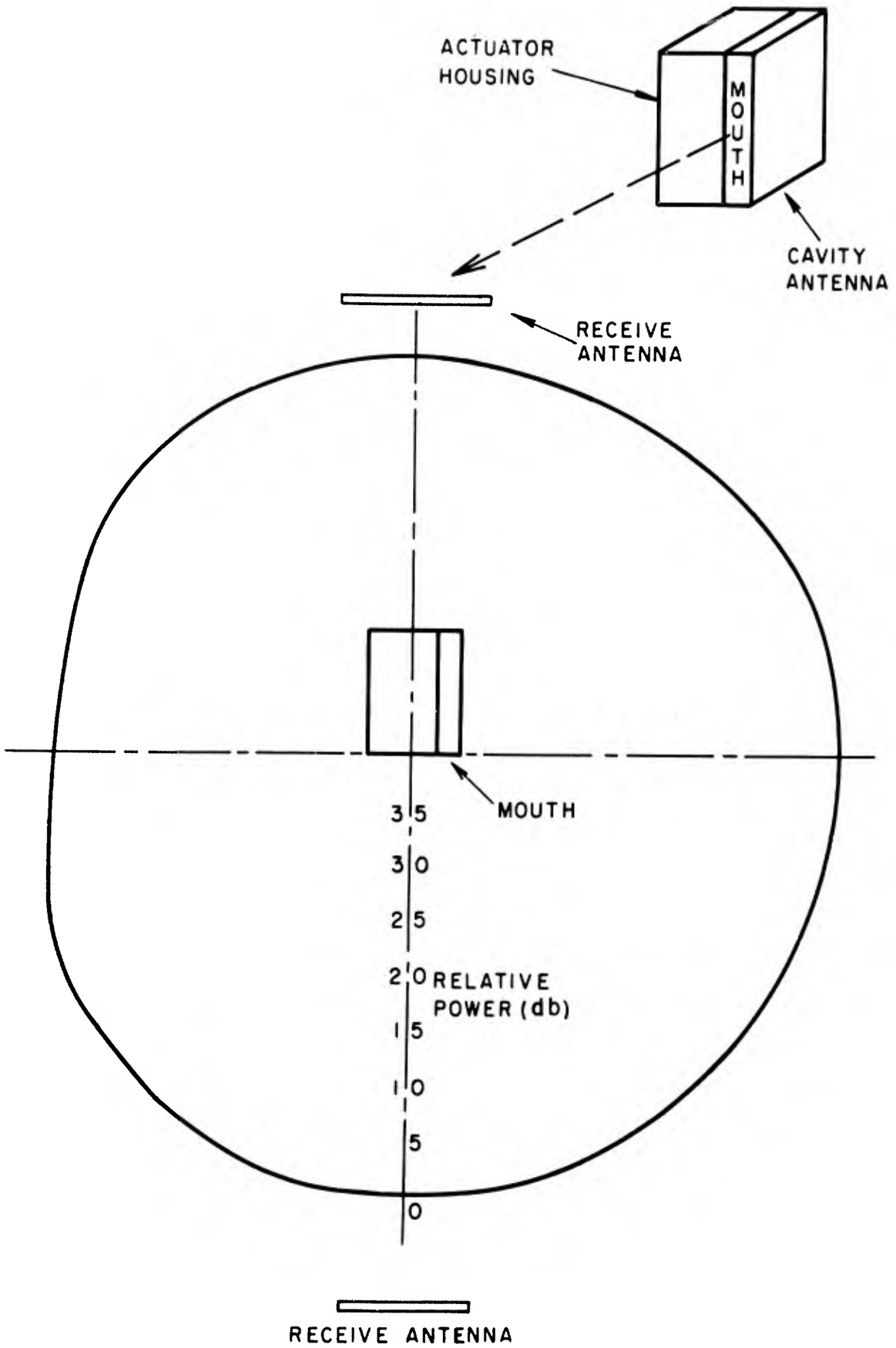

Figure 20. HADOPAD cavity antenna

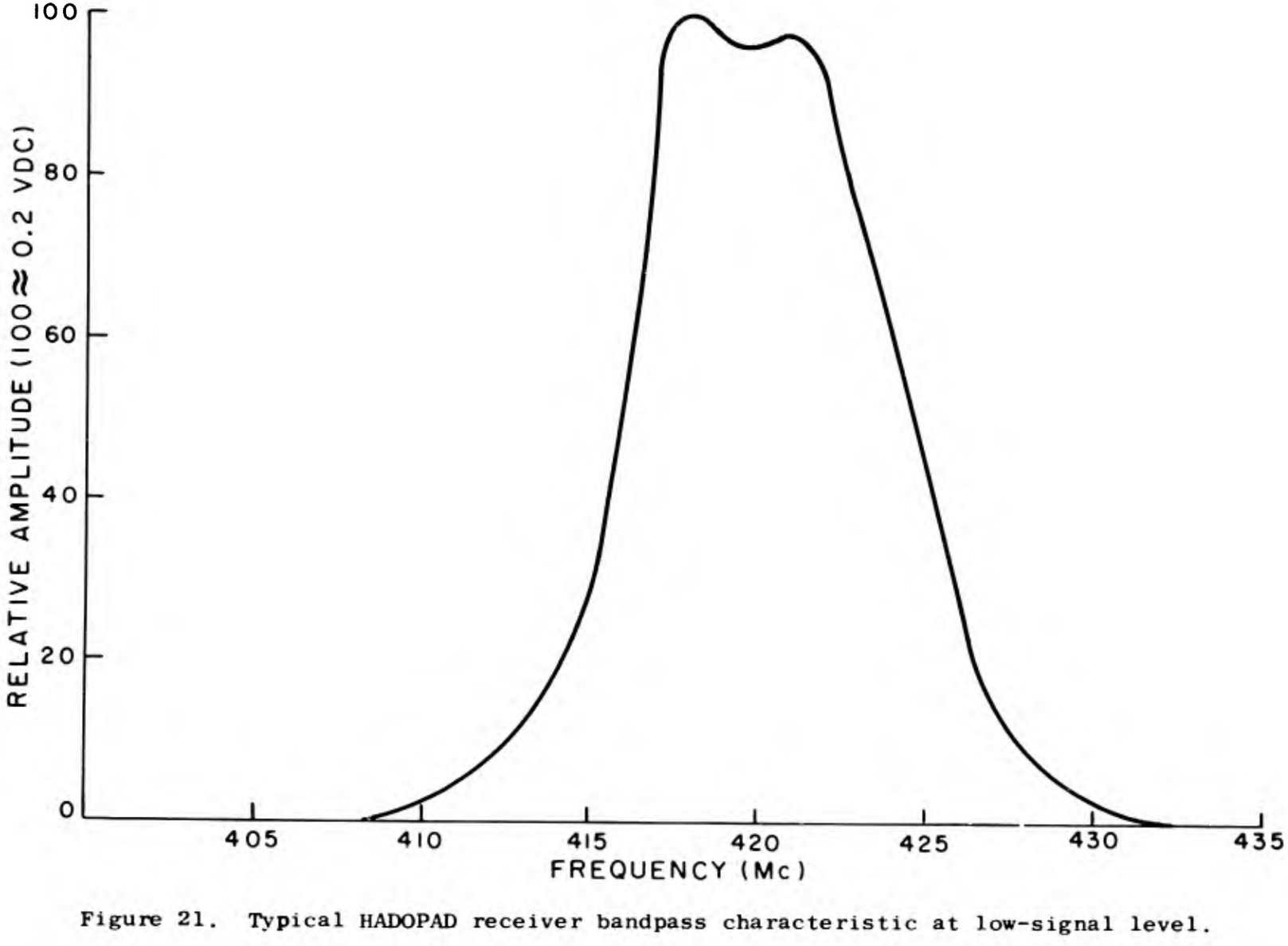

Figure 21. Typical HADOPAD receiver bandpass characteristic at low-signal level.

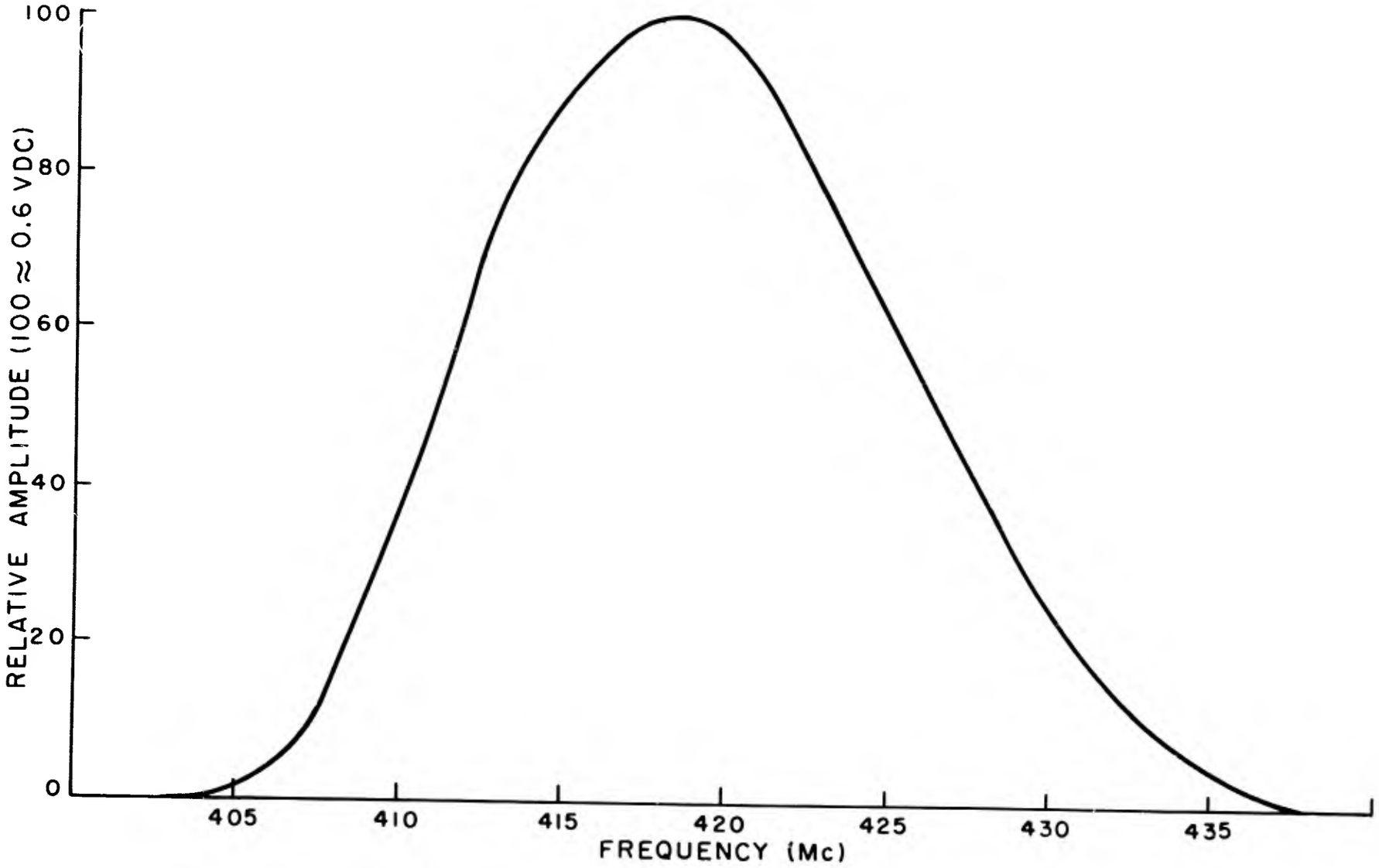

Figure 22. Typical HADOPAD receiver bandpass characteristic at high-signal level.

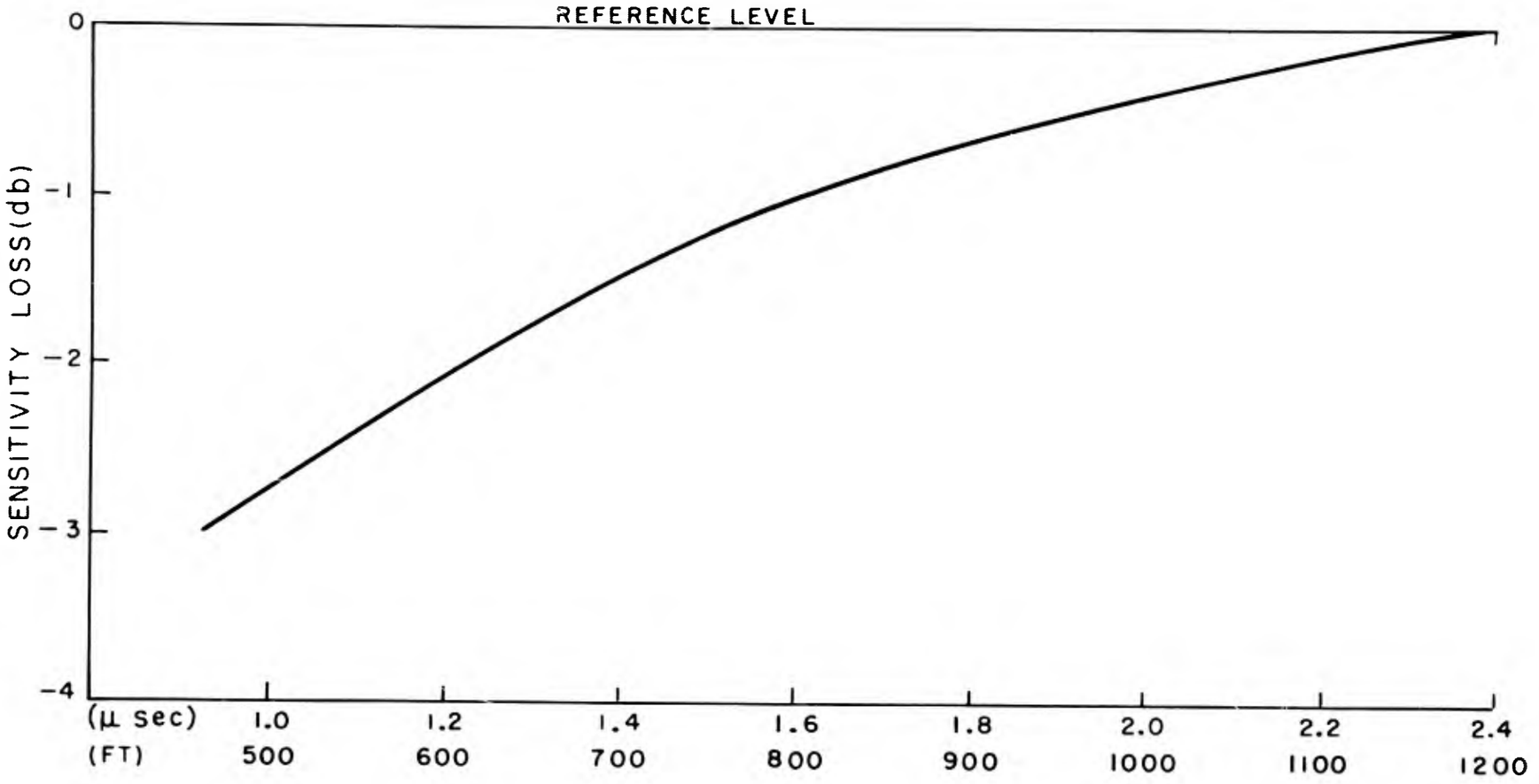

Figure 23. Recovery characteristic of typical HADOPAD receiver.

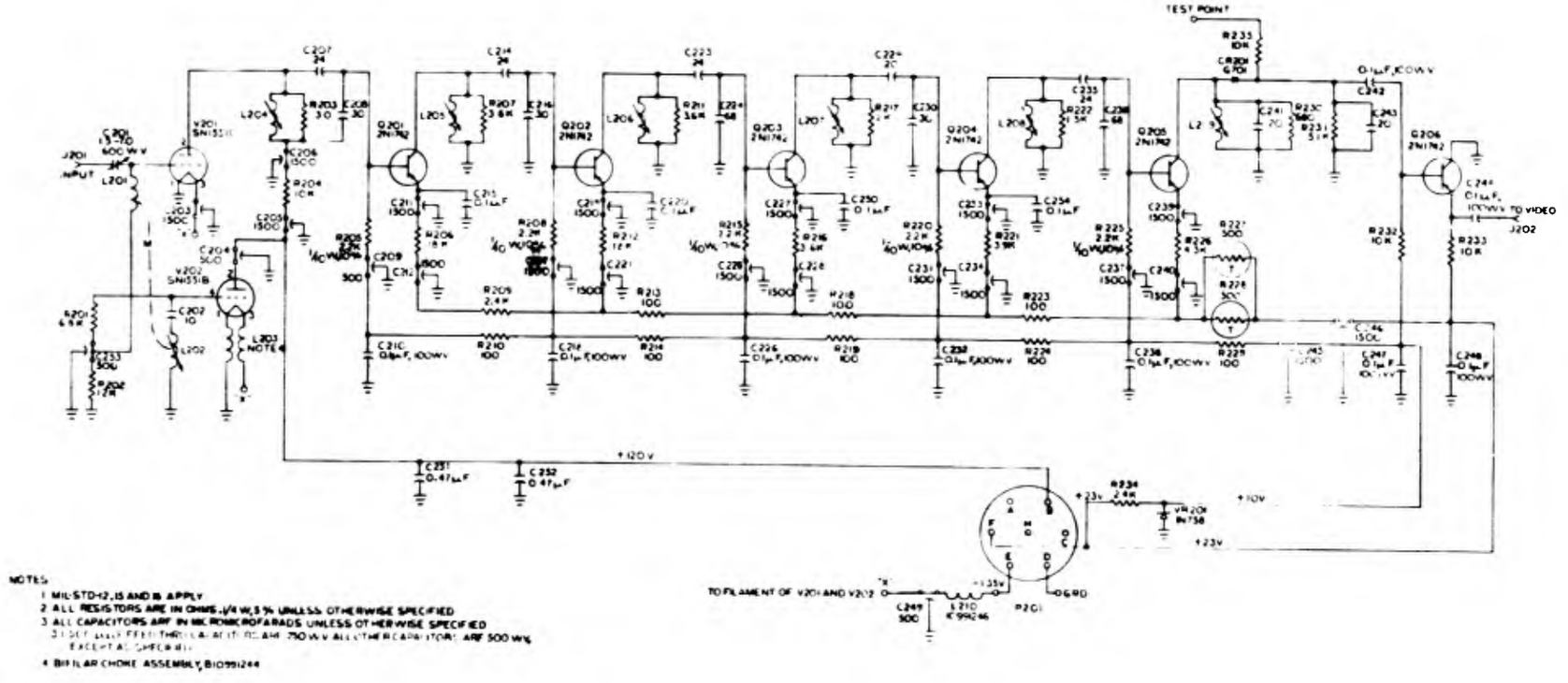

NOTES:
1. MIL-STD-12, IS AND IB APPLY.
2. ALL RESISTORS ARE IN OHMS, 1/4 W, 5% UNLESS OTHERWISE SPECIFIED.
3. ALL CAPACITORS ARE IN MICROMICROFARADS UNLESS OTHERWISE SPECIFIED.
   3) SEE [illegible] FEED THROUGH CAPACITOR: 750 W.V. ALL OTHER CAPACITORS ARE 500 W.V. EXCEPT AS SPECIFIED.
4. BIFILAR CHOKE ASSEMBLY, B10991244

Figure 24. Receiver schematic diagram.

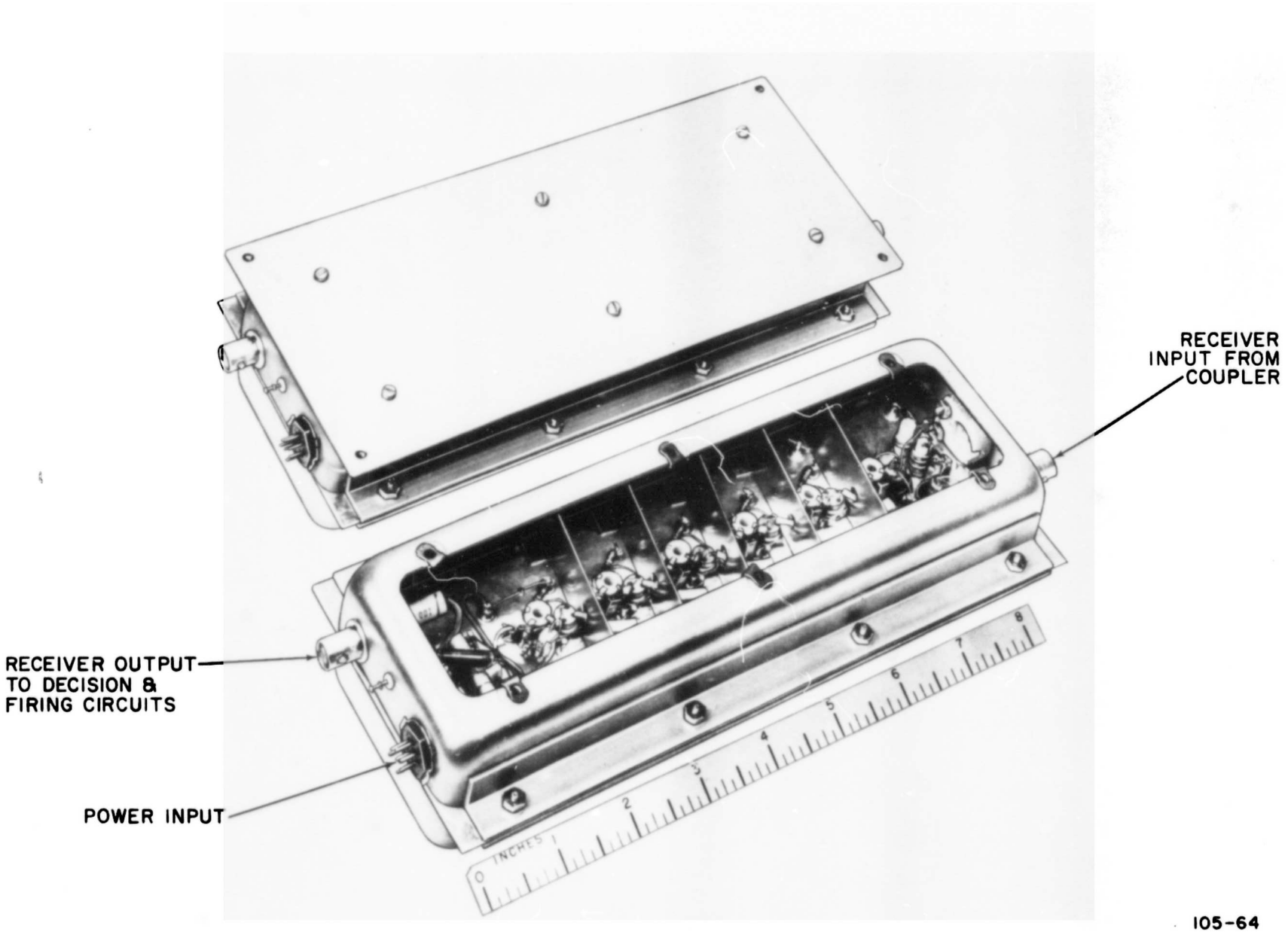

105-64

Fig. 25. Receiver For Radar Actuator.

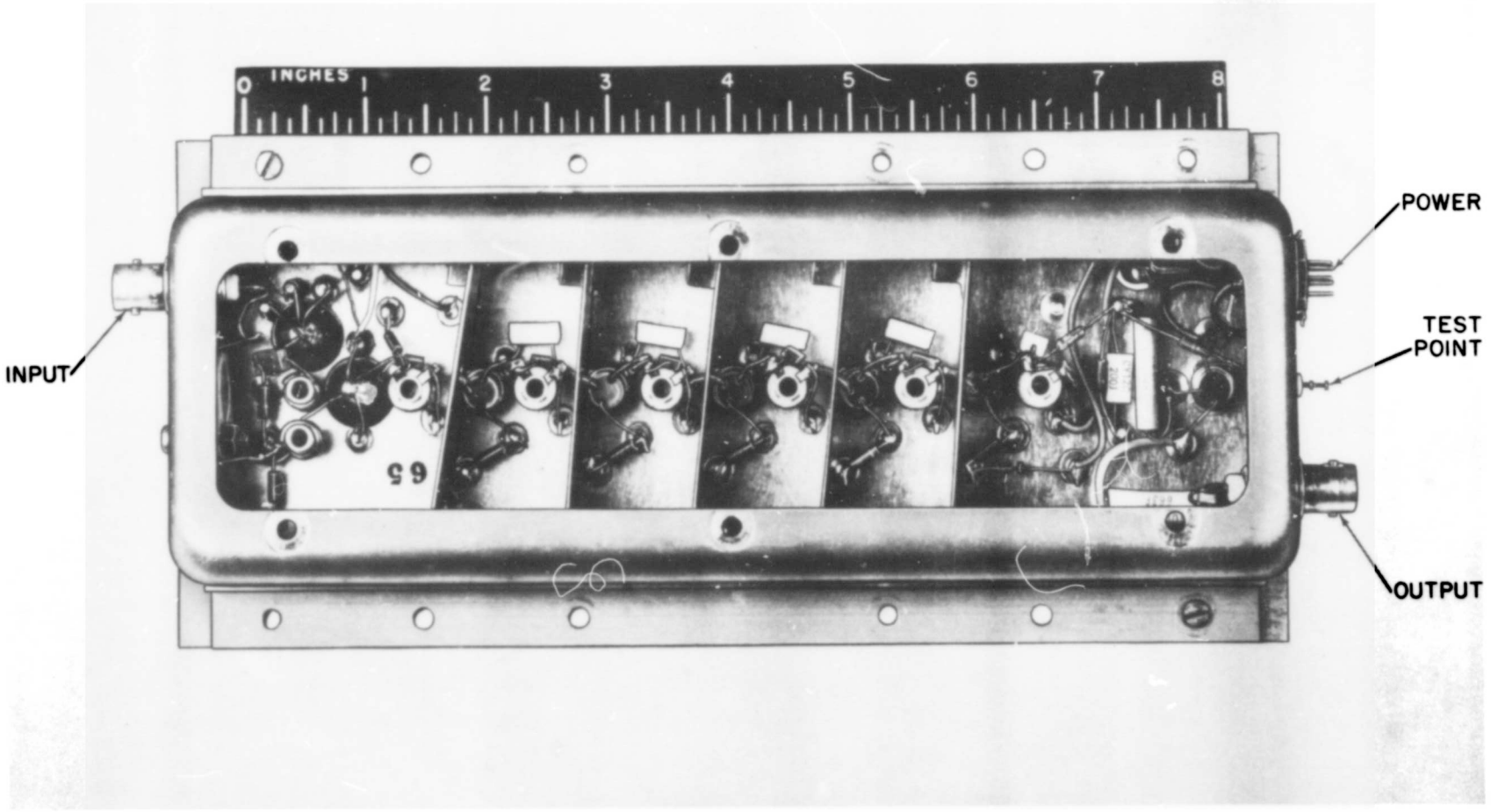

1479-64

Fig. 26. HADOPAD Receiver, Top View, Cover Off.

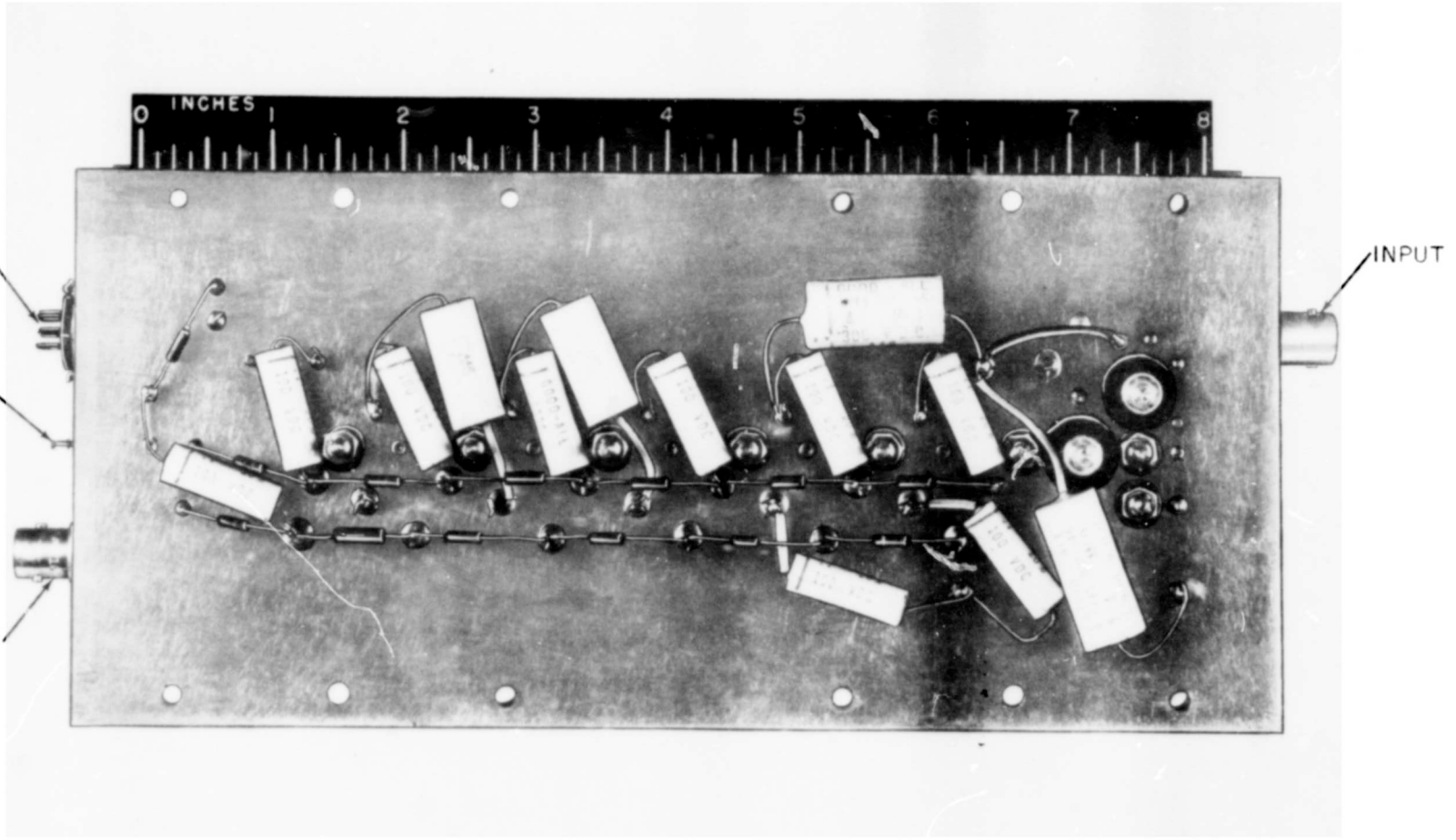

1480-64

Fig. 27. HADOPAD Receiver, Bottom View, Cover Off.

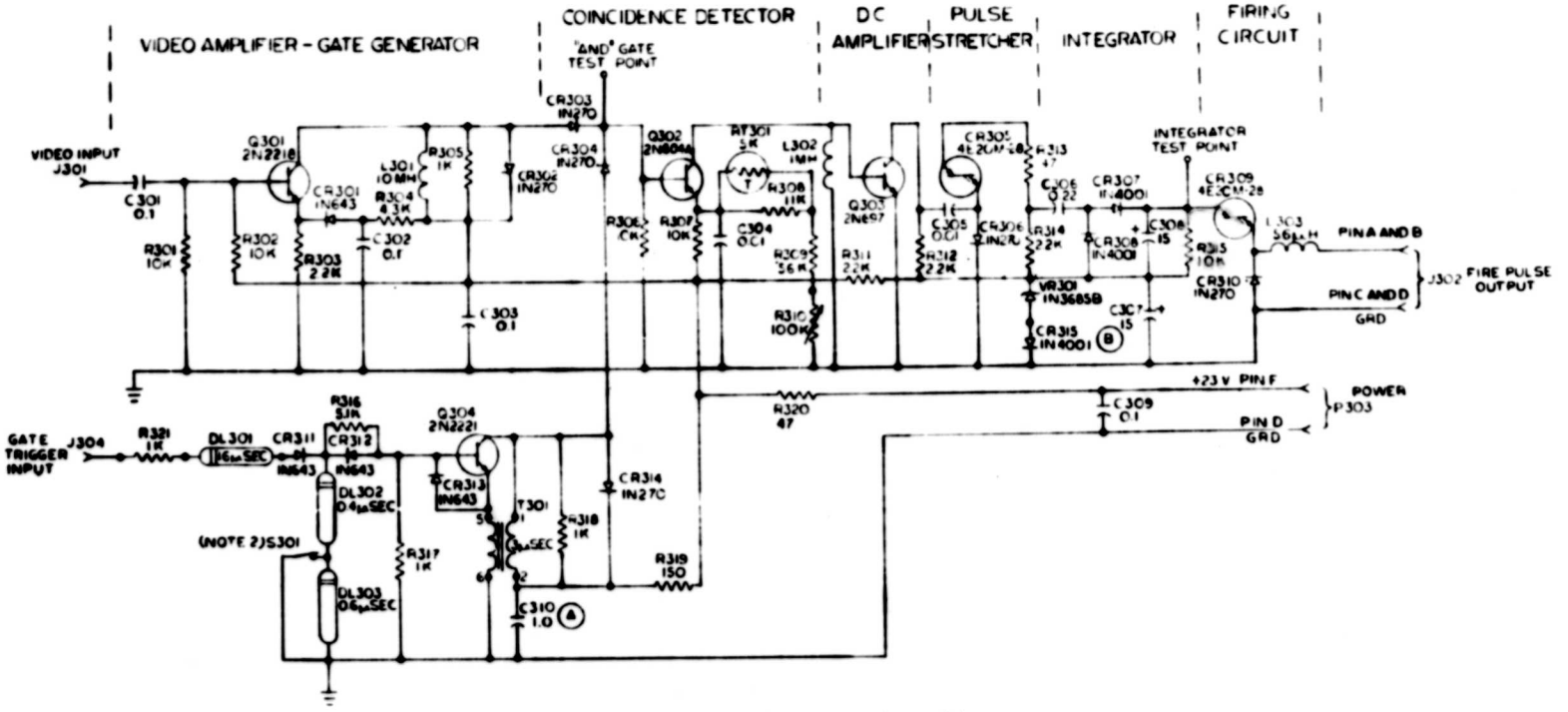

Figure 28. Decision-firing circuit.

1350-64

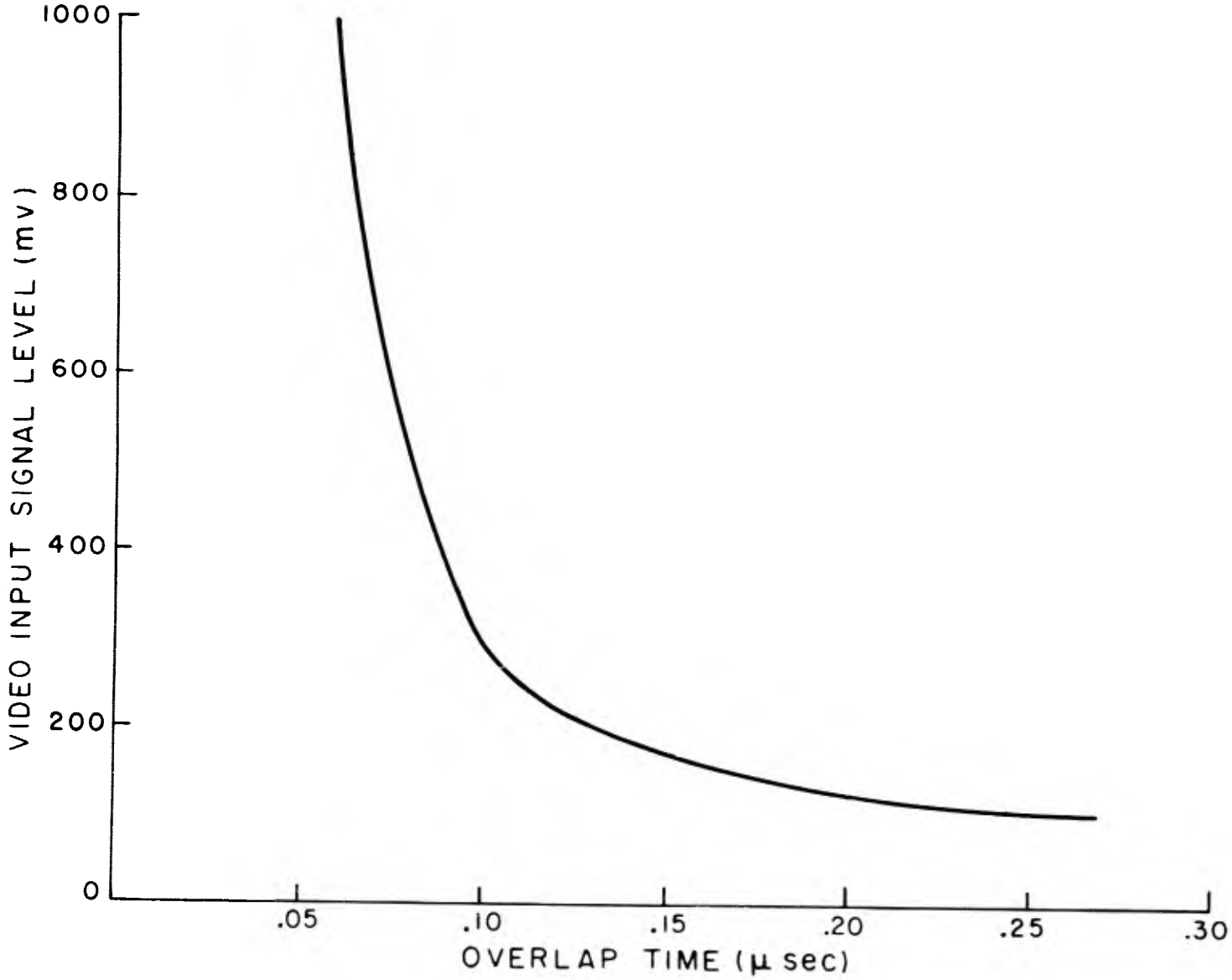

Figure 29. Gate video signal overlap time as function of video signal level in decision-firing circuit.

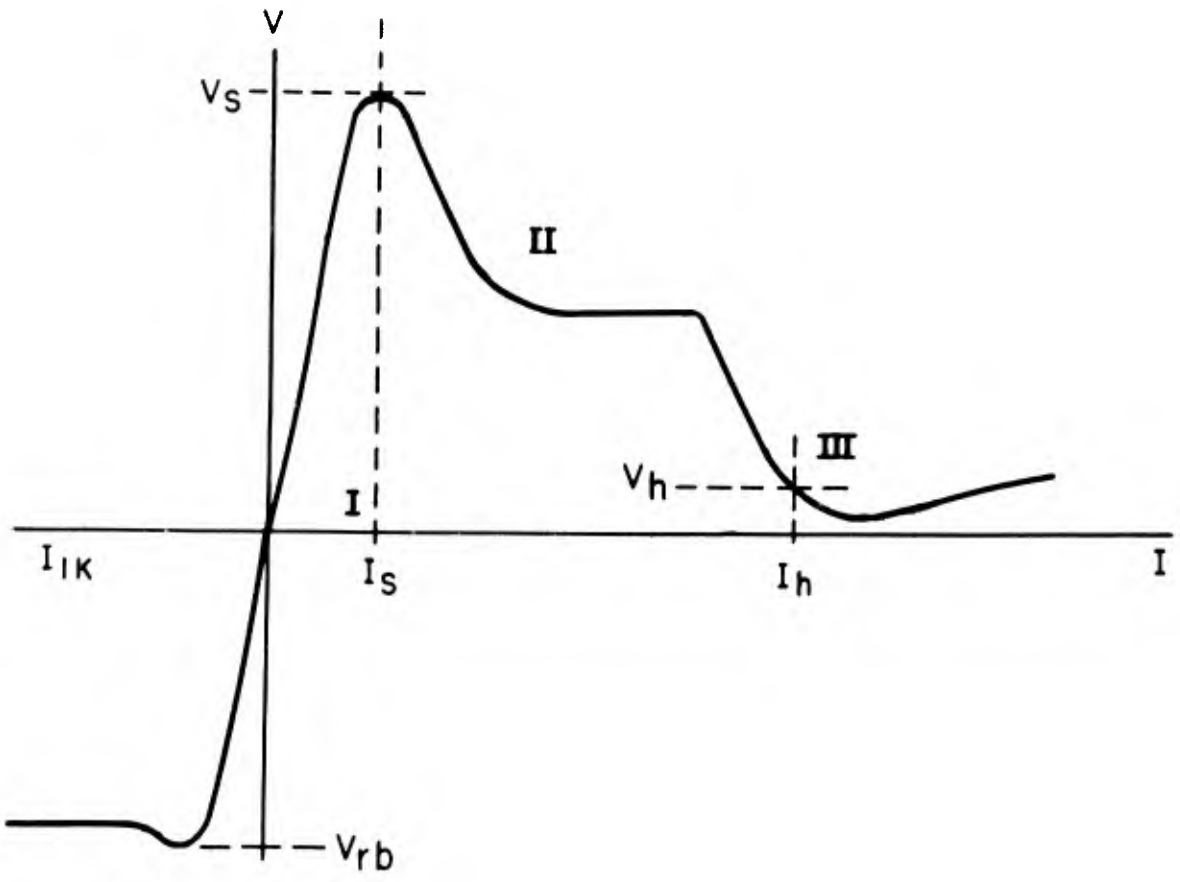

V_S = SWITCHING VOLTAGE
I_S = SWITCHING CURRENT
I_h = HOLDING CURRENT
V_h = HOLDING VOLTAGE
I_{IK} = LEAKAGE CURRENT
V_{rb} = REVERSE BREAKDOWN VOLT.

I = "OFF" – HIGH RESISTANCE STATE

II = TRANSITION (NEGATIVE RESISTANCE) STATE

III = "ON" – LOW RESISTANCE STATE

CONVENTIONAL CURRENT FLOW

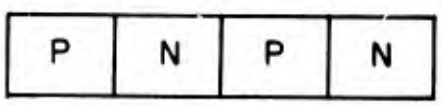

CONSTRUCTION

Figure 30. Typical V-I characteristic curve for four-layer diode.

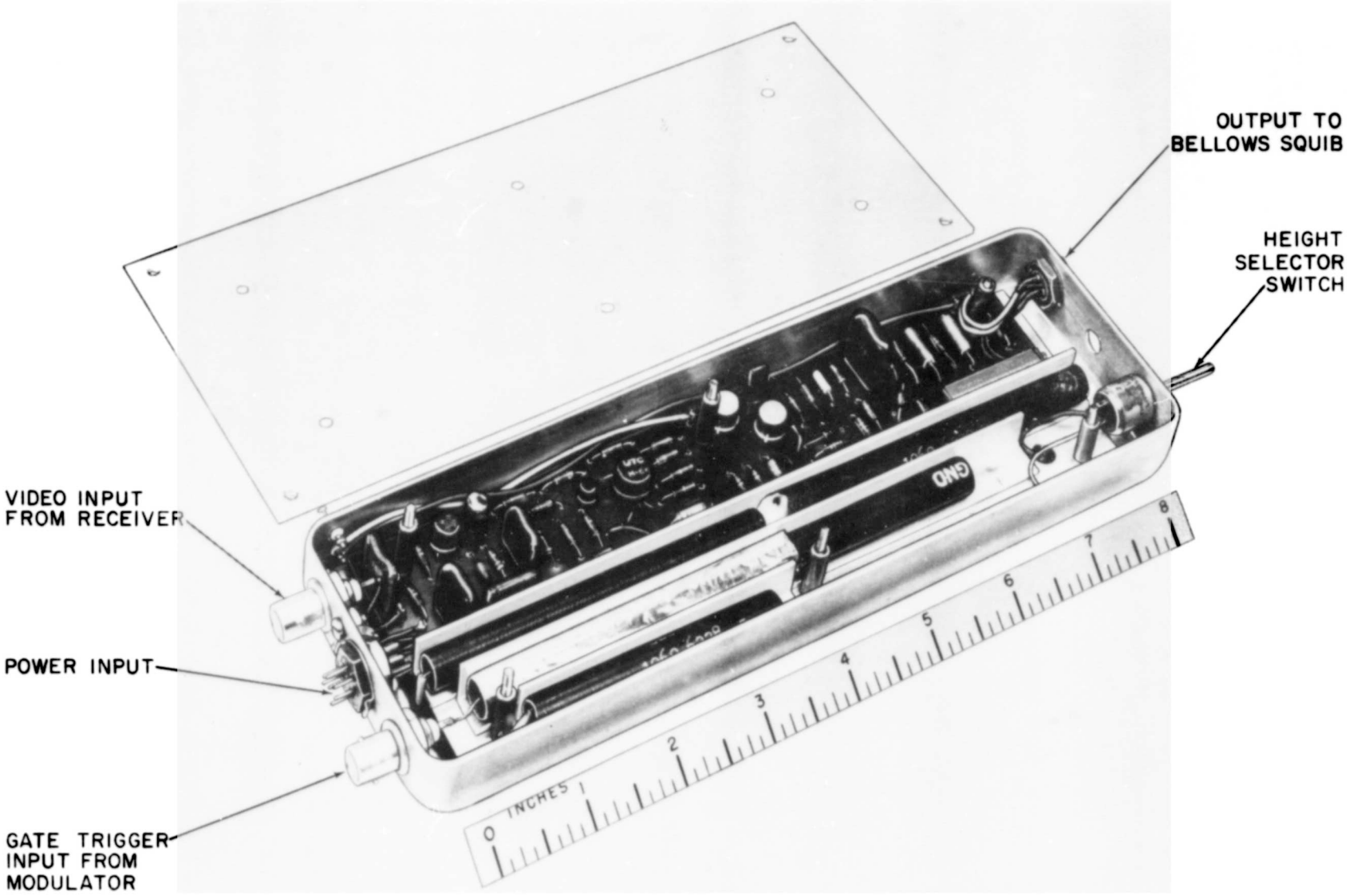

098-64

Fig 31. Decision Firing Circuits For Radar Actuator.

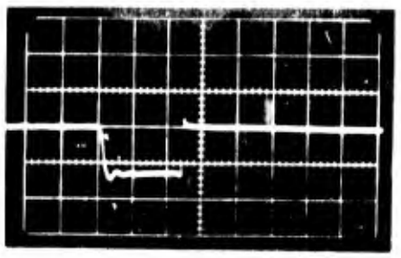

Gate Generator Out
Collector of Q304
20v/cm 0.5μs/cm

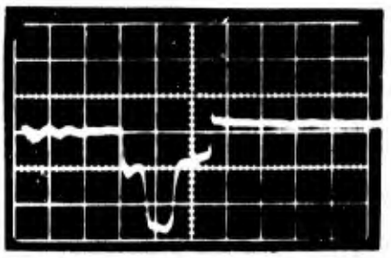

AND Gate Test Point
Base of Q302
1v/cm 0.5μs/cm

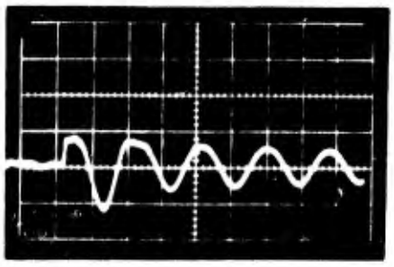

Coincidence Detector Out
Base of Q303
1v/cm 1μs/cm

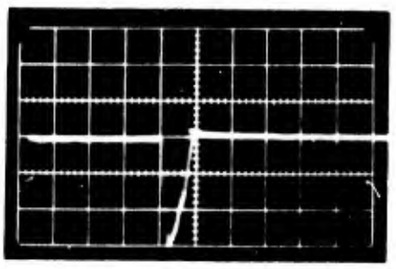

D-C Amplifier Out
Cathode of CR305
5v/cm 0.5μs/cm

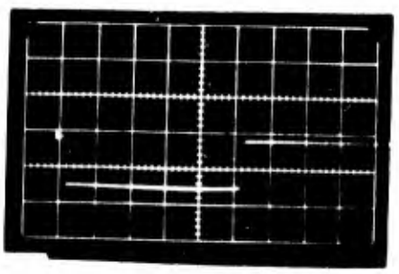

Pulse Stretcher Out
Anode of CR305
5v/cm 10μs/cm

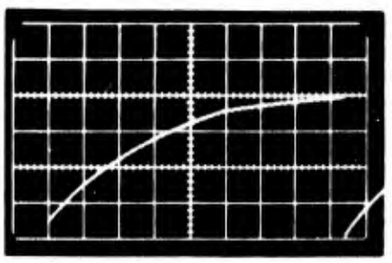

Integrator Test Point
Anode of CR309
5v/cm 10ms/cm

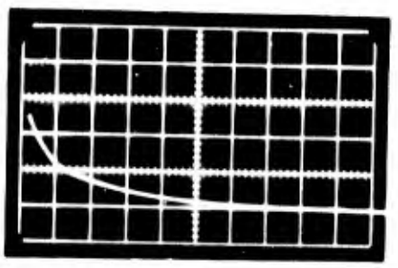

Squib Firing Pulse
50hm Load
5v/cm 50μs/cm

1349-64

Fig. 32 Waveforms in Decision-Firing Circuits. Each major Division Shown is 1cm

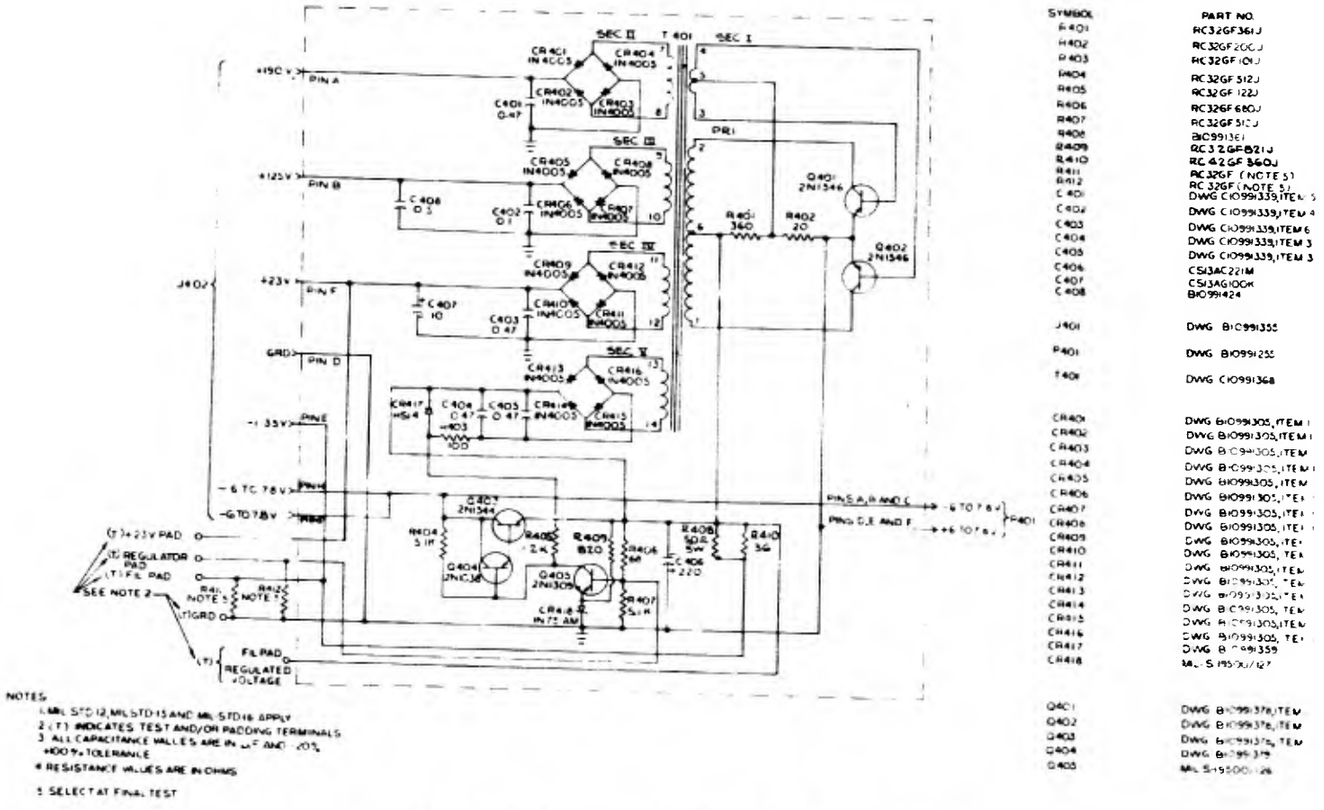

SYMBOL	PART NO.
R401	RC32GF361J
R402	RC32GF200J
R403	RC32GF101J
R404	RC32GF512J
R405	RC32GF122J
R406	RC32GF680J
R407	RC32GF512J
R408	BIC991361
R409	RC32GF821J
R410	RC42GF360J
R411	RC32GF (NOTE 5)
R412	RC32GF (NOTE 5)
C401	DWG CIO991339,ITEM 5
C402	DWG CIO991339,ITEM 4
C403	DWG CIO991339,ITEM 6
C404	DWG CIO991339,ITEM 3
C405	DWG CIO991339,ITEM 3
C406	CS13AC221M
C407	CS13AG100K
C408	BIC991424
J401	DWG BIC991355
P401	DWG BIC991255
T401	DWG CIO991368
CR401	DWG BIC991305,ITEM 1
CR402	DWG BIC991305,ITEM 1
CR403	DWG BIC991305,ITEM
CR404	DWG BIC991305,ITEM 1
CR405	DWG BIC991305,ITEM
CR406	DWG BIC991305,ITEM
CR407	DWG BIC991305,ITEM
CR408	DWG BIC991305,ITEM
CR409	DWG BIC991305,ITEM
CR410	DWG BIC991305,ITEM
CR411	DWG BIC991305,ITEM
CR412	DWG BIC991305,ITEM
CR413	DWG BIC991305,ITEM
CR414	DWG BIC991305,ITEM
CR415	DWG BIC991305,ITEM
CR416	DWG BIC991305,ITEM
CR417	DWG BIC991359
CR418	MIL-S-19500/627
Q401	DWG BIC991378,ITEM
Q402	DWG BIC991378,ITEM
Q403	DWG BIC991378,ITEM
Q404	DWG BIC991379
Q405	MIL-S-19500/628

NOTES:
1. MIL-STD-12, MIL-STD-15 AND MIL-STD-16 APPLY
2. (T) INDICATES TEST AND/OR PADDING TERMINALS
3. ALL CAPACITANCE VALUES ARE IN μF AND ±20% ±100% TOLERANCE
4. RESISTANCE VALUES ARE IN OHMS
5. SELECT AT FINAL TEST

Figure 33. Schematic of dc-dc converter.

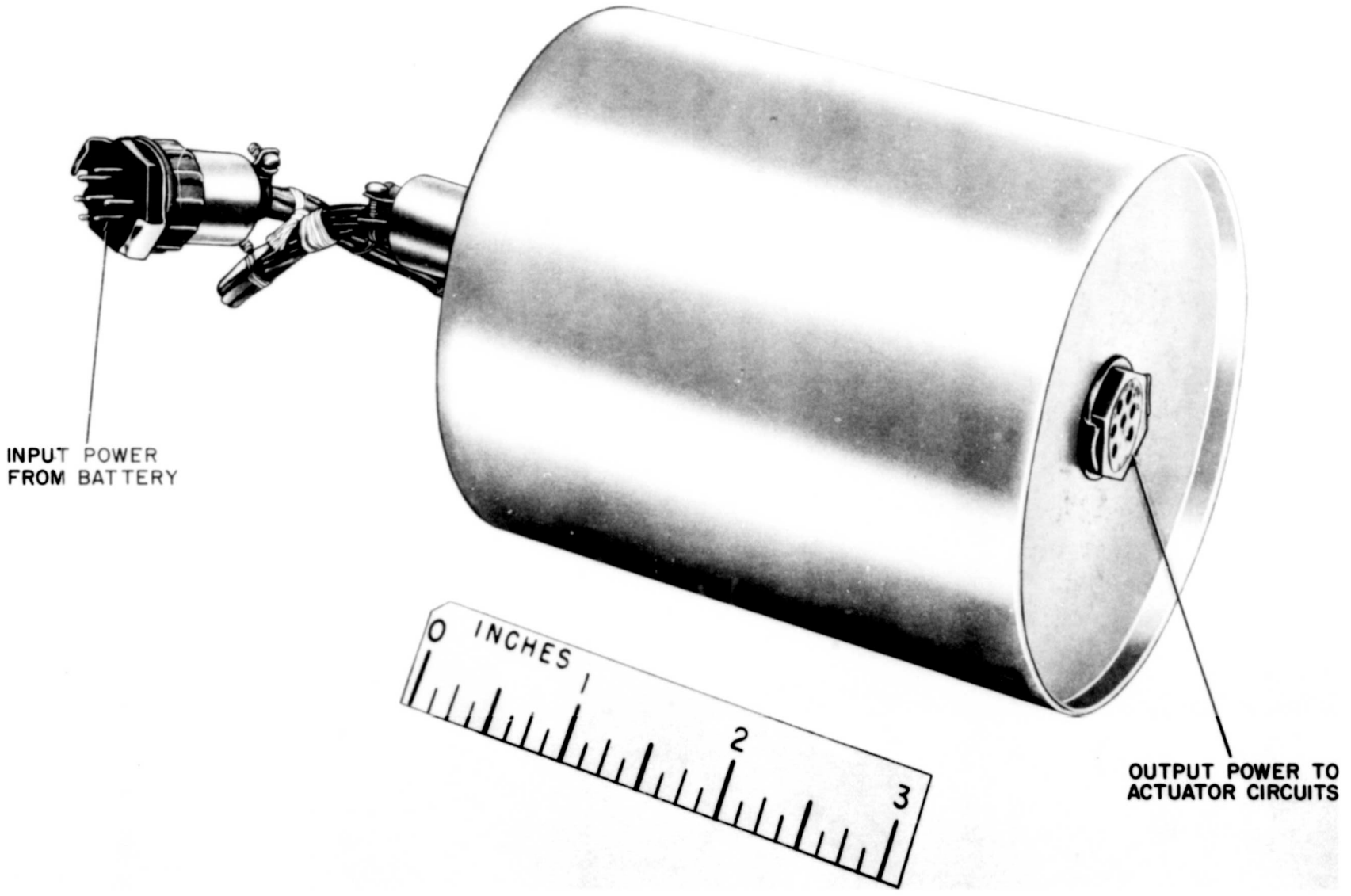

099-64

Fig. 34. DC-DC Converter For Radar Actuator.

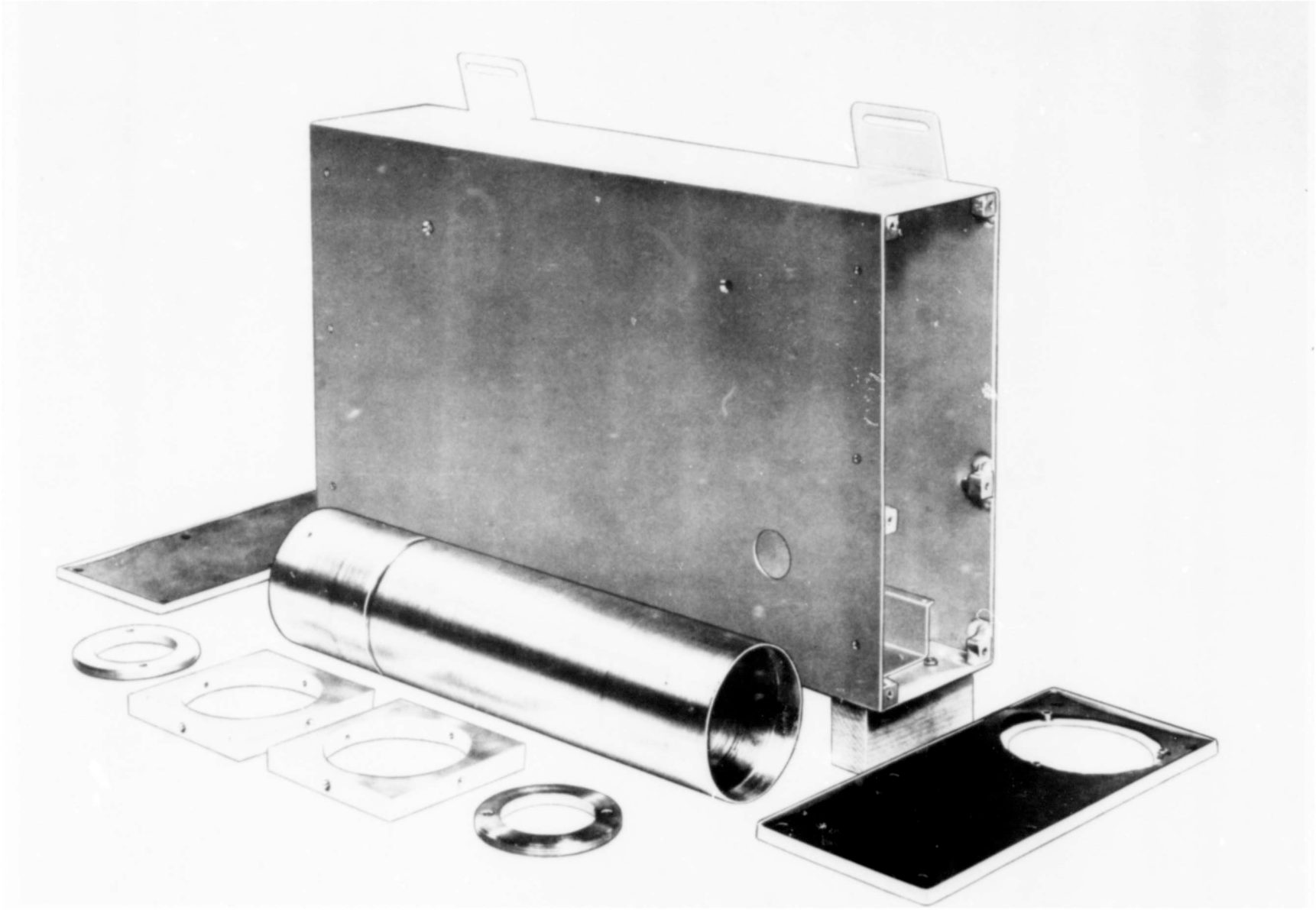

100-64

Fig. 35. Housing For Radar Actuator.

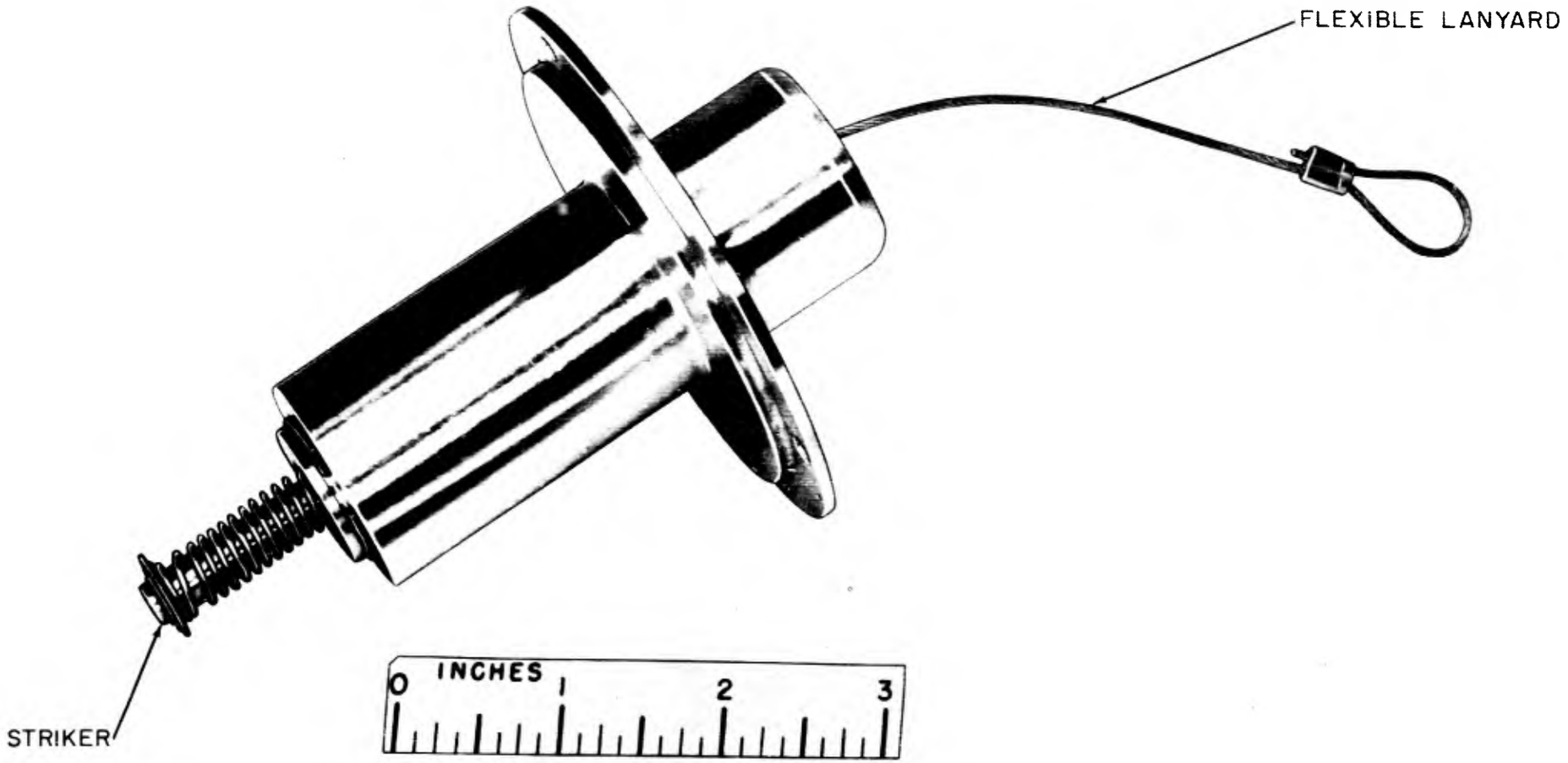

095-64

Fig. 36. Battery Striker Mechanism For Radar Actuator.

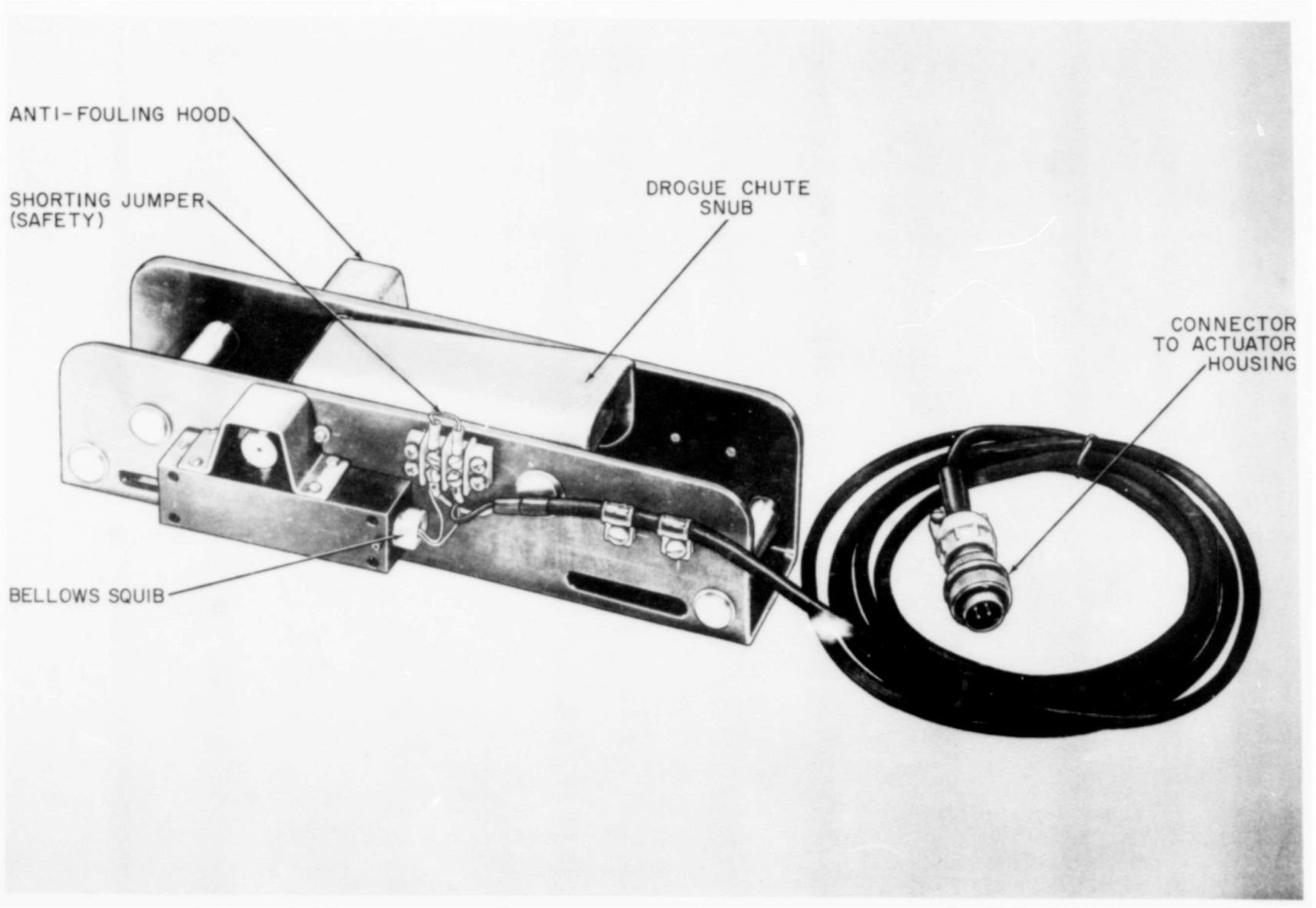

1973-64

Fig. 37. Parachute Release Mechanism For HADOPAD.

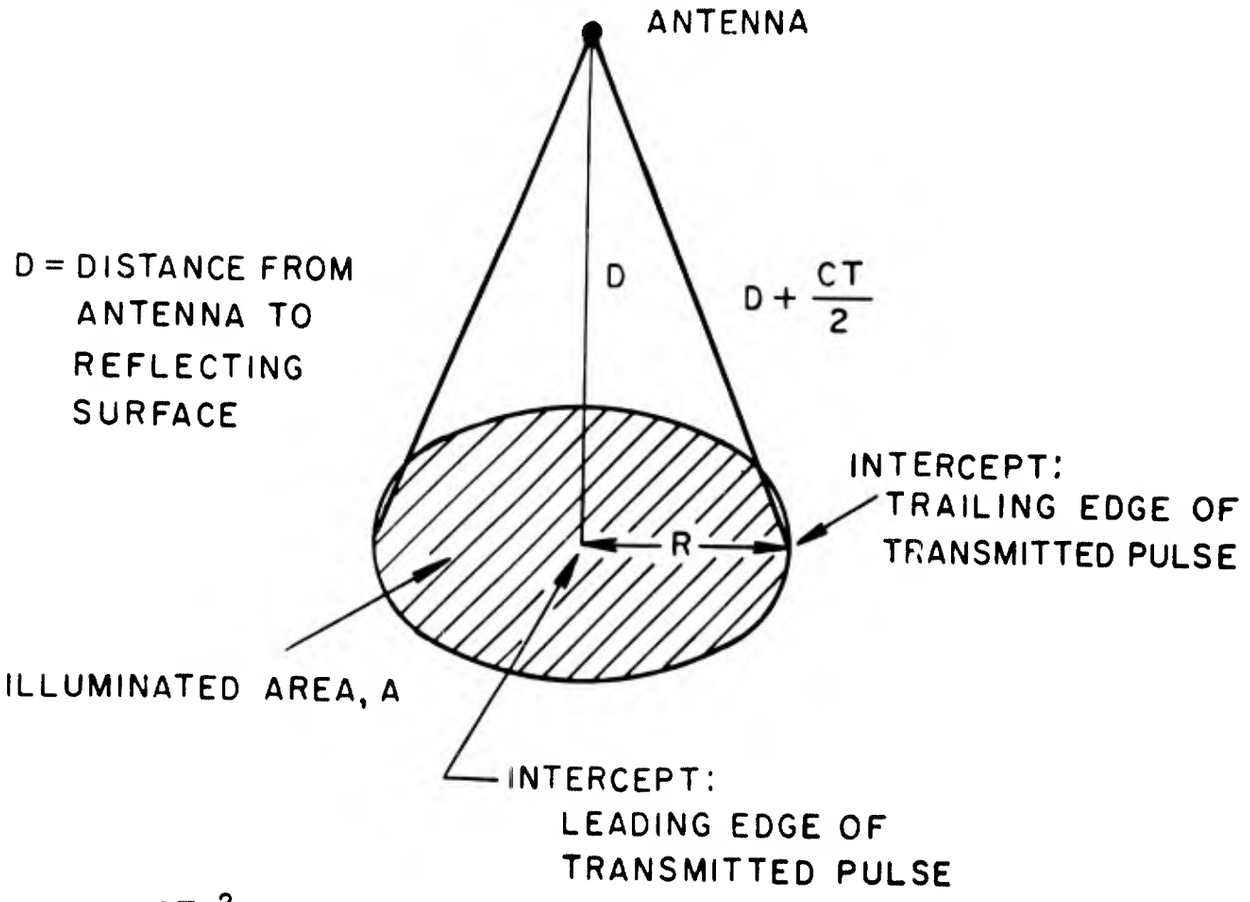

$$R^2 = \left(D + \frac{CT}{2}\right)^2 - D^2$$

C = VELOCITY OF ELECTROMAGNETIC RADIATION = 984 FT/μ sec

T = WIDTH OF TRANSMITTED PULSE

FOR $T = 0.14\ \mu$ sec, $\frac{CT}{2} = 69$ FT

AT D = 1700 FT
R = 458 FT
A = 660,000 SQ FT

AT D = 1000 FT
R = 378 FT
A = 442,000 SQ FT

Figure 38. Pulse width limiting of radar.

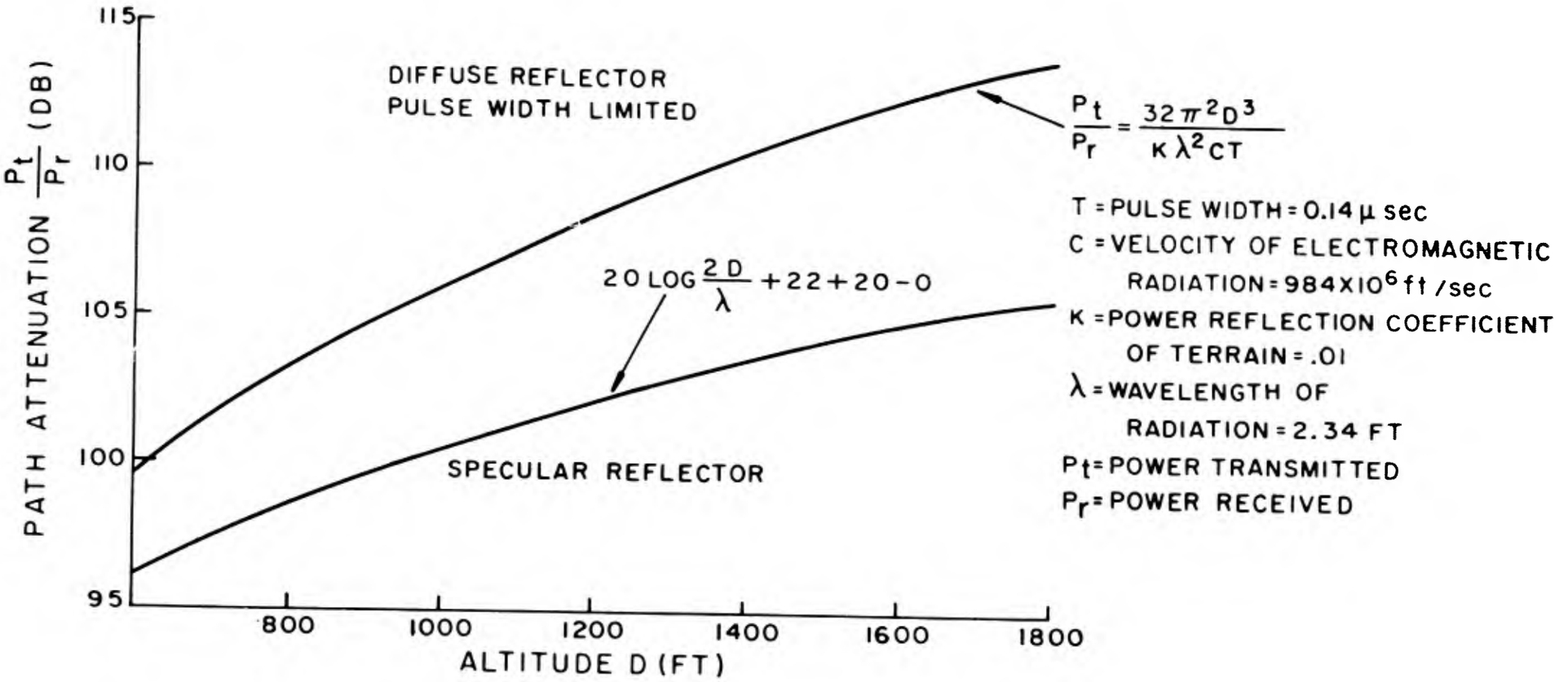

Figure 39. Path attentuation versus altitude with isotropic radiator.

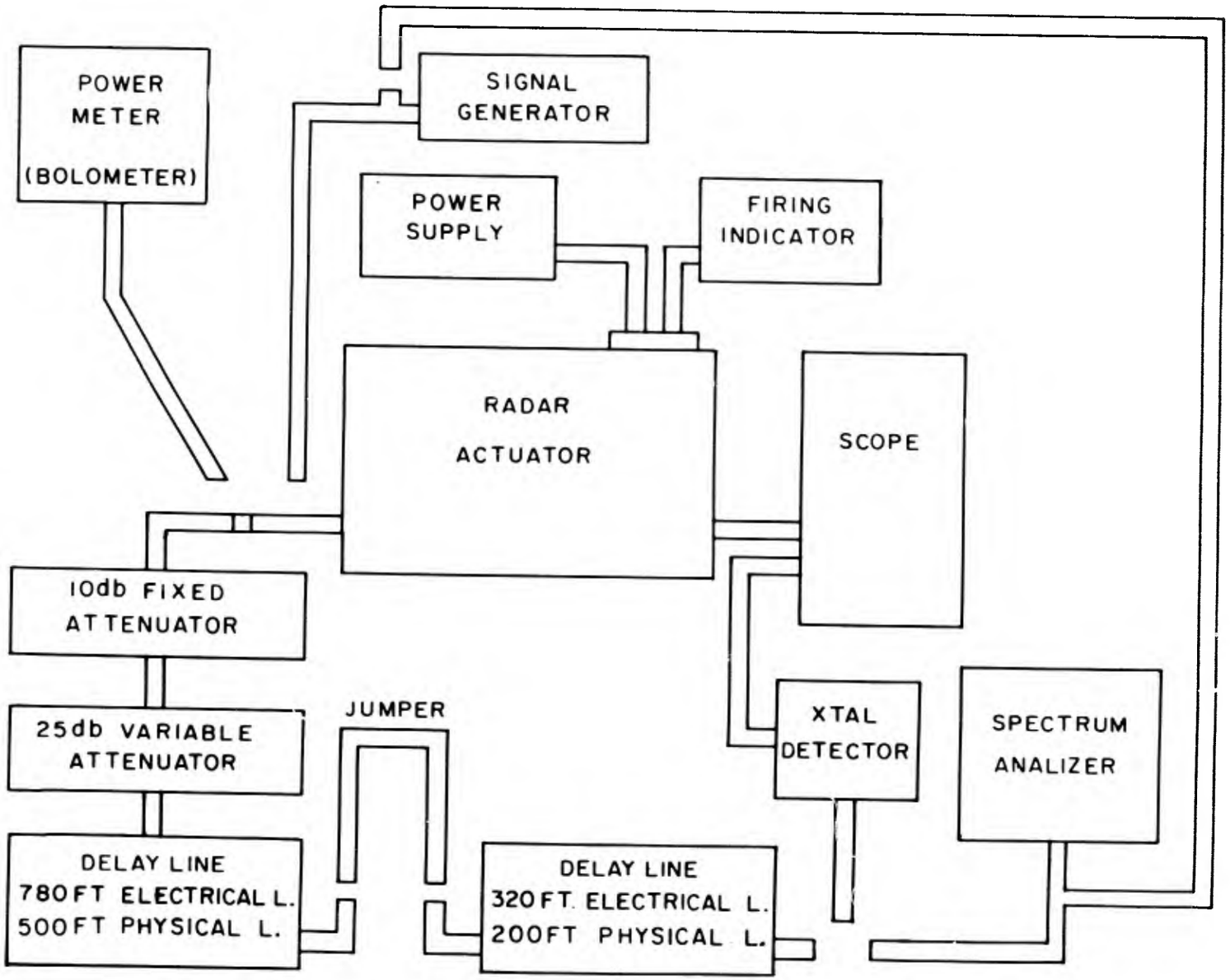

Figure 40. Final test setup for radar actuator.

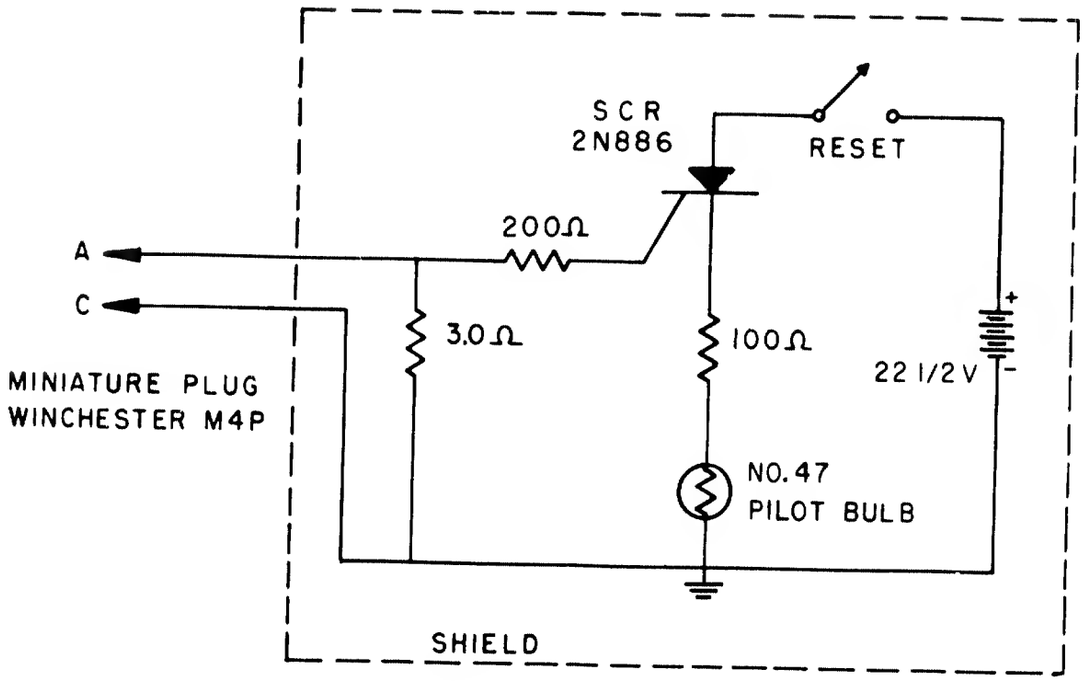

Figure 41. Circuit diagram of firing indicator.

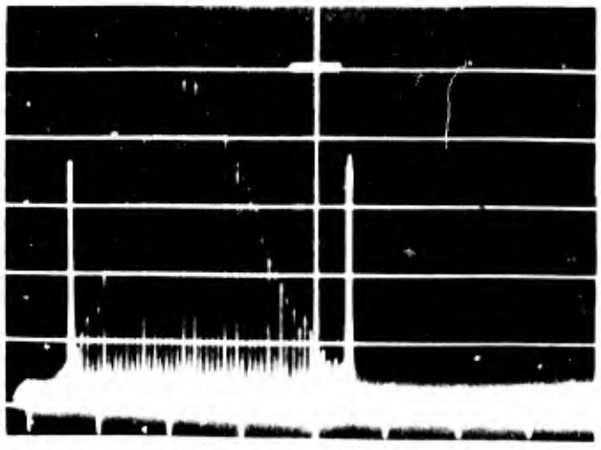

Typical Transmitted Spectrum
HADOPAD Markers at 415 and 425 mc.

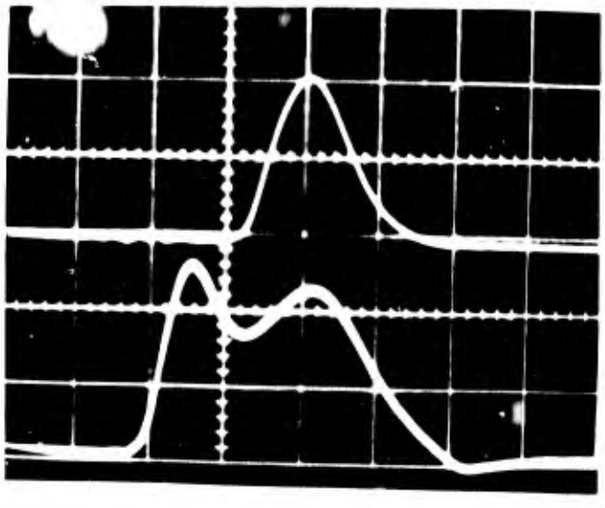

Upper: Detected Transmitted Pulse.
Time Base: 0.1 μ sec/cm
Lower: Modulator Output Pulse.
Time Base: 0.1 μ sec/cm
Vertical: 500 v/cm

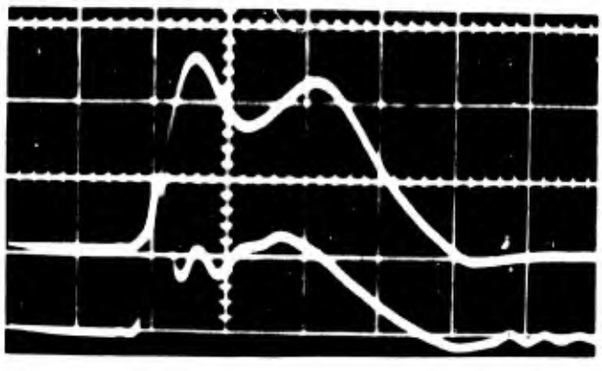

Upper: Modulator Output Pulse.
Time Base: 0.1 μ sec/cm
Vertical: 500 v/cm
Lower: Gate Trigger Pulse.
Time Base: 0.1 μ sec/cm
Vertical: 100 v/cm

060-65

Fig. 42 Typical Data.

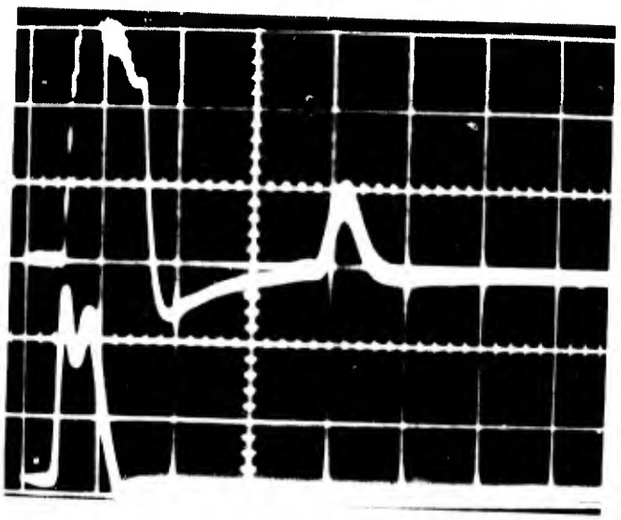

Upper: Emitter Follower Output, Showing "Main Bang" and Echo Pulse Out of 780 Ft. Delay Line.
Time Base: 0.5 μ sec/cm
Vertical: 0.1 v/cm

Lower: Modulator Output Pulse
Time Base: 0.5 μ sec/cm
Vertical: 500 v/cm

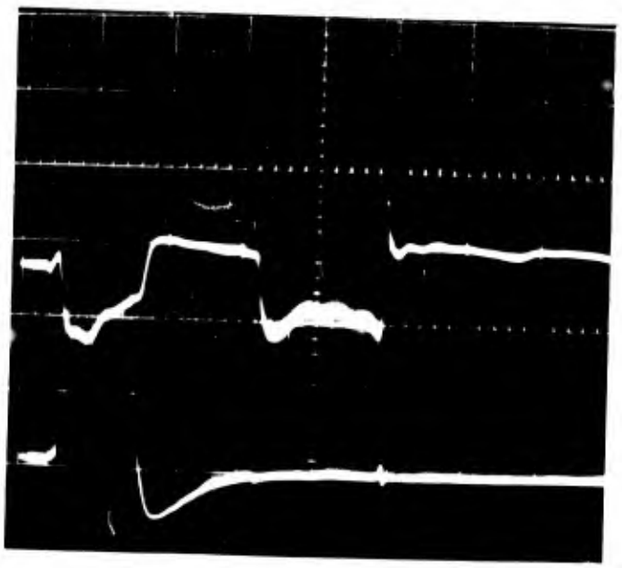

Upper: Video Test Point Showing "Main Bang" and 1000 Ft. Gate Output Pulse. No Echo Signal Present.
Time Base: 0.5 μ sec/cm
Vertical: 1.0 v/cm

Lower: Emitter Follower Output, Showing "Main Bang", No Echo Pulse Present. (Pips on Base Line Are Reaction to Gate Generator Switching).
Time Base: 0.5 μ sec/cm
Vertical: 0.1 v/cm

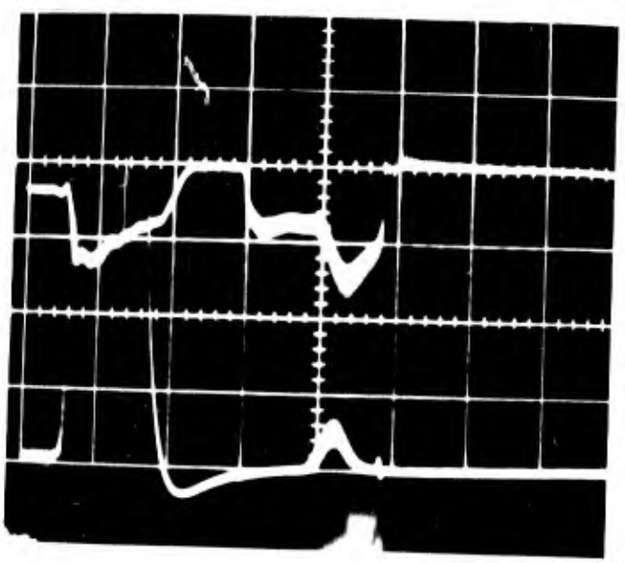

Upper: Video Test Point, Showing "Main Bang" and 1000 Ft. Gate Output Pulse With Echo Signal Superimposed. (Echo Pulse Out of 780 Ft. Delay Line).
Time Base: 0.5 μ sec/cm
Vertical: 1.0 v/cm

Lower: Emitter Follower Output Showing "Main Bang" and Echo Pulse Out of 780 Ft. Delay Line.
Time Base: 0.5 μ sec/cm
Vertical: 0.1 v/cm

061-65

Fig. 43 Typical Data

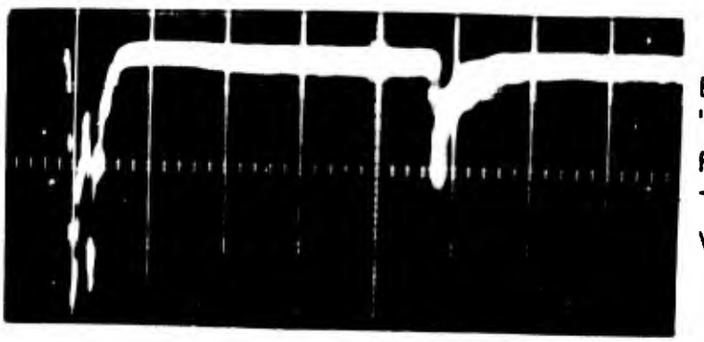

Emitter Follower Output, Showing "Main Bang" and Signal Return From Water at Altitude of 2400 Ft.
Time Base: 1.0 μ sec/cm
Vertical: 0.5 v/cm
(Amplitude = 0.8 v)

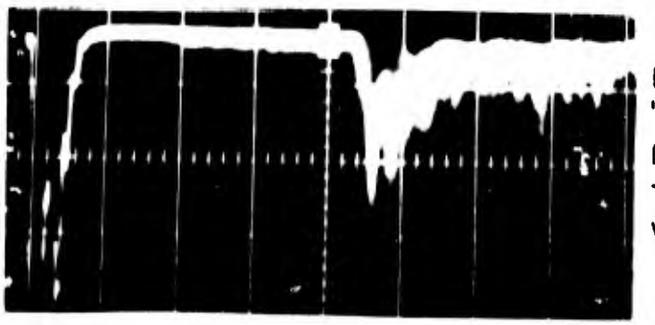

Emitter Follower Output, Showing "Main Bang" and Signal Return From Water at Altitude of 2200 Ft.
Time Base: 1.0 μ sec/cm
Vertical: 0.2 v/cm
(Amplitude = 0.45 v)

062-65

Photographs Taken in Early R & D Phase of Emitter Follower Output Showing Signal Return From Water and Land Along With the "Main Bang". Water Return From Potomac River, Land Return From Typical Farmland in Vicinity of Fredricksburg, Va. Trailing Wire Antenna 116 in. Long. Helicopter: H 21. HADOPAD Actuator Mounted on 12 Ft. Boom Set at Right Angles to Helicopter With Boom Extended From Rear Door.

Fig. 44 Typical Data.

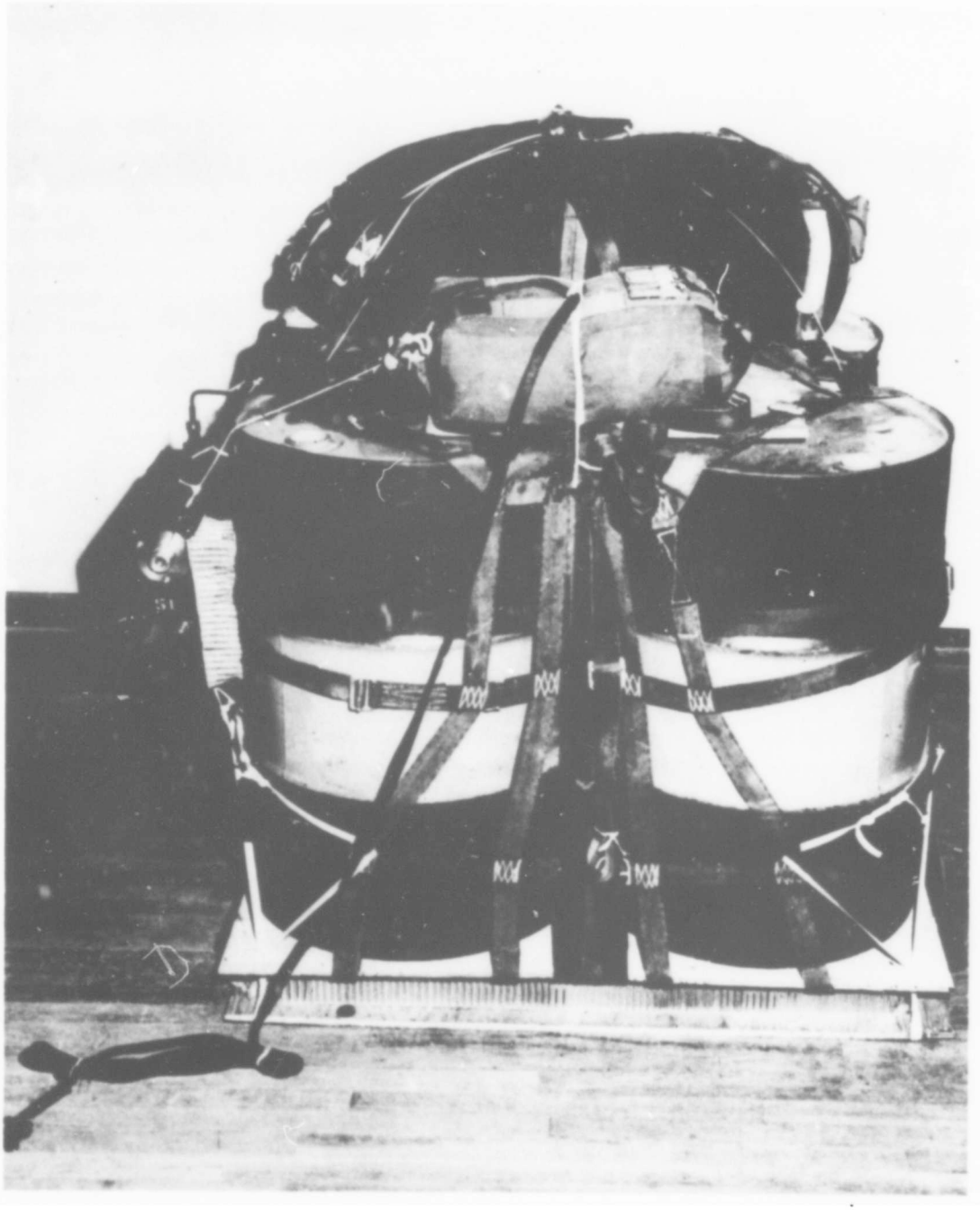

2696-64

Fig. 45 HADOPAD Actuator Mounted on 2200-Lb Load

Fig. 46. HADOPAD Actuator Mounted On 500lb. Load.

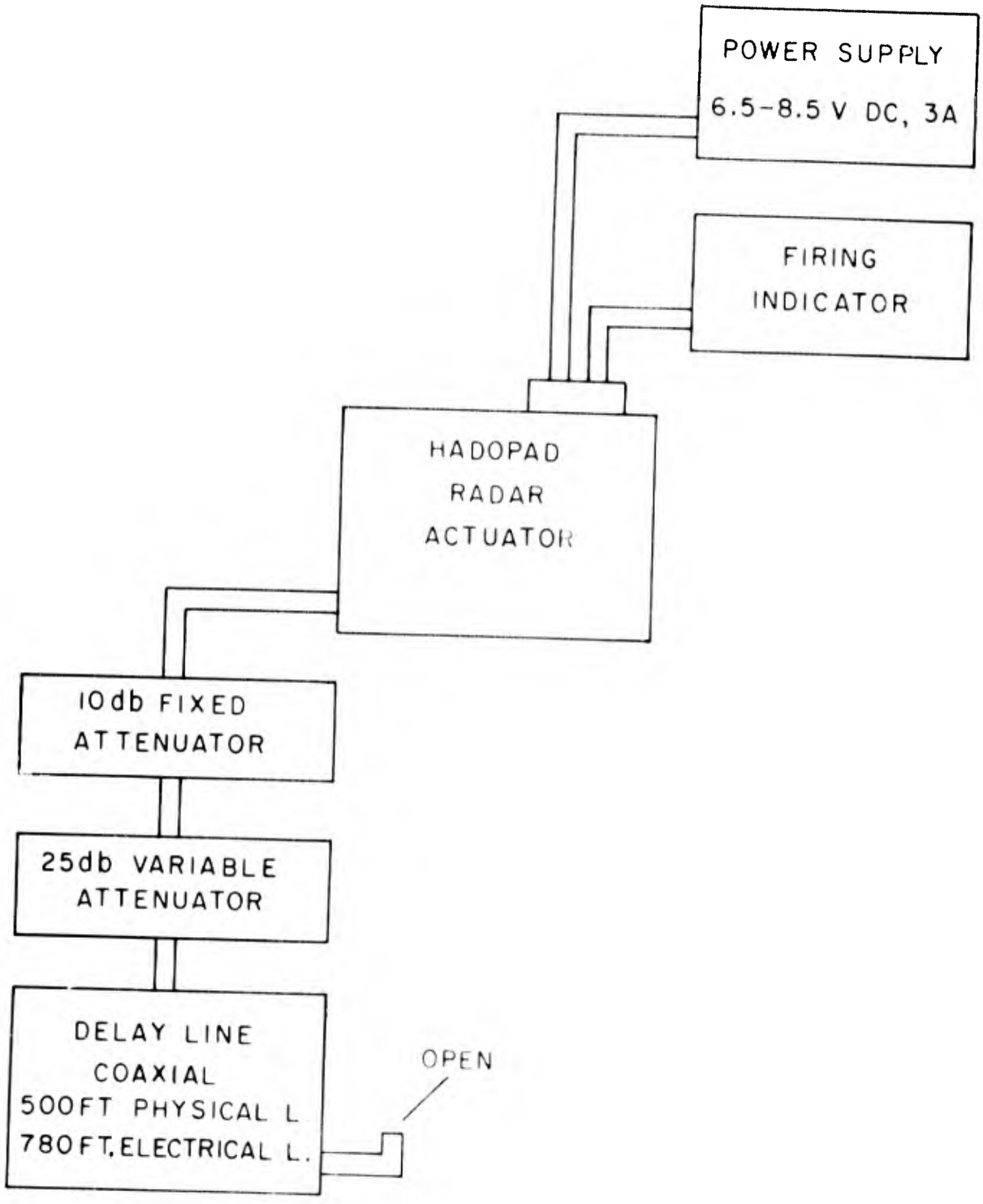

Figure 47. Block diagram of HADOPAD go, no-go test.

DOCUMENT CONTROL DATA - R&D

(Security classification of title, body of abstract and indexing annotation must be entered when the overall report is classified)

1. ORIGINATING ACTIVITY *(Corporate author)*

Harry Diamond Laboratories, Washington, D. C.

2a. REPORT SECURITY CLASSIFICATION

UNCLASSIFIED

2b. GROUP

3. REPORT TITLE

HADOPAD RADAR ACTUATOR DESIGN AND PERFORMANCE

4. DESCRIPTIVE NOTES *(Type of report and inclusive dates)*

5. AUTHOR(S) *(Last name, first name, initial)*

Roach, John J.
Wiseman, Malcolm L.

6. REPORT DATE	7a. TOTAL NO. OF PAGES	7b. NO. OF REFS
February 1966	94	11

8a. CONTRACT OR GRANT NO.	9a. ORIGINATOR'S REPORT NUMBER(S)
b. PROJECT NO. DA-1W542703D346	TM-66-2
c. AMCMS Code: 5520.22.46803	9b. OTHER REPORT NO(S) *(Any other numbers that may be assigned this report)*
d. HDL Proj 47100	

10. AVAILABILITY/LIMITATION NOTICES

Qualified requesters may obtain copies of this report from DDC. DDC release to CFSTI is authorized.

11. SUPPLEMENTARY NOTES	12. SPONSORING MILITARY ACTIVITY
	U.S. Army Natick Laboratories

13. ABSTRACT

A low-cost radar actuator for use as a component in a delayed-opening parachute aerial-delivery system has been developed at HDL at the request of the U.S. Army Natick Laboratories. This device is known as HADOPAD (High-Altitude Delayed-Opening Parachute Actuating Device).

The device, based on radar principles, will open a main recovery parachute at either of two preset heights (1000 or 1700 ft) above the ground. The complete system utilizes a drogue-parachute stabilizing stage for free fall from high altitude followed by a main-parachute recovery stage which is initiated at low altitude by the radar actuator.

Limited field testing of the radar actuator at Fort Devens, Mass. has shown the feasibility of the device as a parachute actuator, but some additional engineering and complete environmental tests are necessary before initiation of quantity production

Forty actuators were constructed by HDL during the research and development phase.

DD FORM 1 JAN 64 1473

14. KEY WORDS	LINK A		LINK B		LINK C	
	ROLE	WT	ROLE	WT	ROLE	WT
HADOPAD Radar actuator Two-stage parachute delivery system						

INSTRUCTIONS

1. ORIGINATING ACTIVITY: Enter the name and address of the contractor, subcontractor, grantee, Department of Defense activity or other organization *(corporate author)* issuing the report.

2a. REPORT SECURITY CLASSIFICATION: Enter the overall security classification of the report. Indicate whether "Restricted Data" is included. Marking is to be in accordance with appropriate security regulations.

2b. GROUP: Automatic downgrading is specified in DoD Directive 5200.10 and Armed Forces Industrial Manual. Enter the group number. Also, when applicable, show that optional markings have been used for Group 3 and Group 4 as authorized.

3. REPORT TITLE: Enter the complete report title in all capital letters. Titles in all cases should be unclassified. If a meaningful title cannot be selected without classification, show title classification in all capitals in parenthesis immediately following the title.

4. DESCRIPTIVE NOTES: If appropriate, enter the type of report, e.g., interim, progress, summary, annual, or final. Give the inclusive dates when a specific reporting period is covered.

5. AUTHOR(S): Enter the name(s) of author(s) as shown on or in the report. Enter last name, first name, middle initial. If military, show rank and branch of service. The name of the principal author is an absolute minimum requirement.

6. REPORT DATE: Enter the date of the report as day, month, year, or month, year. If more than one date appears on the report, use date of publication.

7a. TOTAL NUMBER OF PAGES: The total page count should follow normal pagination procedures, i.e., enter the number of pages containing information.

7b. NUMBER OF REFERENCES: Enter the total number of references cited in the report.

8a. CONTRACT OR GRANT NUMBER: If appropriate, enter the applicable number of the contract or grant under which the report was written.

8b, 8c, & 8d. PROJECT NUMBER: Enter the appropriate military department identification, such as project number, subproject number, system numbers, task number, etc.

9a. ORIGINATOR'S REPORT NUMBER(S): Enter the official report number by which the document will be identified and controlled by the originating activity. This number must be unique to this report.

9b. OTHER REPORT NUMBER(S): If the report has been assigned any other report numbers *(either by the originator or by the sponsor)*, also enter this number(s).

10. AVAILABILITY/LIMITATION NOTICES: Enter any limitations on further dissemination of the report, other than those imposed by security classification, using standard statements such as:

(1) "Qualified requesters may obtain copies of this report from DDC."

(2) "Foreign announcement and dissemination of this report by DDC is not authorized."

(3) "U. S. Government agencies may obtain copies of this report directly from DDC. Other qualified DDC users shall request through _____."

(4) "U. S. military agencies may obtain copies of this report directly from DDC. Other qualified users shall request through _____."

(5) "All distribution of this report is controlled. Qualified DDC users shall request through _____."

If the report has been furnished to the Office of Technical Services, Department of Commerce, for sale to the public, indicate this fact and enter the price, if known.

11. SUPPLEMENTARY NOTES: Use for additional explanatory notes.

12. SPONSORING MILITARY ACTIVITY: Enter the name of the departmental project office or laboratory sponsoring *(paying for)* the research and development. Include address.

13. ABSTRACT: Enter an abstract giving a brief and factual summary of the document indicative of the report, even though it may also appear elsewhere in the body of the technical report. If additional space is required, a continuation sheet shall be attached.

It is highly desirable that the abstract of classified reports be unclassified. Each paragraph of the abstract shall end with an indication of the military security classification of the information in the paragraph, represented as *(TS), (S), (C), or (U)*.

There is no limitation on the length of the abstract. However, the suggested length is from 150 to 225 words.

14. KEY WORDS: Key words are technically meaningful terms or short phrases that characterize a report and may be used as index entries for cataloging the report. Key words must be selected so that no security classification is required. Identifiers, such as equipment model designation, trade name, military project code name, geographic location, may be used as key words but will be followed by an indication of technical context. The assignment of links, rules, and weights is optional.